LA-10342-T
Thesis

UC-34A
Issued: February 1985

LA--10342-T

DE85 011889

Stresses and Elastic Constants of Crystalline Sodium, from Molecular Dynamics

Sheila K. Schiferl

Los Alamos National Laboratory
Los Alamos, New Mexico 87545

TABLE OF CONTENTS

Table of Contents -- Continued

LIST OF TABLES

LIST OF ILLUSTRATIONS

ABSTRACT

The stresses and the elastic constants of bcc sodium are calculated by molecular dynamics (MD) for temperatures to T = 340 K. The total adiabatic potential of a system of sodium atoms is represented by a pseudopotential model. The resulting expression has two terms: a large, strictly volume-dependent potential, plus a sum over ion pairs of a small, volume-dependent two-body potential.

The stresses and the elastic constants are given as strain derivatives of the Helmholtz free energy. The resulting expressions involve canonical ensemble averages (and fluctuation averages) of the position and volume derivatives of the potential. An ensemble correction relates the results to MD equilibrium averages.

Evaluation of the potential and its derivatives requires the calculation of integrals with infinite upper limits of integration, and integrand singularities. Methods for calculating these integrals and estimating the effects of integration errors are developed.

A method is given for choosing initial conditions that relax quickly to a desired equilibrium state. Statistical methods developed earlier for MD data are extended to evaluate uncertainties in fluctuation averages, and to test for symmetry.

The fluctuation averages make a large contribution to the elastic constants, and the uncertainties in these averages are the dominant uncertainties in the elastic constants. The strictly

volume-dependent terms are very large. The ensemble correction is small but significant at higher temperatures. Surprisingly, the volume derivatives of the two-body potential make large contributions to the stresses and the elastic constants. The effects of finite potential range and finite system size are discussed, as well as the effects of quantum corrections and electronic excitations.

The agreement of theory and experiment is very good for the magnitudes of C_{11} and C_{12}. The magnitude of C_{44} is consistently small by ~ 9 kbar for finite temperatures. This discrepancy is most likely due to the neglect of three-body contributions to the potential. The agreement of theory and experiment is excellent for the temperature dependences of all three elastic constants. This result illustrates a definite advantage of MD compared to lattice dynamics for conditions where classical statistics are valid. MD methods involve direct calculations of anharmonic effects; no perturbation treatment is necessary.

CHAPTER 1

INTRODUCTION

The calculation of thermodynamic variables for a real metal at finite temperatures is a many-body problem par excellence. For a small system and at temperatures where quantum effects are negligible, we use a computer to integrate the classical equations of motion and to calculate various mechanical quantities along the system trajectory. Time averages of these quantities, taken after the system has reached equilibrium, can then be related to canonical ensemble averages, and the ensemble averages related to thermodynamic variables.

This kind of computer simulation, molecular dynamics (MD), eliminates a number of many-body difficulties, but it also introduces a number of new problems. These problems, and some proposed solutions, will be discussed in Chapters 4 and 5. A number of many-body problems still remain, principally because the canonical partition function contains an expression for the total energy of a system. We need a form for the total energy that is both mathematically tractable and physically reasonable for a metal.

We will derive an appropriate form for the total energy of a system of sodium atoms, starting with a model of a collection of spherical closed shell ions, and conduction electrons. We treat

the ion-ion interaction as essentially Coulombic, and treat the electron-electron and electron-ion interactions by pseudopotential perturbation theory (see Chapter 2).

In pseudopotential theory, the electrons belong to either rigid cores or conduction bands, and the conduction electron wave functions are orthogonal to the localized core states.[1] The orthogonalization transforms a one-electron 'true' wave equation with an unwieldy potential to a pseudo wave equation[2,3] which can be solved by perturbation theory to give the 'true' energy eigenvalues. We obtain a total energy H of the form

$$H = E_{KI} + \Omega(V) + \sum \phi(r;V) \quad , \tag{1.1}$$

where E_{KI} is the total kinetic energy of the ions, $\Omega(V)$ is a strictly volume-dependent potential, $\phi(r;V)$ is an effective interaction potential between two ions separated by a distance r, and the sum is over all distinct pairs of ions in the system. The detailed expressions for $\Omega(V)$ and $\phi(r;V)$ are derived in Chapter 2; the numerical evaluation of these expressions and their derivatives is discussed in Chapter 3. Note that the form of Eq. (1.1) is appropriate for finite temperature calculations, since the energy can be calculated for an arbitrary ion configuration.

For a model system of metallic sodium at P = 0 and at temperatures up to 2000 K,[4,5] we find that $\Omega(V)$ is a large negative term, responsible for most of the binding energy; this agrees with

our present understanding of metals. The total effective interaction potential is a much smaller term: for temperatures up to melting, the total effective potential comprises ~ 2% of the total potential. The effective potential is also volume dependent, which reflects the importance of screening.

In this dissertation we will use molecular dynamics to calculate stresses and elastic constants for bcc sodium for pressure $P \sim 0$ and for the temperature range 100 K - 340 K, where the melting temperature $T_m \sim 371$ K. This work is part of an ongoing project to obtain a deeper understanding of the physics of metals, including both equilibrium and nonequilibrium properties. Previous work using this model of sodium includes MD calculations of bulk thermodynamic properties for the solid[4] and fluid[5] phases, MD calculations of the P-T phase diagram,[6,7] as well as lattice dynamics calculations of bulk thermodynamic properties,[8] and static lattice calculations of the elastic constants.[9]

The project also focuses on problems inherent in computer simulations, in particular the uncertainties in calculations using MD data, and the nature of computer artifacts. Hence, the calculations of equilibrium properties of metals with a physically reasonable potential represent an effort to evaluate the usefulness of MD techniques, as well as an effort to evaluate the usefulness of pseudopotential theory.

We discuss below some general features of MD techniques. We will also trace the connection between thermodynamic variables

and MD data, and derive expressions for the stresses and adiabatic elastic constants of sodium in terms of MD time averages.

A. Molecular Dynamics Techniques

As discussed above, a molecular dynamics simulation uses a computer to solve the classical equations of motion for N particles in a box of volume V. The result is a trajectory in phase space $\{\underset{\sim}{x},\underset{\sim}{p}\}$ at discrete time steps $t = 0, \Delta t, 2\Delta t..., m\Delta t$. The output consists of mechanical quantities calculated at each time step. For computations of stresses and elastic constants, these mechanical quantities include the total kinetic energy for the particles in the box, plus derivatives with respect to position and volume of the potential. We define an MD system at time t to be the particles in the box plus the mechanical quantities associated with them. The constants of motion for such a system are N, V, H, and the total linear momentum $\underset{\sim}{M}$, where $\underset{\sim}{M} = 0$.

To integrate the equations of motion, we first write the force on a particle L as

$$\underset{\sim}{F}_L = - \nabla_{\underset{\sim}{r}_L} \sum_K' \phi(r_{KL};V) \quad , \tag{1.2}$$

where the sum is taken over all particles K within the range of the effective potential (see below). We then apply two central difference equations for each time step. For the x component of the position of particle L, we have

$$\Delta x_L(t+\Delta t/2) = x_L(t+\Delta t) - x_L(t) \quad , \tag{1.3}$$

where Δx_L is the displacement, and the corresponding velocity is

$$\frac{dx_L(t+\Delta t/2)}{dt} = \frac{\Delta x_L(t+\Delta t/2)}{\Delta t} \quad . \tag{1.4}$$

The central difference equation for the position is then

$$x_L(t+\Delta t) = x_L(t) + \Delta x_L(t+\Delta t/2) \quad . \tag{1.5}$$

For the x component of the force on particle L, we have

$$F_{xL}(t) = \frac{md^2x_L(t)}{dt^2} = \frac{m}{(\Delta t)^2}\,[(\Delta x_L(t+\Delta t/2) - \Delta x_L(t-\Delta t/2)] \quad . \tag{1.6}$$

The central difference equation for the displacement is then

$$\Delta x_L(t+\Delta t/2) = \Delta x_L(t-\Delta t/2) + \frac{F_{xL}(t)}{m}\,(\Delta t)^2 \quad . \tag{1.7}$$

Equations (1.5) and (1.7) comprise the integration algorithm. The choice of the time step Δt and the initial set of velocities and positions is discussed in Chapter 4.

To begin an MD calculation, we introduce periodic boundary conditions, where the computer program sets up a three-dimensional lattice of identical boxes with a set of N particles in each box.

The boxes are indistinguishable for all time with regard to the positions and velocities of the particles inside. We pick one box and call it the computational cell. A particle in the computational cell will have an image particle in every other cell.

With periodic boundary conditions, a particle can interact with all other particles within the range of a central pairwise potential; this allows interactions across cell boundaries. However, we need to restrict the range of the potential so that a particle cannot interact with both a second particle and the second particle's image. For a cubic computational cell with side ℓ the maximum range $r_{max} < \ell/2$.

In an actual MD calculation, we integrate the equations of motion only for the particles in the computational cell, and move each image particle along the same trajectory as its corresponding computational cell particle. If the equations of motion move a particle out of the computational cell, the particle's image moves into the cell at the opposite face. Hence, linear momentum for the computational cell will be conserved (within the limits of the integration algorithm), but angular momentum will fluctuate.

Molecular dynamics output, as discussed above, consists of a set of mechanical quantities calculated at each time step. A graph of a mechanical quantity vs time for an MD system has the appearance of a fluctuating signal which evolves to a steady state, where the steady state has a constant mean and a constant bandwidth (see Figs. 1 and 2). Different mechanical quantities evolve to the

steady state at different rates. We define an MD system to be in equilibrium with respect to a given mechanical quantity when the mean and bandwidth show no significant trend over time. Statistical procedures for determining equilibration times and for establishing confidence limits for MD time averages are given in Schiferl and Wallace;[10] an extension of these procedures for evaluating fluctuation averages is given in Chapter 4.

B. The Connection to Thermodynamics

In order to compute the elastic constants, we need to make an explicit connection between thermodynamic variables and MD equilibrium time averages. We begin by writing the Helmholtz free energy for the canonical ensemble

$$F = - kT \ell nZ \quad , \tag{1.8}$$

where Z is the canonical partition function

$$Z = \frac{1}{N! h^{3N}} \int \ldots \int e^{-\beta H} \Pi_L \, d\underset{\sim}{x}_L \, d\underset{\sim}{p}_L \quad , \tag{1.9}$$

$$\beta = (kT)^{-1} \quad , \tag{1.10}$$

and $d\underset{\sim}{x}_L$ goes over the volume V.

The stresses τ_{ij} and isothermal elastic constants C^T_{ijkl} are defined as strain derivatives of F:

$$V\tau_{ij} = \left(\frac{\partial F}{\partial \eta_{ij}}\right)_{\eta',T} \quad , \tag{1.11}$$

$$VC^{T}_{ijk\ell} = \left(\frac{\partial^2 F}{\partial \eta_{ij}\partial \eta_{k\ell}}\right)_{\eta',T} \quad , \tag{1.12}$$

where the η_{ij} are the Lagrangian strains

$$\eta_{ij} = \frac{1}{2}\left[\sum_k \alpha_{ki}\,\alpha_{kj} - \delta_{ij}\right] \quad , \tag{1.13}$$

the α_{ij} are the strain transformation coefficients, and the strain derivatives are evaluated at $\eta_{ij} = 0$.

We use the form for the total energy given in Eq. (1.1) to write

$$Z = \frac{V^N}{N!\,\lambda^{3N}}\, e^{-\beta\Omega(V)}\, \hat{Q} \quad , \tag{1.14}$$

where

$$\lambda = (2\pi\hbar^2/mkT)^{1/2} \quad , \tag{1.15}$$

and the configuration integral $\hat{Q}$ is given by

$$\hat{Q} = V^{-N} \int\cdots\int \exp[-\beta \sum \phi(r;V)]\,\Pi_L d\underset{\sim}{x}_L \quad . \tag{1.16}$$

This gives, for the strain derivatives:

$$V\tau_{ij} = - NkT \frac{\partial \ell n V}{\partial \eta_{ij}} + \frac{\partial \Omega(V)}{\partial \eta_{ij}} - \frac{kT}{\hat{Q}} \frac{\partial \hat{Q}}{\partial \eta_{ij}} \quad , \tag{1.17}$$

$$VC^{T}_{ijk\ell} = - NkT \frac{\partial^2 \ell n V}{\partial \eta_{k\ell} \partial \eta_{ij}} + \frac{\partial^2 \Omega(V)}{\partial \eta_{k\ell} \partial \eta_{ij}} - \frac{kT}{\hat{Q}} \frac{\partial^2 \hat{Q}}{\partial \eta_{k\ell} \partial \eta_{ij}}$$

$$+ \frac{kT}{\hat{Q}^2} \frac{\partial \hat{Q}}{\partial \eta_{k\ell}} \frac{\partial \hat{Q}}{\partial \eta_{ij}} \quad . \tag{1.18}$$

We evaluate the above expressions by the method given in Wallace, Schiferl and Straub.[11] If the stress is isotropic pressure, we have

$$\tau_{ij} = - P\delta_{ij} \quad , \tag{1.19}$$

and

$$PV = - \Omega^* + NkT - \langle \sum (\phi^* + \frac{1}{3} \phi') \rangle \quad , \tag{1.20}$$

where

$$\Omega^* = \frac{V \partial \Omega(V)}{\partial V} \quad , \tag{1.21}$$

$$\phi^* = V \frac{\partial \phi(r;V)}{\partial V} \quad , \tag{1.22}$$

$$\phi' = r \frac{\partial \phi(r;V)}{\partial r} \quad . \tag{1.23}$$

The sums are taken over all distinct pairs of ions within the range of the potential, and the brackets indicate ensemble averages.

For a cubic crystal, where the Cartesian indices coincide with crystal axes, we have three independent elastic constants. In Voigt notation:

$$VC_{11}^{T} = \Omega^{**} - \Omega^{*} + 2NkT + \beta\left[\langle\textstyle\sum\phi_{xx}\rangle^2 - \langle(\sum\phi_{xx})^2\rangle\right] + \langle\textstyle\sum[\phi^{**} - \phi^{*} + \frac{2}{3}\phi'^{*} + (\phi''-\phi')f_x^4]\rangle \quad , \tag{1.24}$$

$$VC_{12}^{T} = \Omega^{**} + \Omega^{*} + \beta[\langle\textstyle\sum\phi_{xx}\rangle\langle\sum\phi_{yy}\rangle - \langle\sum\phi_{xx}\sum\phi_{yy}\rangle] + \langle\textstyle\sum[\phi^{**} + \phi^{*} + \frac{2}{3}\phi'^{*} + (\phi''-\phi')f_x^2 f_y^2]\rangle \quad , \tag{1.25}$$

$$VC_{44}^{T} = -\Omega^{*} + NkT + \beta\left[\langle\textstyle\sum\phi_{xy}\rangle^2 - \langle(\sum\phi_{xy})^2\rangle\right] + \langle\textstyle\sum[-\phi^{*} + (\phi''-\phi')f_x^2 f_y^2]\rangle \quad , \tag{1.26}$$

where

$$\Omega^{**} = V^2\frac{\partial^2\Omega(V)}{\partial V^2} \quad , \tag{1.27}$$

$$\phi_{ij} = \phi^{*}\delta_{ij} + \phi' f_i f_j \quad , \tag{1.28}$$

$$\phi^{**} = V^2\frac{\partial^2\phi(r;V)}{\partial V^2} \quad , \tag{1.29}$$

$$\phi'' = r^2 \frac{\partial^2 \phi(r;V)}{\partial r^2} \quad , \tag{1.30}$$

$$\phi'^* = rV \frac{\partial^2 \phi(r;V)}{\partial r \partial V} \quad , \tag{1.31}$$

and

$$\hat{r}_i = r_i / r \quad . \tag{1.32}$$

The expressions (1.20) and (1.24)-(1.26) involve canonical ensemble averages. We now proceed to relate the canonical ensemble averages to MD ensemble averages.[12] An MD ensemble[13] is characterized by constant N, V, H, and $\underset{\sim}{M}$. The corresponding canonical ensemble has constant N and V, and a distribution of $\underset{\sim}{M}$, with $\langle \underset{\sim}{M} \rangle = 0$. The average $\langle A \rangle$ of a mechanical quantity in the two ensembles differs by relative order N^{-1}; for our MD systems, $N \sim 700$ and this difference can be ignored. In contrast, the average of a fluctuation differs by relative order 1 for the two ensembles, where a fluctuation average is defined as

$$\langle AB \rangle - \langle A \rangle \langle B \rangle \quad . \tag{1.33}$$

To relate the canonical ensemble averages to MD ensemble averages, we evaluate the ensemble differences of the fluctuation terms in Eqs. (1.24)-(1.26) by the method given in Wallace and Straub.[12] The corrections to be added to the MD ensemble averages are:

$$VC_{11}^T = VC_{11}^T(MD) + \Delta \quad , \tag{1.34}$$

$$VC_{12}^T = VC_{12}^T(MD) + \Delta \ , \tag{1.35}$$

$$VC_{44}^T = VC_{44}^T(MD) \ , \tag{1.36}$$

where

$$\Delta = - NkT \ (\gamma c-1)^2/c \ , \tag{1.37}$$

$$c = C_v/Nk \ , \tag{1.38}$$

C_v is the constant-volume heat capacity, and γ is the Grüneisen parameter.

We can obtain the adiabatic elastic constants from the relations[14]

$$VC_{11}^S - VC_{11}^T = VC_{12}^S - VC_{12}^T = NkT\gamma^2 c \ , \tag{1.39}$$

$$VC_{44}^S = VC_{44}^T \ . \tag{1.40}$$

We obtain values for C_v and γ for bcc sodium from the MD calculations of Swanson et al.[4] These bulk thermodynamic calculations and our elastic constant calculations use the same pseudopotential model.

The expressions given above for the stresses and elastic constants involve MD ensemble averages. We now relate the MD ensemble averages to the MD equilibrium time averages through the quasi-ergodic hypothesis. The hypothesis is stated by Reif[15] as

$$\langle A \rangle = \overline{A(t)} \ , \tag{1.41}$$

where $\langle A \rangle$ is an ensemble average and $\overline{A(t)}$ is an equilibrium time

average for a single system in the ensemble. The averaging time τ must be long enough so that $\overline{A(t)}$ is independent of τ.

In practice, the MD equilibrium time average is never completely independent of the averaging time. Hence, the MD time average can only be considered as an estimate of $\overline{A(t)}$ and hence as an estimate of the MD ensemble average $\langle A \rangle$. This introduces a statistical uncertainty into the ensemble averages, and for fluctuation averages this uncertainty can be very large (see Chapter 5). The calculation of these uncertainties will be discussed in Chapter 4.

CHAPTER 2

DERIVATION OF THE TOTAL ADIABATIC POTENTIAL

In the previous chapter we described the general theory we will use in our computation of the elastic constants of sodium. We will need to calculate the molecular dynamics time averages of the total energy and of its derivatives with respect to position and volume (density). In this chapter we will derive an expression for the total adiabatic potential of a system of N atoms of metallic sodium in its ground state. We will discuss the numerical evaluation of this expression and of its derivatives in Chapter 3.

We begin with a model of closed shell ions, (Z = + 1), in a compensating background charge. We first simplify this intractable many-body problem by taking the Born-Oppenheimer, or adiabatic approximation.[14] In this approximation the electrons adiabatically follow the motion of the ions.

We can write the adiabatic Hamiltonian as

$$H = E_{KI} + \Omega_{II} + E_g + NI_z \quad , \tag{2.1}$$

where E_{KI} is the kinetic energy of the ions, Ω_{II} is the ion-ion interaction energy and E_g is the ground state energy of the electrons. We include NI_z, the ionization energy of the system, in

the Hamiltonian since the zero of energy for this model of sodium is a system of neutral atoms at infinite separation.

The last three terms in the adiabatic Hamiltonian are called the total adiabatic potential Φ, where

$$\Phi = Q_{II} + E_g + NI_z \quad . \tag{2.2}$$

Our model, even with the adiabatic approximation, is still intractable. We simplify further by using a central potential model. Since the ions have closed shells, we consider them to be spherically symmetric. In addition, we will treat each interaction potential as a sum of two-body terms centered on the ion cores. Such a two-body term moves rigidly with an ion, regardless of the positions of any other ions. This eliminates many-body polarization effects on the ion cores. Also, the central potential model enables us to separate out ion position information from details of the potential due to a single ion. This separation into structure and form factors will be described below.

The use of the adiabatic approximation and the central potential model makes possible a form for the total energy suitable for molecular dynamics calculations. From the adiabatic Hamiltonian, the ion kinetic energy can be separated out and calculated at each time step by the standard molecular dynamics techniques described in Chapter 1. We are left with the sum of central potentials. Since individual molecular dynamics runs are

done at constant volume, we want to express the total adiabatic potential as a strictly volume-dependent term, plus a sum in real space of effective ion-ion potentials, $\phi(r_{KL};V)$, over all distinct pairs of ions:

$$\Phi - NI_z = \Omega(V) + \frac{1}{2} \sum_{K,L}' \phi(r_{KL};V) \quad , \tag{2.3}$$

where r_{KL} is the distance between ions K and L, and V is the volume of the system. The numerical evaluation of $\phi(r;V)$ and $\Omega(V)$ and their derivatives with respect to r and V will be done in Chapter 3.

We can write Ω_{II}, the ion-ion interaction energy, as a sum of two-body central potentials in real space. Conversely, we can write E_g, the electron ground state energy, as a sum over reciprocal space. For the purposes of molecular dynamics calculations, we want to write our entire expression for Φ in real space. Hence, we will keep Ω_{II} in its original form and transform E_g; this is the opposite of the usual procedure in lattice dynamics.

For all of these calculations we will use atomic units for length and energy. With length in Bohr radii (a_0) and energy in Rydbergs, we have

$$a_0 = \hbar^2/me^2 = 1 \quad ,$$

$$e^2/2a_0 = 1 \quad ; \; e^2 = 2 \quad , \tag{2.4}$$

where m is the mass of the electron and e is the charge of the electron. We will also take Z = 1 for the valence of sodium.

We consider an appropriate form for Ω_{II} first. We can write

$$\Omega_{II} = \frac{1}{2} \sum_{K,L}' \left[\frac{2}{r_{KL}} + \alpha_B \exp(-\gamma_B r_{KL})\right] . \qquad (2.5)$$

The first term in Eq. (2.5) is the ordinary Coulomb potential energy of two point ions. The second term is a Born-Mayer repulsive potential, and represents an empirical correction for core-core repulsion. This latter term is needed for alkali metals, since the ion cores are large, and some core overlap is possible as the ions move. The core charge distributions are still treated as rigid; overlap is not prohibited by the central potential model. α_B and γ_B are parameters.

We now consider an appropriate form for the electron ground state energy, E_g. It should be noted that molecular dynamics calculations are fundamentally classical; quantum mechanics only enters in the treatment of E_g.

The calculation of the electronic ground state energy is still an intractable many-body problem; we reduce E_g to an expression we can calculate by two approximations. First, we will write the energy as a sum over states of a one-electron Hamiltonian, minus double-counting corrections. Second, we will

solve the one-electron problem by second-order perturbation theory, where the perturbation is a local, central pseudopotential.

The perturbation theory treatment gives us the sum over states in reciprocal space and the double-counting corrections in real space. We will write the entire expression for E_g as a sum over reciprocal space to allow for cancellation of divergent terms. We then convert the sums to integrals which can be evaluated numerically, and obtain

$$E_g = \Omega(V) + \frac{1}{2} \sum_{K,L}' g(r_{KL};V) \quad , \tag{2.6}$$

where $g(r_{KL};V)$ is an integral over reciprocal space and $\Omega(V)$ is a function independent of r_{KL}. We will then show that the full expression for the total adiabatic potential per atom, Φ/N, is bounded.

We can write the one-electron wave equation as

$$h\psi_{\underset{\sim}{k}} = \varepsilon_{\underset{\sim}{k}}\psi_{\underset{\sim}{k}} \quad , \tag{2.7}$$

where the one-electron Hamiltonian is

$$h = - \nabla^2 + V_{sc}(\underset{\sim}{r}) \quad , \tag{2.8}$$

and $V_{sc}(\underset{\sim}{r})$ is a self-consistent potential. We will not solve

Eq. (2.7) explicitly. Instead, we will solve a one-electron pseudo wave equation:[2,3]

$$h_p \phi_{\underset{\sim}{k}} = \varepsilon_{\underset{\sim}{k}} \phi_{\underset{\sim}{k}} \quad , \tag{2.9}$$

where

$$h_p = - \nabla^2 + W \quad , \tag{2.10}$$

and $\phi_{\underset{\sim}{k}}$ is a pseudo wave function. The non-Hermitian operator W is a pseudopotential, where $W\phi_{\underset{\sim}{k}}$ is small compared to the free electron energy.[16,17] Equation (2.9) can be solved by second-order perturbation theory to give the same energy eigenvalues as Eq. (2.7).

From formal perturbation theory, we can write, to first order in the pseudopotential,

$$\phi_{\underset{\sim}{k}} = \sum_{\underset{\sim}{q}} A(\underset{\sim}{q},\underset{\sim}{k}) |\underset{\sim}{k} + \underset{\sim}{q}\rangle \quad , \tag{2.11}$$

where

$$|\underset{\sim}{k}\rangle = \frac{1}{\sqrt{V}} e^{i\underset{\sim}{k}\cdot\underset{\sim}{r}} \quad , \tag{2.12}$$

$$A(\underset{\sim}{q},\underset{\sim}{k}) = \langle \underset{\sim}{k}+\underset{\sim}{q} | W | \underset{\sim}{k} \rangle \, (e_{\underset{\sim}{k}} - e_{\underset{\sim}{k}+\underset{\sim}{q}})^{-1}, \; \underset{\sim}{q} \neq 0 \quad , \tag{2.13}$$

and $A(0,\underset{\sim}{k})$ is determined from a normalization condition.

To second order, we have

$$\varepsilon_{\underset{\sim}{k}} = e_{\underset{\sim}{k}} + \langle \underset{\sim}{k}|W|\underset{\sim}{k}\rangle + \sum_{\underset{\sim}{q}}{}' A(\underset{\sim}{q},\underset{\sim}{k})\langle \underset{\sim}{k}|W|\underset{\sim}{k}+\underset{\sim}{q}\rangle \quad , \tag{2.14}$$

where $e_{\underset{\sim}{k}}$ is the free electron energy.

To simplify Eqs. (2.11) and (2.14), we approximate the operator W by a local pseudopotential $W(\underset{\sim}{r})$. We then obtain for the matrix elements:

$$\langle \underset{\sim}{k}+\underset{\sim}{q}|W(\underset{\sim}{r})|\underset{\sim}{k}\rangle = \frac{1}{V}\int W(\underset{\sim}{r})e^{-i\underset{\sim}{q}\cdot\underset{\sim}{r}}d\underset{\sim}{r} = W(\underset{\sim}{q}) \quad . \tag{2.15}$$

Note that the matrix elements of $W(\underset{\sim}{r})$ are independent of $\underset{\sim}{k}$. We also obtain, to first order in $W(\underset{\sim}{r})$,[14]

$$\phi_{\underset{\sim}{k}} = \psi_{\underset{\sim}{k}} \quad . \tag{2.16}$$

We can now write, for the one-electron wave function and energy,

$$\psi_{\underset{\sim}{k}} = |\underset{\sim}{k}\rangle + \sum_{\underset{\sim}{q}}{}' W(\underset{\sim}{q})|\underset{\sim}{k}+\underset{\sim}{q}\rangle\,(e_{\underset{\sim}{k}}-e_{\underset{\sim}{k}+\underset{\sim}{q}})^{-1} \quad , \tag{2.17}$$

$$\varepsilon_{\underset{\sim}{k}} = e_{\underset{\sim}{k}} + W(\underset{\sim}{q}=0) + \sum_{\underset{\sim}{q}}{}' |W(\underset{\sim}{q})|^2\,(e_{\underset{\sim}{k}}-e_{\underset{\sim}{k}+\underset{\sim}{q}})^{-1} \quad . \tag{2.18}$$

We take the sum over states of Eq. (2.18) to obtain the electronic ground state energy:

$$E_g = \sum_{\underset{\sim}{k}} g_{\underset{\sim}{k}} e_{\underset{\sim}{k}} + NW(\underset{\sim}{q}=0) + \sum_{\underset{\sim}{q}}{}' |W(\underset{\sim}{q})|^2 \sum_{\underset{\sim}{k}} g_{\underset{\sim}{k}} (e_{\underset{\sim}{k}} - e_{\underset{\sim}{k}+\underset{\sim}{q}})^{-1}$$
$$- \text{(double-counting corrections)}, \qquad (2.19)$$

where $g_{\underset{\sim}{k}}$ is the ground state occupation number and N is the number of conduction electrons.

We calculate the zeroth-order term in E_g first, where the sum over $\underset{\sim}{k}$ is taken up to the Fermi surface. To zeroth order, the Fermi surface is a sphere in reciprocal space with radius k_f, where $\underset{\sim}{k}_f$ is the Fermi wave vector, and with all states within the sphere occupied. Wallace[14] and Harrison[3] show that the total ground state conduction electron kinetic energy, correct to second order in the pseudopotential, is equal to the total ground state free electron energy. This can be understood by considering that the distortion of the Fermi sphere is second order, and the energy change of an electron moving from inside to outside the original Fermi sphere is of higher order than zero.

We find the Fermi wave vector, $\underset{\sim}{k}_f$, by requiring all states in reciprocal space to be filled up to the surface of the Fermi sphere. We have N conduction electrons and hence N states in a volume V. Hence,

$$N = \sum_{\underset{\sim}{k}} g_{\underset{\sim}{k}} = \frac{2V}{(2\pi)^3} \int_0^{k_f} k^2 dk \int d\Omega \quad , \qquad (2.20)$$

where $\int d\Omega$ is the angular integral, $V/(2\pi)^3$ is the density of states

in reciprocal space, and the factor of 2 indicates two electrons of opposite spin per state. This gives

$$k_f = \left(\frac{3\pi^2}{V_a}\right)^{1/3} , \tag{2.21}$$

where

$$V_a = V/N = \text{volume per atom} . \tag{2.22}$$

We calculate the zeroth-order term by converting the sum over $\underset{\sim}{k}$ to an integral over the Fermi sphere, as in Eq. (2.20), and by taking $e_k = k^2$ in atomic units. This gives

$$\sum_{\underset{\sim}{k}} g_{\underset{\sim}{k}} e_{\underset{\sim}{k}} = \frac{2V}{(2\pi)^3} \int_0^{k_f} k^4 dk \int d\Omega = \frac{3}{5} N e_f , \tag{2.23}$$

where e_f is the Fermi energy, and

$$e_f = k_f^2 . \tag{2.24}$$

To determine the first and second order terms and the double-counting corrections, we take the form of the one-electron pseudopotential $W(\underset{\sim}{r})$ to be the sum of three local central potentials:

$$W(\underset{\sim}{r}) = W_B(\underset{\sim}{r}) + W_S(\underset{\sim}{r}) + W_X(\underset{\sim}{r}) , \tag{2.25}$$

where $W_B(\underset{\sim}{r})$ is a model bare-ion potential, consisting of the electron-ion potential from unscreened closed shell ions. $W_S(\underset{\sim}{r})$ is a self-consistent screening potential, involving Coulomb interactions among the electrons. $W_X(\underset{\sim}{r})$ is a one-electron approximation for exchange and correlation effects, and is only dependent on the density of conduction electrons.

This form allows two further simplifications. First, since each of the three parts of the pseudopotential is a sum of two-body central potentials, we can factor $W(\underset{\sim}{q})$, or any of its three components, into two parts: a) a structure factor, $S(\underset{\sim}{q})$, a function only of ion positions, and b) a form factor, $w(q)$, or $w_B(q)$, etc., a function only of the details of a single-ion potential, independent of ion positions.

We show this factoring explicitly with $W_B(\underset{\sim}{r})$. We can write the bare-ion potential as

$$W_B(\underset{\sim}{r}) = \sum_{L=1}^{N} w_B(|\underset{\sim}{r}-\underset{\sim}{R}_L|) \quad , \tag{2.26}$$

where $\underset{\sim}{R}_L$ is the position of the Lth ion. The Fourier components are

$$W_B(\underset{\sim}{q}) = \sum_{L=1}^{N} \frac{1}{V} \int \exp(-i\underset{\sim}{q}\cdot\underset{\sim}{r}) w_B(|\underset{\sim}{r}-\underset{\sim}{R}_L|)\, d\underset{\sim}{r}$$

$$= \frac{1}{N} \sum_{L=1}^{N} \exp(-i\underset{\sim}{q}\cdot\underset{\sim}{R}_L) \frac{1}{V_a} \int \exp[-i\underset{\sim}{q}\cdot(\underset{\sim}{r}-\underset{\sim}{R}_L)] w_B(|\underset{\sim}{r}-\underset{\sim}{R}_L|) d\underset{\sim}{r} \quad . \tag{2.27}$$

Since $\underset{\sim}{r}$ is independent of $\underset{\sim}{R}_L$, we can treat $(\underset{\sim}{r}-\underset{\sim}{R}_L)$ in the integrand as a dummy variable, and we can write

$$W_B(\underset{\sim}{q}) = S(\underset{\sim}{q})w_B(q) \quad , \tag{2.28}$$

where

$$S(\underset{\sim}{q}) = \frac{1}{N}\sum_{L=1}^{N}\exp(-i\underset{\sim}{q}\cdot\underset{\sim}{R}_L) \quad , \tag{2.29}$$

and

$$w_B(q) = \frac{1}{V_a}\int \exp(-i\underset{\sim}{q}\cdot\underset{\sim}{r})w_B(r)d\underset{\sim}{r} \quad . \tag{2.30}$$

Note that the form factor, $w_B(q)$, is dependent only on the magnitude of $\underset{\sim}{q}$.

For the second simplification, with $W_S(\underset{\sim}{r})$ and $W_X(\underset{\sim}{r})$ as described, we can relate the Fourier components $W_S(\underset{\sim}{q})$ and $W_X(\underset{\sim}{q})$ to the Fourier component of the total pseudopotential, $W(\underset{\sim}{q})$, and hence we can relate $W(\underset{\sim}{q})$ to $W_B(\underset{\sim}{q})$. Since we can factor out $S(\underset{\sim}{q})$ from $W_B(\underset{\sim}{q})$, we can write $W(\underset{\sim}{q})$ in terms of the model form factor, $w_B(q)$, and the structure factor.

We now consider each of the three parts of the pseudopotential in detail.

A. $W_B(\underset{\sim}{r})$, Bare-ion Potential

We take the one-electron potential, $W_B(\underset{\sim}{r})$, to be the sum of the interactions of one electron with all the ions, independent of

the presence of any other electrons. We calculate the form factor, $w_B(q)$, from a single-ion model potential, $w_B(r)$:

$$w_B(r) = w_z(r) + w_c(r) \quad , \tag{2.31}$$

where $w_z(r)$ is the Coulomb potential energy of an electron at a distance r from a point ion with charge Z = + 1, and $w_c(r)$ is a term, negligible outside the ion core, which cancels the Coulomb contribution inside the core. Harrison[3] takes the core term, $w_c(r)$, to be proportional to a 1s electron wave function, $\alpha\exp(-r/\rho)$, where ρ is a positive parameter. The single-ion potential then becomes

$$w_B(r) = -2/r + \alpha\exp(-r/\rho) \quad , \tag{2.32}$$

with Fourier components

$$w_B(q) = \frac{1}{V_a}\int \frac{-2}{r}\exp(-i\underset{\sim}{q}\cdot\underset{\sim}{r})d\underset{\sim}{r} + \frac{1}{V_a}\int\alpha\exp(-r/\rho)\exp(-i\underset{\sim}{q}\cdot\underset{\sim}{r})d\underset{\sim}{r} \quad . \tag{2.33}$$

For the first integral in Eq. (2.33), we introduce a convergence factor δ, to give

$$w_z(q) = \lim_{\delta\to 0}\frac{1}{V_a}\int\frac{-2}{r}\exp(-\delta r)\exp(-i\underset{\sim}{q}\cdot\underset{\sim}{r})d\underset{\sim}{r} = \lim_{\delta\to 0}\frac{1}{V_a}\frac{-8\pi}{q^2+\delta^2}$$

$$= \frac{-8\pi}{V_a q^2} \quad , \; q \neq 0 \quad . \tag{2.34}$$

For the second integral, we obtain

$$w_c(q) = \frac{8\pi\alpha\rho^3}{V_a(1+q^2\rho^2)^2} \quad . \tag{2.35}$$

This can be written as

$$w_c(q) = \frac{\beta}{V_a} \frac{1}{(1+q^2\rho^2)^2} \quad , \tag{2.36}$$

where β and ρ are positive, and will be treated as adjustable parameters.

Hence, we can write the bare-ion form factor as

$$w_B(q) = \frac{1}{V_a} \left[\frac{-8\pi}{q^2} + \frac{\beta}{(1+q^2\rho^2)^2}\right] \quad , \; q \neq 0 \quad , \tag{2.37}$$

and

$$w_c(q = 0) = \beta/V_a. \tag{2.38}$$

The Fourier component of the Coulomb term, $w_z(q)$, diverges as $q \to 0$. We will show the cancellation of such divergent terms when we write the full expression for E_g.

B. $W_S(\underline{r})$, Screening Potential

We take the one-electron screening potential, $W_S(\underline{r})$, to be the ordinary electron-electron Coulomb potential energy:

$$W_S(\underset{\sim}{r}) = \int \frac{2}{|\underset{\sim}{r}-\underset{\sim}{r}'|} \rho(\underset{\sim}{r}')d\underset{\sim}{r}' \quad , \tag{2.39}$$

where $\rho(\underset{\sim}{r})$ is the number density of conduction electrons, and

$$\rho(\underset{\sim}{r}) = \sum_{\underset{\sim}{k}} g_{\underset{\sim}{k}} \phi^*_{\underset{\sim}{k}}(\underset{\sim}{r})\phi_{\underset{\sim}{k}}(\underset{\sim}{r}) \quad . \tag{2.40}$$

This potential is determined self-consistently, in the sense that the electron density depends on the eigenfunctions $\phi_{\underset{\sim}{k}}$ of the entire one-electron Hamiltonian.

Note that when we sum over all states, we count the Coulomb energy of each pair of electrons twice; this is the source of the first double-counting correction. Hence, we can write

$$E_g = \{\sum_{\underset{\sim}{k}} g_{\underset{\sim}{k}} \int \phi^*_{\underset{\sim}{k}}(\underset{\sim}{r}) \left[e_{\underset{\sim}{k}} + W_B(\underset{\sim}{r}) + W_S(\underset{\sim}{r}) + W_X(\underset{\sim}{r}) - \frac{1}{2} W_S(\underset{\sim}{r})\right] \phi_{\underset{\sim}{k}}(\underset{\sim}{r})d\underset{\sim}{r}\} - (\text{other double-counting corrections}) \quad . \tag{2.41}$$

If we compare this to Eq. (2.18) for $\varepsilon_{\underset{\sim}{k}}$, and use Eq. (2.40) for $\rho(\underset{\sim}{r})$, we get

$$E_g = \sum_{\underset{\sim}{k}} g_{\underset{\sim}{k}}\varepsilon_{\underset{\sim}{k}} - \frac{1}{2} \int \rho(\underset{\sim}{r})W_S(\underset{\sim}{r})d\underset{\sim}{r} - (\text{other double-counting corrections}) \quad , \tag{2.42}$$

and the first double-counting correction is therefore

$$\frac{1}{2}\int \rho(\underset{\sim}{r})W_S(\underset{\sim}{r})d\underset{\sim}{r} \quad . \tag{2.43}$$

We are also counting the Coulomb energy of each electron in its own potential field. This self-energy per electron is of the order 1/N of the total Coulomb energy per electron, and can be ignored for large N.

The Fourier components of $W_S(\underset{\sim}{r})$ are

$$W_S(\underset{\sim}{q}) = \frac{1}{V}\int W_S(\underset{\sim}{r})\exp(-i\underset{\sim}{q}\cdot\underset{\sim}{r})d\underset{\sim}{r}$$

$$= \frac{1}{V}\int \frac{2}{|\underset{\sim}{r}-\underset{\sim}{r}'|}\exp[-i\underset{\sim}{q}\cdot(\underset{\sim}{r}-\underset{\sim}{r}')]\rho(\underset{\sim}{r}')\exp(-i\underset{\sim}{q}\cdot\underset{\sim}{r}')d\underset{\sim}{r}d\underset{\sim}{r}' \quad . \tag{2.44}$$

Since $\underset{\sim}{r}'$ and $\underset{\sim}{r}$ are independent, $(\underset{\sim}{r}-\underset{\sim}{r}')$ becomes a dummy variable, and we can write

$$W_S(\underset{\sim}{q}) = \frac{1}{V}\int \rho(\underset{\sim}{r}')\exp(-i\underset{\sim}{q}\cdot\underset{\sim}{r}')d\underset{\sim}{r}' \int \frac{2}{r}\exp(-i\underset{\sim}{q}\cdot\underset{\sim}{r})d\underset{\sim}{r}$$

$$= \rho(\underset{\sim}{q}) \int \frac{2}{r}\exp(-i\underset{\sim}{q}\cdot\underset{\sim}{r})d\underset{\sim}{r} \quad . \tag{2.45}$$

From Eq. (2.34) we then obtain

$$W_S(\underset{\sim}{q}) = \frac{8\pi}{q^2}\rho(\underset{\sim}{q}) \quad , \underset{\sim}{q} \neq 0 \quad , \tag{2.46}$$

where the Fourier components of the screening term, $W_S(\underset{\sim}{q})$, diverge

as $\underset{\sim}{q} \to 0$. We will discuss the removal of this divergent part when we write the full expression for E_g.

We can evaluate $\rho(\underset{\sim}{q})$, and hence find $W_S(\underset{\sim}{q})$ in terms of $W(\underset{\sim}{q})$, by writing $\rho(\underset{\sim}{r})$ to first order in the pseudopotential and taking its Fourier components. From Eq. (2.40) for $\rho(\underset{\sim}{r})$ and Eq. (2.17) for $\phi_{\underset{\sim}{k}}(\underset{\sim}{r})$, we get

$$\rho(\underset{\sim}{r}) = \sum_{\underset{\sim}{k}} g_{\underset{\sim}{k}} \left[\langle \underset{\sim}{k}| + \sum_{\underset{\sim}{q}}{}' \frac{\langle \underset{\sim}{k}+\underset{\sim}{q}|W^*(\underset{\sim}{q})}{(e_{\underset{\sim}{k}}-e_{\underset{\sim}{k}+\underset{\sim}{q}})}\right]\left[|\underset{\sim}{k}\rangle + \sum_{\underset{\sim}{q}}{}' \frac{W(\underset{\sim}{q})|\underset{\sim}{k}+\underset{\sim}{q}\rangle}{(e_{\underset{\sim}{k}}-e_{\underset{\sim}{k}+\underset{\sim}{q}})}\right]$$

$$= \frac{1}{V} \sum_{\underset{\sim}{k}} g_{\underset{\sim}{k}} \{1 + \sum_{\underset{\sim}{q}}{}' [(\exp(-i\underset{\sim}{q}\cdot\underset{\sim}{r})W^*(\underset{\sim}{q})$$

$$+ \exp(i\underset{\sim}{q}\cdot\underset{\sim}{r})W(\underset{\sim}{q}))(e_{\underset{\sim}{k}}-e_{\underset{\sim}{k}+\underset{\sim}{q}})^{-1}]\} \quad . \tag{2.47}$$

For the terms of first order in $W(\underset{\sim}{q})$, we take the sum over the zeroth-order Fermi sphere, giving $g_{\underset{\sim}{k}} = g_{-\underset{\sim}{k}}$. From Eq. (2.15), we have $W^*(\underset{\sim}{q}) = W(-\underset{\sim}{q})$. Hence, for $\underset{\sim}{q} \to -\underset{\sim}{q}$ and $\underset{\sim}{k} \to -\underset{\sim}{k}$, we have

$$g_{\underset{\sim}{k}} [(\exp(-i\underset{\sim}{q}\cdot\underset{\sim}{r})W^*(\underset{\sim}{q})+\exp(i\underset{\sim}{q}\cdot\underset{\sim}{r})W(\underset{\sim}{q}))(e_{\underset{\sim}{k}}-e_{\underset{\sim}{k}+\underset{\sim}{q}})^{-1}]$$

$$= g_{-\underset{\sim}{k}} [(\exp(i\underset{\sim}{q}\cdot\underset{\sim}{r})W(\underset{\sim}{q})+\exp(-i\underset{\sim}{q}\cdot\underset{\sim}{r})W^*(\underset{\sim}{q}))(e_{-\underset{\sim}{k}}-e_{-\underset{\sim}{k}-\underset{\sim}{q}})^{-1}] \quad . \tag{2.48}$$

We can then write

$$\rho(\underset{\sim}{r}) = \frac{1}{V} \sum_{\underset{\sim}{k}} g_{\underset{\sim}{k}} + \frac{2}{V} \sum_{\underset{\sim}{q}}{}' \exp(i\underset{\sim}{q}\cdot\underset{\sim}{r})W(\underset{\sim}{q}) \sum_{\underset{\sim}{k}} g_{\underset{\sim}{k}}(e_{\underset{\sim}{k}}-e_{\underset{\sim}{k}+\underset{\sim}{q}})^{-1} \quad . \tag{2.49}$$

We can write down the Fourier components $\rho(\underset{\sim}{q})$ by inspection, since $\rho(\underset{\sim}{r}) = \sum_{\underset{\sim}{q}} \rho(\underset{\sim}{q})\exp(i\underset{\sim}{q}\cdot\underset{\sim}{r})$. Hence,

$$\rho(\underset{\sim}{q}=0) = N/V = 1/V_a \quad , \tag{2.50}$$

and

$$\rho(\underset{\sim}{q}) = \frac{2}{V} W(\underset{\sim}{q}) \sum_{\underset{\sim}{k}} g_{\underset{\sim}{k}}(e_{\underset{\sim}{k}}-e_{\underset{\sim}{k}+\underset{\sim}{q}})^{-1} \quad , \underset{\sim}{q} \neq 0 \quad . \tag{2.51}$$

Since $\rho(\underset{\sim}{q})$ is of first order in the pseudopotential for $\underset{\sim}{q} \neq 0$, and distortions of the Fermi surface are of second order, we take the states $\underset{\sim}{k}$ over the Fermi sphere, as in Eq. (2.23). We then convert the sum over $\underset{\sim}{k}$ to an integral:

$$\sum_{\underset{\sim}{k}} g_{\underset{\sim}{k}}(e_{\underset{\sim}{k}}-e_{\underset{\sim}{k}+\underset{\sim}{q}})^{-1} = \frac{2V}{(2\pi)^3} \int_0^{k_f} \int_0^{\pi} \int_0^{2\pi} \frac{-k^2 \sin\theta \, dk d\theta d\phi}{(q^2 + 2qk\cos\theta)}$$

$$= \frac{-2V}{(2\pi)^2} \int_0^{k_f} k^2 dk \int_{-1}^{1} \frac{dx}{(q^2+2qkx)} \quad . \tag{2.52}$$

There is a singularity in the integrand if

$$\frac{\underset{\sim}{k}\cdot\underset{\sim}{q}}{q} = k\cos\theta = -q/2 \quad . \tag{2.53}$$

This is handled by taking the principal values in the region of the singularity. The limits of integration for x then become

$[-1, -q/2k_f - \delta]$ and $[-q/2k_f + \delta, 1]$. In the limit $\delta \to 0$, this gives

$$\frac{-V}{(2\pi)^2 q} \int_0^{k_f} k \ln\left|\frac{q+2k}{q-2k}\right| dk = \frac{-V}{8\pi^2} k_f \left[\frac{1-\eta^2}{2\eta} \ln\left|\frac{1+\eta}{1-\eta}\right| + 1\right] \quad , (2.54)$$

where $\eta = q/2k_f$. (2.55)

We can therefore write the sum over $\underset{\sim}{k}$ as

$$\sum_{\underset{\sim}{k}} g_{\underset{\sim}{k}} (e_{\underset{\sim}{k}} - e_{\underset{\sim}{k}+\underset{\sim}{q}})^{-1} = \frac{q^2 V}{16\pi} (1-\varepsilon(q)) \quad , \quad (2.56)$$

where $\varepsilon(q)$ is the static Hartree dielectric function for free electrons, and is given by

$$\varepsilon(q) = 1 + \frac{2k_f}{\pi q^2} \left[\frac{1-\eta^2}{2\eta} \ln\left|\frac{1+\eta}{1-\eta}\right| + 1\right] \quad . \quad (2.57)$$

The dielectric function has a singularity at $\eta = 1$ $(q=2k_f)$, caused by the sharp cutoff of screening at the Fermi sphere. The function itself is continuous at $\eta = 1$, since

$$\lim_{\eta \to 1} \left(\frac{1-\eta^2}{2\eta} \ln\left|\frac{1+\eta}{1-\eta}\right|\right) = 0 \quad , \quad (2.58)$$

but all of the derivatives of the dielectric function with respect to q and to k_f (and hence with respect to volume) diverge at $\eta = 1$.

It is the existence of these singularities that will give Friedel oscillations in the potential at large r, as discussed below.

The leading terms in the small-q expansion of $\varepsilon(q)$ are

$$\varepsilon(q) - 1 = \frac{4k_f}{\pi q^2} - \frac{1}{3\pi k_f} \quad . \tag{2.59}$$

The dielectric function diverges as $q \to 0$. This is characteristic of metals, where long-wavelength components of the potential are well screened.

The leading terms in the large-q expansion of $\varepsilon(q) - 1$ are

$$\varepsilon(q) - 1 = \frac{16k_f^3}{3\pi q^4} + \frac{64k_f^5}{15\pi q^6} \quad . \tag{2.60}$$

Hence, short-wavelength components are poorly screened.

We can now write $\rho(\underline{q})$ and $W_S(\underline{q})$ in terms of $W(\underline{q})$. From Eqs. (2.51) and (2.56), we obtain

$$\rho(\underline{q}) = \frac{q^2}{8\pi} W(\underline{q})(1-\varepsilon(q)) \quad , \ \underline{q} \neq 0 \quad , \tag{2.61}$$

and from Eqs. (2.46) and (2.61), we obtain

$$W_S(\underline{q}) = W(\underline{q})(1-\varepsilon(q)) \quad , \ \underline{q} \neq 0 \quad . \tag{2.62}$$

We can also rewrite the first double-counting correction, Eq. (2.43), as a Fourier sum:

$$\frac{1}{2}\int \rho(\underset{\sim}{r})\, W_S(\underset{\sim}{r})d\underset{\sim}{r} = \frac{V}{2}\sum_{\underset{\sim}{q}} \rho(\underset{\sim}{q})W_S(-\underset{\sim}{q}) \quad , \tag{2.63}$$

where the divergent $\underset{\sim}{q} = 0$ term is included in the sum.

C. $W_X(\underset{\sim}{r})$, Exchange and Correlation Potential

We approximate exchange and correlation contributions to the energy of the system by a local potential, $X(\underset{\sim}{r})$, which depends only on the density of conduction electrons. Although local potentials must be explicitly spin-independent, this is a plausible form for an interaction between electrons with parallel spins, since the density of conduction electrons with each spin is $\rho(\underset{\sim}{r})/2$. The one-electron exchange and correlation potential $W_X(\underset{\sim}{r})$ and the associated double-counting correction can be written as functions of $X(\underset{\sim}{r})$ and $\rho(\underset{\sim}{r})$.

To determine the "best" one-electron wave equation and the exchange and correlation double-counting correction, Wallace[14] uses a variational calculation, which minimizes the ground state energy E_g with regard to variation of the one-electron wave functions $\psi_{\underset{\sim}{k}}(\underset{\sim}{r})$, where

$$E_g = \sum_{\underset{\sim}{k}} g_{\underset{\sim}{k}} \int \psi^*_{\underset{\sim}{k}}(\underset{\sim}{r})[e_{\underset{\sim}{k}}+W_B(\underset{\sim}{r}) + \frac{1}{2} W_S(\underset{\sim}{r}) + X(\underset{\sim}{r})]\psi_{\underset{\sim}{k}}(\underset{\sim}{r})d\underset{\sim}{r} \quad . \tag{2.64}$$

Note that the double-counting correction of the screening potential $W_S(\underset{\sim}{r})$ has been included here.

The results of the variational calculation give

$$W_X(\underset{\sim}{r}) = \frac{\partial}{\partial\rho(\underset{\sim}{r})}\,(\rho(\underset{\sim}{r})X(\underset{\sim}{r})) = \rho(\underset{\sim}{r})\,\frac{\partial X(\underset{\sim}{r})}{\partial\rho(\underset{\sim}{r})} + X(\underset{\sim}{r}) \quad . \tag{2.65}$$

The sum over states of the one-electron energies, minus the double-counting corrections, can now be written

$$E_g = \sum_{\underset{\sim}{k}} g_{\underset{\sim}{k}} \int \phi^*_{\underset{\sim}{k}}(\underset{\sim}{r})[e_{\underset{\sim}{k}} + W_B(\underset{\sim}{r}) + W_S(\underset{\sim}{r}) + W_X(\underset{\sim}{r}) - (\tfrac{1}{2}\,W_S(\underset{\sim}{r}) + W_X(\underset{\sim}{r}) - X(\underset{\sim}{r}))]\phi_{\underset{\sim}{k}}(\underset{\sim}{r})d\underset{\sim}{r} \quad . \tag{2.66}$$

In effect, we subtract a second double-counting correction, where this exchange and correlation correction is

$$\sum_{\underset{\sim}{k}} g_{\underset{\sim}{k}} \int \phi^*_{\underset{\sim}{k}}(\underset{\sim}{r})\phi_{\underset{\sim}{k}}(\underset{\sim}{r})(W_X(\underset{\sim}{r}) - X(\underset{\sim}{r}))d\underset{\sim}{r} = \int \rho(\underset{\sim}{r})(W_X(\underset{\sim}{r}) - X(\underset{\sim}{r}))d\underset{\sim}{r} \quad . \tag{2.67}$$

We will write this integral as a Fourier sum later.

In order to write $W_X(\underset{\sim}{q})$ in terms of $W(\underset{\sim}{q})$, we must consider that we have no explicit form for the Fourier components $X(\underset{\sim}{q})$, except for the many-body result at $\underset{\sim}{q} = 0$. At $\underset{\sim}{q} = 0$, $X(\underset{\sim}{q}) = X(\rho_0)$, the exchange and correlation energy per electron of a uniform electron gas. For the limit of $W_X(\underset{\sim}{q})$ as $\underset{\sim}{q} \to \infty$, Hubbard[18] argues

that the effect of exchange and correlation is to cancel half of the screening. We use these results to write an interpolation approximation for $W_X(\underset{\sim}{q})$, of first order in the pseudopotential:

$$W_X(\underset{\sim}{q}) = - Y(q)W_S(\underset{\sim}{q}) \quad , \ \underset{\sim}{q} \neq 0 \quad , \tag{2.68}$$

where

$$Y(q) = \frac{q^2}{2(q^2 + \xi k_f^2)} \quad . \tag{2.69}$$

The parameter ξ is chosen to give the proper behavior for $Y(q)$ in the limit as $q \to 0$.

To find ξ in terms of $X(\rho_0)$, we expand $W_X(\underset{\sim}{r})$ in powers of the pseudopotential around the uniform component of the conduction electron density $\rho_0 = \rho(\underset{\sim}{q} = 0)$, Eq. (2.50). The expansion of $W_X(\underset{\sim}{r})$ is done through an expansion of the density $\rho(\underset{\sim}{r})$ in powers of the pseudopotential. To second order in the pseudopotential, we can write

$$\rho(\underset{\sim}{r}) = \rho_0 + \rho_1 + \rho_2 \quad , \tag{2.70}$$

where

$$\rho_1 = \sum_{\underset{\sim}{g}}{}' \rho(\underset{\sim}{g})\exp(i\underset{\sim}{g}\cdot\underset{\sim}{r}) \quad , \tag{2.71}$$

and $\rho(\underset{\sim}{q})$ is given by Eq. (2.51). The explicit form of the second

order term, ρ_2, will not be needed. Derivatives with respect to $\rho(\underset{\sim}{r})$ are evaluated at ρ_0.

For simplicity, we can drop the r-dependent notation. We have, to first order,

$$W_X = W_X(\rho_0) + \rho_1 W_X'$$

$$= W_X(\rho_0) + \sum_{\underset{\sim}{q}}' \left[\frac{\partial^2(\rho X)}{\partial \rho^2}\right]_{\rho_0} \rho(\underset{\sim}{q}) \exp(i\underset{\sim}{q}\cdot\underset{\sim}{r}) \quad . \tag{2.72}$$

We then equate the corresponding Fourier components in the expansion and in the interpolation approximation:

$$\left[\frac{\partial^2(\rho X)}{\partial \rho^2}\right]_{\rho_0} \rho(\underset{\sim}{q}) = - Y(q) W_S(\underset{\sim}{q}) \quad . \tag{2.73}$$

We then take the limit as $\underset{\sim}{q} \to 0$ to give the defining equation for ξ:

$$\frac{\partial^2[\rho_0 X(\rho_0)]}{\partial \rho_0^2} = \lim_{q \to 0} \left[\frac{-q^2}{2(q^2 + \xi k_f^2)} \frac{8\pi}{q^2}\right] = \frac{-4\pi}{\xi k_f^2} \quad . \tag{2.74}$$

For a uniform electron gas, the exchange and correlation energy per electron can be written as

$$X(\rho_0) = \frac{-3}{2} \left(\frac{3\rho_0}{\pi}\right)^{1/3} + (-0.115 + 0.031 \ln r_s) \quad , \tag{2.75}$$

where the first term is the exchange energy[19] and the second term

is the correlation energy. The correlation energy is obtained from an interpolation by Pines and Nozières[20] for metallic densities, and

$$\frac{4}{3}\pi r_s^3 = 1/\rho_0 \quad . \tag{2.76}$$

By combining Eqs. (2.74) and (2.75), we obtain

$$\xi = 2/(1 + 0.0155\pi/k_f) \quad . \tag{2.77}$$

Finally, writing $W_X(\underset{\sim}{q})$ in terms of $W(\underset{\sim}{q})$, we have

$$W_X(\underset{\sim}{q}) = - Y(q)W(\underset{\sim}{q})[1-\varepsilon(q)] \quad . \tag{2.78}$$

We can express the exchange and correlation double-counting correction, Eq. (2.67), as a Fourier sum of known functions of $W(\underset{\sim}{q})$, by expanding the integrand in powers of the pseudopotential, as in Eqs. (2.70) through (2.72). We obtain, to second order in the pseudopotential,

$$\begin{aligned}\int \rho(W_X - X)d\underset{\sim}{r} &= \int [\rho_0(W_X(\rho_0) - X(\rho_0)) + (\rho_1+\rho_2)\rho_0 W_X' \\ &\quad + \frac{1}{2}\rho_1^2(\rho_0 W_X'' + W_X')]d\underset{\sim}{r} \\ &= \int \rho_0[W_X(\rho_0) - X(\rho_0]d\underset{\sim}{r} + \int \rho_0(W_{X1} + W_{X2})d\underset{\sim}{r} \\ &\quad + \int \frac{1}{2}\rho_1 W_{X1} d\underset{\sim}{r} \quad ,\end{aligned} \tag{2.79}$$

where W_{X1} and W_{X2} are the first and second-order terms in the expansion of $W_X(\underset{\sim}{r})$.

The first integral in Eq. (2.79) can be written

$$\rho_0 V[W_X(\underset{\sim}{q}=0) - X(\rho_0)] \quad . \tag{2.80}$$

The second integral in Eq. (2.79) vanishes:

$$\rho_0 \int (W_{X1}+W_{X2})d\underset{\sim}{r} = \rho_0 \sum_{\underset{\sim}{q}}' (W_{X1}(\underset{\sim}{q})+W_{X2}(\underset{\sim}{q})) \int \exp(i\underset{\sim}{q}\cdot\underset{\sim}{r})d\underset{\sim}{r} = 0 \quad . \tag{2.81}$$

The third integral can be written as a nonvanishing Fourier sum:

$$\frac{1}{2} \int \rho_1 W_{X1} d\underset{\sim}{r} = \frac{V}{2} \sum_{\underset{\sim}{q}}' \rho(\underset{\sim}{q}) W_X(-\underset{\sim}{q}) \quad . \tag{2.82}$$

Hence, we can write the total exchange and correlation double-counting correction as

$$N(W_X(\underset{\sim}{q}=0) - X(\rho_0)) + \frac{V}{2} \sum_{\underset{\sim}{q}}' \rho(\underset{\sim}{q}) W_X(-\underset{\sim}{q}) \quad , \tag{2.83}$$

correct to second order in the pseudopotential.

D. E_g, Electron Ground State Energy

We can now write the full expression for E_g, correct to second order in the pseudopotential. If we rewrite Eq. (2.19), using Eqs. (2.63) and (2.83) for the double-counting corrections,

Eq. (2.23) for the first sum over $\underset{\sim}{k}$, and Eq. (2.56) for the second sum over $\underset{\sim}{k}$, we obtain

$$E_g = N \left(\frac{3}{5} e_f + W(\underset{\sim}{q}=0) - W_X(\underset{\sim}{q}=0) + X(\rho_0)\right)$$

$$+ \frac{V}{2} \sum_{\underset{\sim}{q}}' W(\underset{\sim}{q})W(-\underset{\sim}{q}) \frac{q^2}{8\pi} (1-\varepsilon(q)) - \frac{V}{2} \sum_{\underset{\sim}{q}}' \rho(\underset{\sim}{q})W_X(-\underset{\sim}{q})$$

$$- \frac{V}{2} \sum_{\underset{\sim}{k}} \rho(\underset{\sim}{q})W_S(-\underset{\sim}{q}) \quad . \tag{2.84}$$

We then rewrite the first sum in Eq. (2.84):

$$\frac{V}{2} \sum_{\underset{\sim}{q}}' W(\underset{\sim}{q})W(-\underset{\sim}{q}) \frac{q^2}{8\pi} (1-\varepsilon(q)) = \frac{V}{2} \sum_{\underset{\sim}{q}}' \rho(\underset{\sim}{q})W(-\underset{\sim}{q}) \quad . \tag{2.85}$$

When we transform to real space, we will want to convert these sums to integrals. We begin by adding and subtracting the limits as $\underset{\sim}{q} \to 0$:

$$E_g = N \left[\frac{3}{5} e_f + X(\rho_0) + W(\underset{\sim}{q}=0) - W_X(\underset{\sim}{q}=0)\right.$$

$$\left. - \frac{1}{2} \lim_{\underset{\sim}{q}\to 0} (W(\underset{\sim}{q}) - W_X(\underset{\sim}{q}))\right] + \frac{V}{2} \sum_{\underset{\sim}{q}} \rho(\underset{\sim}{q})W_B(-\underset{\sim}{q}) \quad . \tag{2.86}$$

We can use Eqs. (2.62) and (2.78) to write $W(\underset{\sim}{q})$ in terms of $W_B(\underset{\sim}{q})$:

$$W(\underset{\sim}{q}) = \frac{W_B(\underset{\sim}{q})}{1 + (\varepsilon(q)-1)\ (1 - Y(q))} \quad . \tag{2.87}$$

We can use Eqs. (2.61) and (2.87) to write $\rho(\underset{\sim}{q})$ in terms of $W_B(\underset{\sim}{q})$. We then separate $W_B(\underset{\sim}{q})$ and $W_B(-\underset{\sim}{q})$ into structure and form factors:

$$E_g = N\left(\frac{3}{5}e_f + X(\rho_0)\right) + N\sum_{\underset{\sim}{q}} S(\underset{\sim}{q})S(-\underset{\sim}{q})F(q) + NS(\underset{\sim}{q}=0)$$

$$\times \left[w_B(q=0) + w_S(q=0) - \frac{1}{2}\lim_{\underset{\sim}{q}\to 0}\left(w_B(\underset{\sim}{q}) + w_S(\underset{\sim}{q})\right)\right] , \quad (2.88)$$

where

$$F(q) = \frac{-V_a q^2 |w_B(q)|^2\,(\varepsilon(q)-1)}{16\pi[1 + (\varepsilon(q)-1)(1-Y(q))]} . \quad (2.89)$$

We evaluate the structure factors from Eq. (2.29):

$$S(\underset{\sim}{q}=0) = \frac{1}{N}\sum_{L=1}^{N} 1 = 1 , \quad (2.90)$$

$$S(\underset{\sim}{q})S(-\underset{\sim}{q}) = \frac{1}{N^2}\sum_{K,L}{}' \exp[i\underset{\sim}{q}\cdot(\underset{\sim}{R}_K - \underset{\sim}{R}_L)] + \frac{1}{N^2}\sum_{L=1}^{N} 1 , \quad (2.91)$$

and convert the sum over $\underset{\sim}{q}$ to an integral:

$$E_g = N\left[\frac{3}{5}e_f + X(\rho_0) + \frac{V_a}{(2\pi)^3}\int F(q)dq\right]$$

$$+ N\left[w_B(q=0) + w_S(q=0) - \frac{1}{2}\lim_{q\to 0}\left(w_B(q) + w_S(q)\right)\right]$$

$$+ \frac{1}{2}\sum_{K,L}{}' \frac{2V_a}{(2\pi)^3}\int F(q)\exp\left(i\underset{\sim}{q}\cdot\underset{\sim}{r}_{KL}\right)d\underset{\sim}{q} , \quad (2.92)$$

where $\underset{\sim}{r}_{KL} = \underset{\sim}{R}_K - \underset{\sim}{R}_L$.

We can write the sum of the two q = 0 terms as

$$w_B(q=0) + w_S(q=0) = \lim_{q\to 0} [w_B(q) + w_S(q)] \quad , \qquad (2.93)$$

since both the bare ion form factor, $w_B(q)$, and the screening form factor, $w_S(q)$, diverge as $q\to 0$, but the limit of the sum exists. We now use Eqs. (2.62) and (2.87) to write $w_S(q)$ in terms of $w_B(q)$:

$$\lim_{q\to 0} [w_B(q) + w_S(q)] = \lim_{q\to 0} \left\{\frac{w_B(q)}{D(q)} - \frac{w_B(q)(\varepsilon(q)-1)Y(q)}{D(q)}\right\} \quad , \qquad (2.94)$$

where

$$D(q) = 1 + (\varepsilon(q)-1)(1-Y(q)) \quad . \qquad (2.95)$$

We can evaluate the limit in Eq. (2.94), using Eq. (2.37) for $w_B(q)$, Eq. (2.69) for $Y(q)$, and Eq. (2.59) for $\varepsilon(q)-1$ at small q:

$$\lim_{q\to 0} [w_B(q) + w_S(q)] = \frac{-2e_f}{3} + \frac{4k_f}{3\xi\pi} \quad . \qquad (2.96)$$

Finally, we substitute the above results into E_g and perform the angular integrations:

$$E_g = N\left[\frac{4}{15}e_f + \frac{2}{3}\frac{k_f}{\xi\pi} + X(\rho_0) + \frac{V_a}{2\pi^2}\int_0^\infty F(q)q^2dq\right]$$

$$+\frac{1}{2}\sum_{K,L}{}' \frac{V_a}{\pi^2}\int_0^\infty F(q)q^2\frac{\sin(qr_{KL})}{qr_{KL}}dq \quad . \qquad (2.97)$$

E. Total Adiabatic Potential

Equation (2.97) gives E_g in real space. We can now combine E_g with Ω_{II} and NI_z to give the total adiabatic potential per atom, Φ/N, where

$$\Phi/N - I_z = \frac{\Omega(V)}{N} + \frac{1}{2N}\sum_{K,L}{}' \phi(r_{KL};V) \quad , \qquad (2.98)$$

$$\frac{\Omega(V)}{N} = \frac{4}{15}e_f + \frac{2k_f}{3\xi\pi} + X(\rho_0) + \frac{V_a}{2\pi^2}\int_0^\infty F(q)q^2dq \quad , \qquad (2.99)$$

and

$$\phi(r;V) = \frac{2}{r} + \alpha_B\exp(-\gamma_B r) + \frac{V_a}{\pi^2}\int_0^\infty F(q)q^2\frac{\sin qr}{qr}dq \quad . \qquad (2.100)$$

We collect here the expressions in Eqs. (2.99) and (2.100) for later reference:

$$X(\rho_0) = \frac{-3k_f}{2\pi} - 0.115 + 0.031\ \ln r_s \quad , \qquad (2.75)$$

$$r_s = (3V_a/4\pi)^{1/3} \quad , \qquad (2.76)$$

$$\xi = 2/(1 + 0.0155\pi/k_f) \quad , \tag{2.77}$$

$$F(q) = \frac{-V_a q^2 \, |w_B(q)|^2 \, (\varepsilon(q)-1)}{16\pi \, [1 + (\varepsilon(q)-1)(1 - Y(q)]} \quad , \tag{2.89}$$

$$w_B(q) = \frac{1}{V_a} \left[\frac{-8\pi}{q^2} + \frac{\beta}{(1 + q^2\rho^2)^2}\right] \quad , \; q \neq 0 \quad , \tag{2.37}$$

$$\varepsilon(q) - 1 = \frac{2k_f}{\pi q^2} \left[\frac{1-\eta^2}{2\eta} \, \ln \left|\frac{1+\eta}{1-\eta}\right| + 1\right] \quad , \tag{2.57}$$

$$\eta = q/2k_f \quad , \tag{2.55}$$

$$Y(q) = \frac{q^2}{2(q^2+\xi k_f^2)} \quad , \tag{2.69}$$

$$e_f = k_f^2 \quad , \tag{2.24}$$

$$k_f = \left(\frac{3\pi^2}{V_a}\right)^{1/3} \quad , \tag{2.21}$$

$$V_a = V/N \quad . \tag{2.22}$$

Equation (2.98) gives the appropriate form of the total adiabatic potential for use in molecular dynamics calculations. Note that $\Omega(V)$ is strictly volume-dependent; all of the position information is in the effective potential, $\phi(r_{KL};V)$. The determination of the parameters α_B, γ_B, β, and ρ will be discussed in Chapter 3.

We need to show that the total adiabatic potential per atom, Φ/N, is bounded. To demonstrate this, we first show that the

two integral terms in Φ/N exist, and then show that the sum over all neighbors, $\sum_L' \phi(r_{KL};V)$, converges.

To show that the integrals in Eqs. (2.99) and (2.100) exist, we take the limits of the integrands as $q \to 0$ and as $q \to \infty$, where $F(q)$ is given in Eq. (2.89).

At small q, the leading terms in the factors of $F(q)$ are

$$\varepsilon(q) - 1 = \frac{4k_f}{\pi q^2} \quad , \tag{2.101}$$

$$1 - Y(q) = 1 \quad , \tag{2.102}$$

$$|w_B(q)|^2 = \frac{1}{V_a^2} \frac{64\pi^2}{q^4} \quad . \tag{2.103}$$

Since $\lim_{q \to 0} \left(\frac{\sin qr}{qr}\right) = 1$, both integrands go as q^0 as $q \to 0$.

At large q, the leading terms in the factors of $F(q)$ are

$$\varepsilon(q) - 1 = \frac{16k_f^3}{3\pi q^4} \quad , \tag{2.104}$$

$$1 - Y(q) = 1/2 \quad , \tag{2.105}$$

$$|w_B(q)|^2 = \frac{1}{V_a^2} \frac{64\pi^2}{q^4} \quad , \tag{2.106}$$

and the integrands go as q^{-4} and q^{-5} as $q \to \infty$.

At $q = 2k_f$ the dielectric function $\varepsilon(q)$ has a logarithmic singularity. As indicated in the previous discussion of $\varepsilon(q)$, the function is continuous at $q = 2k_f$. Hence, the integrands do not

diverge at this point. Since the limits of the integrands as $q \to 0$ exist, and the integrands vanish faster than q^{-1} for large q, both integrals exist.

We now need to show that the sum over all neighbors converges. For large r, the number of neighbors from r to $r + \delta r$ goes as $r^2 \delta r$. Hence, the effective potential, $\phi(r;V)$, for large r must vanish faster than r^{-3} for the sum $\sum_L{}' \phi(r_{KL};V)$ to converge.

We cannot find an analytical form for the r-dependent integral in Eq. (2.100) at large r, but we can find an expansion in powers of r^{-1} by successive integrations by parts, obtaining a higher power of r^{-1} in each resulting integral. This is the procedure suggested by Harrison[3] for the large-r expansion of a simpler effective potential with no exchange and correlation contribution. Unlike Harrison's expression, however, the integral in Eq. (2.100) cannot be integrated by parts in its present form. We will rewrite this integral in a more suitable form for partial integration. Two successive integrations by parts will then give the leading term of $\phi(r;V)$ at large r.

From Eq. (2.100) we have

$$\phi(r;V) = \frac{2}{r} + \alpha_B \exp(-\gamma_B r) + \zeta(r) \quad , \tag{2.107}$$

where

$$\zeta(r) = \frac{V_a}{\pi^2} \int_0^\infty F(q) q \, \frac{\sin qr}{r} \, dq \quad . \tag{2.108}$$

If we attempt a partial integration of Eq. (2.108), we obtain

$$\zeta(r) = \frac{-V_a}{\pi^2} \left|_0^\infty \frac{\cos qr}{r^2} F(q)\, q + \frac{V_a}{\pi^2} \int_0^\infty \frac{\cos qr}{r^2} (F(q)q)' dq \right. . \quad (2.109)$$

The integrated term of Eq. (2.104) is infinite at its lower limit, since $F(q)q$ goes as q^{-1} at small q. In addition, the integral on the right does not exist, since the derivative $(F(q)q)'$ goes as q^{-2} at small q.

This suggests that the leading term of $\zeta(r)$ at large r goes as r^{-1}. Accordingly, we rewrite $\zeta(r)$ to explicitly contain such a Coulomb term:

$$\zeta(r) = \frac{-V_a^2}{16\pi^3} \int_0^\infty \left[q^3 |w_B(q)|^2 \frac{\sin qr}{r} \right.$$

$$\left. \times \left\{1 - 1 + \frac{\varepsilon(q) - 1}{[1+(\varepsilon(q)-1)(1-Y(q))]}\right\}\right] dq$$

$$= \frac{-V_a^2}{16\pi^3} \int_0^\infty q^3 |w_B(q)|^2 \frac{\sin qr}{r}\, dq + \int_0^\infty \frac{\sin qr}{r}\, g(q) dq \quad , (2.110)$$

where

$$g(q) = \frac{h(q)}{D(q)} [1 - Y(q)(\varepsilon(q)-1)] \quad , \quad (2.111)$$

$$h(q) = \frac{V_a^2}{16\pi^3} |w_B(q)|^2 q^3 \quad , \quad (2.112)$$

and

$$D(q) = 1 + (\varepsilon(q)-1)(1-Y(q)) \quad . \tag{2.95}$$

The leading terms at large r of the first integral in Eq. (2.110) are

$$\frac{-2}{r} + j(r)\exp(-r/\rho) \quad , \tag{2.113}$$

where $j(r)$ is a quadratic polynomial in r. Note that the $-2/r$ term in $\zeta(r)$ cancels the Coulomb term in $\phi(r;V)$.

The second integral in Eq. (2.110) exists, since $g(q)$ goes as q at small q, and as q^{-1} at large q. This form can be integrated by parts twice. We note that $Y(q)$ and its derivatives are bounded and continuous for $0 \leq q \leq \infty$, and that $h(q)$ and its derivatives are bounded and continuous for $0 < q \leq \infty$. $\varepsilon(q)$ is bounded and continuous for $0 < q \leq \infty$, but its derivatives with respect to q contain singularities at $q = 2k_f$; the contributions of these singularities to $\zeta(r)$ will enable us to find the leading term of $\phi(r;V)$ at large r.

We integrate by parts once:

$$\int_0^\infty \frac{\sin qr}{r}\, g(q) = -\left|_0^\infty \frac{\cos qr}{r^2}\, g(q) + \int_0^\infty \frac{\cos qr}{r^2}\, g'(q)dq \right. \quad , \tag{2.114}$$

where

$$g'(q) = \frac{h'}{D}\,[D-(\varepsilon-1)] - \frac{h}{D^2}\,[\varepsilon'+Y'(\varepsilon-1)^2] \quad , \qquad (2.115)$$

$$\varepsilon'(q) = \frac{2k_f}{\pi}\,\left[\frac{q^2-12k_f^2}{4k_f q^4}\,\ln\left|\frac{q+2k_f}{q-2k_f}\right| - \frac{1}{q^3}\right] \quad , \qquad (2.116)$$

and we omit the q-dependent notation in Eq. (2.115) for simplicity. The integrated part in Eq. (2.114) vanishes, since $g(q)\to 0$ at both limits. The integrand on the right in Eq. (2.14) is bounded at the limits of integration, since $g'(q)$ goes as q^0 at small q, and as q^{-2} at large q. This integrand also contains a logarithmic singularity at $q = 2k_f$, from the first derivative of the dielectric function, $\varepsilon'(q)$.

We integrate by parts once more, and take principal values in the region of the singularity:

$$P\int_0^\infty \frac{\cos qr}{r^2}\,g'(q)dq = \lim_{\delta\to 0}\left\{\left|_0^{2k_f-\delta} + \left|_{2k_f+\delta}^{\infty}\right.\right.\right. \frac{\sin qr}{r^3}\,g'(q)\Big\}$$

$$- P\int_0^\infty \frac{\sin qr}{r^3}\,g''(q)dq \quad , \qquad (2.117)$$

where

$$g'' = \frac{h''}{D}\,[1-Y(\varepsilon-1)] - \frac{2h'}{D^2}\,[\varepsilon'+Y'(\varepsilon-1)^2] - \frac{h}{D^2}\,[Y''(\varepsilon-1)^2+\varepsilon'']$$

$$+ \frac{2h}{D^3}\,[(\varepsilon')^2(1-Y) - 2\varepsilon'Y'(\varepsilon-1) - (Y')^2(\varepsilon-1)^3] \quad , \qquad (2.118)$$

$$\varepsilon''(q) = \frac{2k_f}{\pi}\,\left[\frac{24k_f^2-q^2}{4k_f q^5}\,\ln\left|\frac{q+2k_f}{q-2k_f}\right| + \frac{2}{q^2(q^2-4k_f^2)}\right] \quad , \qquad (2.119)$$

and we omit the q-dependence in Eq. (2.118).

We can rewrite the limit term in Eq. (2.117) as

$$\lim_{\delta\to 0}\left\{\int_0^{\infty}\frac{\sin qr}{r^3}\,g'(q)+\int_{2k_f+\delta}^{2k_f-\delta}\frac{\sin 2k_f r}{r^3}\,C(2k_f)\ln|2k_f-q|\right\}\quad,(2.120)$$

where the slowly varying terms in sin qr g'(q) in the interval $[2k_f-\delta,\ 2k_f+\delta]$ are taken at $q=2k_f$, and $C(2k_f)$ is a constant. The first term in Eq. (2.120) vanishes, since sin qr $g'(q)\to 0$ at both limits. The second term also vanishes, since

$$\lim_{\delta\to 0}\int_{2k_f+\delta}^{2k_f-\delta}\ln|2k_f-q| = 0\quad . \qquad (2.121)$$

The integrand on the right of Eq. (2.117) is bounded at the limits of integration, since the leading terms of g"(q) go as q^{-3} at large q, and as q^{-1} at small q. In addition, in the limit $q\to 0$ the q^{-1} terms cancel and the next leading terms go as q. This integrand contains logarithmic singularities at $q=2k_f$, from $\varepsilon'(q)$ and $\varepsilon''(q)$, and a simple pole at $q=2k_f$, from $\varepsilon''(q)$. This integral exists, as will be shown below, and we can evaluate its leading term for large r. We drop the principal parts notation, and write

$$\zeta(r) = \frac{-2}{r} + j(r)\exp(-r/\rho) + \zeta_1(r)\quad , \qquad (2.122)$$

where

$$\zeta_1(r) = - \int_0^\infty \frac{\sin qr}{r^3} g''(q)dq \quad . \tag{2.123}$$

To find the leading term of $\zeta_1(r)$ at large r, we discard all terms formally of order greater than r^{-3}. We can evaluate the leading order of each of the terms in $\zeta_1(r)$ by considering the asymptotic behavior of the integral

$$\int_0^\infty \sin qr \; G(q)dq \quad , \tag{2.124}$$

where G(q) represents one of the nine terms of g"(q). We consider two cases: 1) for G(q) bounded and continuous, and 2) for G(q) containing a finite number of singularities.

For G(q) bounded and continuous, the integral in Eq. (2.124) will vanish as $r \to \infty$ because of the rapid oscillations of sin qr. Hence, all terms of g"(q) that are bounded and continuous will contribute terms formally of order greater than r^{-3} to $\zeta_1(r)$. The only possible contributions of order r^{-3} will be from singularities in g"(q). Of the nine terms in g"(q), only the last term, which goes as q as $q \to 0$ and contains no derivatives of $\varepsilon(q)$, is bounded and continuous and can be discarded. Of the remaining eight terms, seven contain singularities at q=0 and four at $q=2k_f$.

For G(q) containing a finite number of singularities, we can evaluate the leading orders of the contribution of each singularity at large r. From Lighthill,[21] we can find the leading terms at large r of the Fourier transform, (F.T.), of G(q) by

expanding the continuous part of G(q) around each singularity. Since each G(q) is an odd function, we have

$$\int_0^\infty G(q)\sin qr\, dq = -\frac{1}{2}\,\mathrm{Im}\int_{-\infty}^{\infty} G(q)\exp(-iqr)dq$$

$$= -\frac{1}{2}\,\mathrm{Im}\,[\text{F.T. } G(q)] \quad . \qquad (2.125)$$

Around each singularity $q=q_s$ in G(q), where G(q) is now defined on $[-\infty,\infty]$, we can write G(q) as the product

$$G(q) = c(q)G_s(q-q_s) \quad , \qquad (2.126)$$

where c(q) is a continuous function in the interval including the singularity, and $G_s(q-q_s)$ is a generalized function which diverges at the singularity. We can expand c(q) around the singularity to give

$$G(q) = c(q_s)G_s(q-q_s) + c'(q_s)[(q-q_s)G_s(q-q_s)]$$

$$+ \frac{1}{2}\,c''(q_s)[(q-q_s)^2G_s(q-q_s)] + \ldots \quad . \qquad (2.127)$$

The two leading terms of the contribution of the singularity to Eq. (2.125) become

$$-\frac{1}{2}\,\{c(q_s)\mathrm{Im}[\text{F.T. } G_s(q-q_s)]+c'(q_s)\mathrm{Im}[\text{F.T.}((q-q_s)G_s(q-q_s))] \quad , (2.128)$$

and the leading term of the contribution of the singularity at $q=q_s$ to $\zeta_1(r)$ can then be written as

$$\frac{1}{2r^3}\, c(q_s)\,\mathrm{Im}[\mathrm{F.T.}\ G_s(q-q_s)] \quad . \tag{2.129}$$

We need only apply Eq. (2.129) to the singularities in $g''(q)$ on the interval $[-\infty, \infty]$, and discard terms of order greater than r^{-3}, to find the leading term of $\zeta_1(r)$ at large r. We now consider the effect of each singularity in $g''(q)$ in detail.

The first seven terms in $g''(q)$ each go as q^{-1} for small q, and hence diverge at q=0. If we apply Eq. (2.129) to each of these terms and take the sum, we obtain

$$\frac{1}{2r^3}\,\mathrm{Im}[\mathrm{F.T.}\ (\frac{1}{q})] \sum_{i=1}^{7} c_i(0) = 0 \quad , \tag{2.130}$$

since the q^{-1} terms cancel in the limit $q \to 0$. The next order contribution to $\zeta_1(r)$ from these singularities goes as r^{-4} and can be ignored.

The third, sixth, seventh and eighth terms in $g''(q)$ contain singularities at $q = \pm 2k_f$, from $\varepsilon'(q)$ and $\varepsilon''(q)$. From Eqs. (2.116) and (2.119), we have three generalized functions for the singular parts of $\varepsilon'(q)$, $(\varepsilon'(q))^2$ and $\varepsilon''(q)$ at $q = \pm 2k_f$:

$$G_{s1}(q\mp 2k_f) = \ln|q\mp 2k_f| \quad ,$$

$$G_{s2}(q\mp 2k_f) = [\ln|q\mp 2k_f|]^2 \quad ,$$

$$G_{s3}(q\mp 2k_f) = 1/(q\mp 2k_f) \quad . \qquad (2.131)$$

From Lighthill,[21] the Fourier transforms of $G_{s1}(q\mp 2k_f)$ and $G_{s2}(q\mp 2k_f)$ go as r^{-1}. If we apply Eq. (2.129) to these singularities, we obtain contributions to $\zeta_1(r)$ of leading order r^{-4}; these contributions can be ignored.

The Fourier transforms of $G_{s3}(1\mp 2k_f)$ go as r^0 and hence contribute two terms of leading order r^{-3} to $\zeta_1(r)$, from the simple poles at $q = \pm 2k_f$. Since the contributions from the two singularities are equal, we apply Eq. (2.129) and write the leading term of $\zeta_1(r)$ at large r as

$$\zeta_1(r) = \frac{1}{r^3}\left[\frac{h(q)}{D^2(q)}\frac{4k_f}{\pi q^2}\frac{1}{q+2k_f}\right]_{q=2k_f} \mathrm{Im}\left[\mathrm{F.T.}\left(\frac{1}{q-2k_f}\right)\right]$$

$$= \frac{A\cos(2k_f r)}{r^3} \quad , \qquad (2.132)$$

where

$$A = \frac{V_a^2 k_f |w_B(2k_f)|^2}{8\pi^3(1+b)^2} \quad , \qquad (2.133)$$

and

$$b = \frac{1}{2\pi k_f} \left(\frac{2 + \xi}{4 + \xi}\right) \quad . \tag{2.134}$$

We then have, for the leading term of the effective potential at large r,

$$\phi(r;V) = \frac{A \cos(2k_f r)}{r^3} \quad , \tag{2.135}$$

where A is given by Eq. (2.133). Hence, the sum over all neighbors converges and the total adiabatic potential per atom, Φ/N, is bounded.

Equation (2.135) has the form of Friedel oscillations, and it can be seen now that these oscillations are a mathematical result of the singularities in the derivatives of the integrand in $\phi(r;V)$ at $q=2k_f$. The singularities, in turn, are caused by the cutoff of screening at the Fermi sphere; the screening cancels the Coulomb potential at large r, leaving a small oscillatory tail in the effective potential, $\phi(r;V)$. The form of this potential is shown in Fig. 3.

CHAPTER 3

NUMERICAL TECHNIQUES

In the previous chapter we derived an expression for the total adiabatic potential of metallic sodium. In Chapter 1 we gave the expressions needed to calculate the elastic constants of sodium, in terms of the total adiabatic potential and its derivatives with respect to position and volume. We now discuss the numerical evaluation of these expressions.

We need to evaluate eight expressions to determine the elastic constants. Three of these expressions depend only on volume (V-dependent); the remaining five expressions depend on both position and volume ((r;V)-dependent). Using the notation of Chapter 1, we write the three V-dependent expressions:

$$\frac{\Omega}{N} = g_1(V) + \int_0^\infty \frac{Q\varepsilon_1}{D}\, dq \quad , \tag{3.1}$$

$$\frac{\Omega^*}{N} = g_2(V) + \int_0^\infty [f_1(q) + f_2(q)\ln|\eta-1|]dq \quad , \tag{3.2}$$

$$\frac{\Omega^{**}}{N} = g_3(V) + \int_0^\infty [f_3(q) + f_4(q)\ln|\eta-1| + f_5(q)\ln^2|\eta-1| + f_6(q)(\eta-1)^{-1}]dq \quad , \tag{3.3}$$

where

$$g_1(V) = \frac{4}{15} k_f^2 + \frac{2k_f}{3\xi\pi} - \frac{3k_f}{2\pi} - 0.115 + .031 \ln r_s \quad , \qquad (3.4)$$

$$g_2(V) = -\frac{8}{45} k_f^2 + \frac{7}{18} \frac{k_f}{\pi} + \frac{.031}{3} \quad , \qquad (3.5)$$

$$g_3(V) = \frac{8}{27} k_f^2 - \frac{14k_f}{27\pi} - \frac{.031}{3} \quad , \qquad (3.6)$$

$$f_1(q) = \frac{V_a Q}{D^2} (\varepsilon_1^2 Y_1 - \varepsilon_2 \ln|\eta+1|) \quad , \qquad (3.7)$$

$$f_2(q) = \frac{V_a Q}{D^2} \varepsilon_2 \quad , \qquad (3.8)$$

$$f_3(q) = \frac{V_a^2 Q}{D^2} \left[\frac{2\varepsilon_1^2 Y_1^2(1+\varepsilon_1)}{DY} + \frac{\varepsilon_1^2 Y_1}{V_a} \left(\frac{\xi-4}{3} + \frac{4}{\xi-6}\right)\right.$$

$$\left. + \varepsilon_2 \ln|\eta+1| \left(\frac{5}{3V_a} - \frac{4\varepsilon_1 Y_1}{D} - \frac{2\varepsilon_2(1-Y)}{D} \ln|\eta+1|\right)\right] \quad , \qquad (3.9)$$

$$f_4(q) = \frac{V_a^2 Q \varepsilon_2}{D^2} \left[\frac{-5}{3V_a} + \frac{4\varepsilon_1 Y_1}{D} + \frac{4\varepsilon_2(1-Y)}{D} \ln|\eta+1|\right] \quad , \qquad (3.10)$$

$$f_5(q) = -\frac{2V_a^2 Q}{D^3} \varepsilon_2^2 (1-Y) \quad , \qquad (3.11)$$

$$f_6(q) = \frac{2}{3} \frac{V_a Q}{D^2} \frac{\varepsilon_2 \eta}{(\eta+1)} \quad , \qquad (3.12)$$

$$Q = -\frac{V_a^2 q^4}{32\pi^3} |w_B(q)|^2 \quad , \qquad (3.13)$$

$$\varepsilon_1 = \varepsilon(q) - 1 \quad , \qquad (3.14)$$

$$\varepsilon_2 = \frac{4k_f^2}{3\pi V_a q^3} \quad , \tag{3.15}$$

$$D = 1 + \varepsilon_1(1-Y) \quad , \tag{3.16}$$

$$Y_1 = \frac{2Y^2k_f^2}{3V_a q^2}\,(3\xi - \xi^2/2) \quad , \tag{3.17}$$

and $\varepsilon(q)$, Y, $w_B(q)$, k_f, ξ, r_s, and η are given by the equations following Eq. (2.100).

The five (r;V)-dependent expressions can be written

$$\phi = h_1(r) + 2\int_0^\infty \frac{Q\varepsilon_1}{D}\frac{\sin qr}{qr}\,dq \quad , \tag{3.18}$$

$$\phi' = h_2(r) + 2\int_0^\infty \frac{Q\varepsilon_1}{D}\left(\cos qr - \frac{\sin qr}{qr}\right) dq \quad , \tag{3.19}$$

$$\phi'' - \phi' = h_3(r) + 2\int_0^\infty \frac{Q\varepsilon_1}{D}\left(\frac{3\sin qr}{qr} - 3\cos qr - qr\sin qr\right)dq \quad , \tag{3.20}$$

$$\phi^* = 2\int_0^\infty \left(f_1(q) + f_2(q)\ln|\eta-1|\right)\frac{\sin qr}{qr}\,dq \quad , \tag{3.21}$$

$$\begin{aligned}\phi^{**} + \frac{2}{3}\phi'^* = 2\int_0^\infty \{&[f_3(q) + f_4(q)\ln|\eta-1| + f_5(q)\ln^2|\eta-1| \\ &+ f_6(q)(\eta-1)^{-1}]\frac{\sin qr}{qr} \\ &+ \frac{2}{3}\left[f_1(q) + f_2(q)\ln|\eta-1|\right]\left(\cos qr - \frac{\sin qr}{qr}\right)\}dq \quad ,\end{aligned} \tag{3.22}$$

where

$$h_1(r) = \frac{2}{r} + \alpha_B \exp(-\gamma_B r) \quad , \tag{3.23}$$

$$h_2(r) = \frac{-2}{r} - \gamma_B \alpha_B r \exp(-\gamma_B r) \quad , \tag{3.24}$$

and

$$h_3(r) = \frac{6}{r} + \gamma_B \alpha_B r(1+\gamma_B r) \exp(-\gamma_B r) \quad . \tag{3.25}$$

There are no general analytic solutions to the integrals above. Hence, we will solve the integrals numerically and obtain the (r;V)-dependent quantities needed during an MD run from tables of our numerical solutions. Details of the table construction will be given in Chapter 4.

Numerical treatment of the integrals in Eqs. (3.1)-(3.3) and (3.18)-(3.22) presents a number of difficulties. The major difficulties include the infinite limits of integration, as well as the singularities at $q = 2k_f$ in several of the integrands; the singularities result from differentiation of the total adiabatic potential with respect to volume.

Previous work on this model of sodium utilized the numerical techniques described in Swanson.[22] Evaluation of Ω, ϕ, and ϕ' involved a Simpson's rule integration over the interval $q = [0,20]$, plus an analytic approximation for the integral over $q = [20,\infty]$. The volume derivatives Ω^* and ϕ^* were obtained from fits of Ω and ϕ vs V. The uncertainties in calculations using these techniques are very difficult to analyze. In addition, the

analytic solution for large q is unsuitable for a slowly converging integrand (such as the integrand in Eq. (3.20)), and the fitting technique is unsuitable for higher derivatives with respect to the volume.

We will use substantially different numerical techniques here. For our calculations of the elastic constants, we will transform the preceding integrals into expressions that can be handled efficiently by adaptive Gaussian quadrature. This method is useable for all of the volume derivatives and for slowly converging integrands. This method also gives better estimates of the errors and is quite efficient in its use of computer time.

We begin by determining the parameters for our model potential and establishing the existence of the preceding integrals. We will then describe the basic integration routine and the necessary transformations of the integrals.

A. Parameters

The total adiabatic potential contains four model parameters: γ_B and α_B from the Born-Mayer repulsion, and β and ρ from Harrison's[3] pseudopotential model. We take the value of γ_B calculated by Fumi and Tosi[23] for NaCl-type sodium halides. We treat the other three parameters as adjustable. Wallace[8] determined the values of α_B, β, and ρ by fitting the total adiabatic potential and its volume derivatives to the measured binding energy and compressibility of sodium at zero temperature and pressure, and requiring agreement between calculated and

experimental values of the average of the phonon frequencies squared, $\langle\omega^2\rangle$. Zero-point vibrations were neglected. The four parameters were found to be

$$\gamma_B = 1.56\ a_0^{-1} \quad , \tag{3.26}$$

$$\alpha_B = 10.5\ \text{Ry} \quad , \tag{3.27}$$

$$\beta = 37.0\ \text{Ry}\ a_0^3 \quad , \tag{3.28}$$

$$\rho = 0.5\ a_0 \quad . \tag{3.29}$$

We also need to consider the typical values of V_a and r that we will use in our simulations. The choice of V_a and the calculation of a minimum and maximum r for a particular MD run will be discussed in Chapter 4. We give the ranges of V_a and r here, since details of the integration procedure depend on the sizes of these variables:

$$254.9\ a_0^3 \lesssim V_a \lesssim 269.0\ a_0^3 \quad , \tag{3.30}$$

$$5\ a_0 \lesssim r \lesssim 27\ a_0 \quad . \tag{3.31}$$

B. Existence of the Integrals

We have previously shown that the integrals in Eqs. (3.1) and (3.18) exist (see Chapter 2). To demonstrate that each integral in the remaining six expressions exists, we first show that the integrand is bounded at the lower limit of integration and vanishes faster than q^{-1} at the upper limit, and then show that

either the integrand is continuous over the range of integration or the Cauchy principal value exists.

We first take the limits of the integrands as $q \to 0$ and as $q \to \infty$. At small q, the leading terms in the factors of the integrands are

$$Q = \frac{-2}{\pi} \quad , \tag{3.32}$$

$$\varepsilon_1 = \frac{4k_f}{\pi q^2} \quad , \tag{3.33}$$

$$\varepsilon_2 \quad \frac{4k_f^2}{3\pi V_a} \frac{1}{q^3} \quad , \tag{3.34}$$

$$D = \frac{4k_f}{\pi q^2} \quad , \tag{3.35}$$

$$Y = \frac{q^2}{2\xi k_f^2} \quad , \tag{3.36}$$

$$V_1 = \frac{q^2(3-\xi/2)}{6\xi k_f^2 V_a} \quad . \tag{3.37}$$

Since $\lim_{q\to 0} \left(\frac{\sin qr}{qr}\right) = \lim_{q\to 0} (\cos qr) = 1$, and the leading term of $\left(\frac{\sin qr}{qr} - \cos qr\right)$ goes as q^2, as $q \to 0$, the integrands of Eqs. (3.2)-(3.3) and (3.19)-(3.22) go as q^2, as $q \to 0$. Hence, these integrands all vanish at $q = 0$.

At large q, the leading terms in the factors of the integrands are

$$Q = \frac{-2}{\pi} \quad , \tag{3.38}$$

$$\varepsilon_1 = \frac{16k_f^3}{3\pi q^4} \quad , \tag{3.39}$$

$$\varepsilon_2 = \frac{4k_f^2}{3\pi V_a} \frac{1}{q^3} \quad , \tag{3.40}$$

$$D = 1 \quad , \tag{3.41}$$

$$Y = \frac{1}{2} \quad , \tag{3.42}$$

$$Y_1 = \frac{k_f^2 \xi (3-\xi/2)}{6V_a q^2} \quad . \tag{3.43}$$

The integrand in Eq. (3.20) goes as q^{-3}, as $q \to \infty$. The integrands in Eqs. (3.2), (3.3), (3.19) and (3.22) go as q^{-4}, and the integrand in Eq. (3.21) goes as q^{-5}, as $q \to \infty$. Hence, these integrands all vanish faster than q^{-1}, as $q \to \infty$.

We now consider continuity. Q, ε_2, Y, and Y_1, as well as their derivatives with respect to q, are all bounded and continuous for $0 < q \leq \infty$. As indicated in Chapter 2, $\varepsilon(q)$ is bounded and continuous for $0 < q \leq \infty$, but its derivatives with respect to q contain singularities at $q = 2k_f$. Hence, ε_1 and D are bounded and continuous over $0 < q \leq \infty$ but their derivatives are unbounded at $q = 2k_f$.

The integrands in Eq. (3.19) and (3.20) are both continuous for $0 < q < \infty$. Since these integrands are bounded at $q = 0$ and vanish faster than q^{-1} for large q, the integrals in Eq. (3.19) and (3.20) exist.

The integrands in Eqs. (3.2), (3.3), (3.21), and (3.22) are unbounded at $q = 2k_f$ ($\eta=1$). All four expressions contain singular terms of the form $f(q)\ln|\eta-1|$, where $f(q)$ is bounded and continuous for $0 \leq q \leq \infty$, where $f(q)$ vanishes faster than q^{-3} for large q, and where $f(q) \neq 0$ at $\eta=1$. The integrands in Eqs. (3.3) and (3.22) also contain singular terms of the form $f(q)\ln^2|\eta-1|$ and $f(q)(\eta-1)^{-1}$. We can divide each unbounded integrand into two parts: a sum of continuous terms, and a sum of singular terms. The integral over the continuous part obviously exists. For the singular part, we need to show that the Cauchy principal value exists. For simplicity in the following discussion, we will treat $\eta = q/2k_f$ as the variable of integration.

First, we consider an integrand of the form $f(\eta)\ln|\eta-1|$. We divide the range of integration into three parts: $\eta = [0,a]$, $\eta = [a,b]$ and $\eta = [b,\infty]$, where $0 < a < 1 < b < \infty$. The integrals over the first and third intervals clearly exist, since the integrand is bounded and continuous over each interval, and vanishes faster than η^{-1} for large η.

For the second interval, we integrate by parts:

$$P\int_a^b f(\eta)\ln|\eta-1|d\eta = P\left|_a^b f(\eta)[(\eta-1)\ln|\eta-1| - (\eta-1)]\right.$$
$$- P\int_a^b f'(\eta)[(\eta-1)\ln|\eta-1| - (\eta-1)]d\eta \quad . \qquad (3.44)$$

The integrated part in Eq. (3.44) can be rewritten

$$\lim_{\delta\to 0}\left\{\left|_a^b f(\eta)[(\eta-1)\ln|\eta-1|-(\eta-1)]\right.\right.$$
$$\left.\left. - \left|_{1-\delta}^{1+\delta} f(1)[(\eta-1)\ln|\eta-1|-(\eta-1)]\right.\right\} \quad , \quad (3.45)$$

where the slowly varying terms in $f(\eta)$ in the interval $[1-\delta, 1+\delta]$ are taken at $\eta = 1$. The first expression in Eq. (3.45) is bounded for finite b. The second expression vanishes, since

$$\lim_{\delta\to 0}(\delta\ln\delta-\delta) = 0 \quad . \qquad (3.46)$$

The integral on the right in Eq. (3.44) can be rewritten

$$P\int_a^b [t_1(\eta) + t_2(\eta)\ln|\eta-1|][(\eta-1)\ln|\eta-1| - (\eta-1)]d\eta \quad , (3.47)$$

where $t_1(\eta)$ and $t_2(\eta)$ are bounded and continuous over $[a,b]$. The extra factor of $\ln|\eta-1|$ arises from the singular derivative of the dielectric function $\varepsilon_1' = \varepsilon'(q)$ (see Eq. (2.116)). The integrand in Eq. (3.47) is continuous at $\eta = 1$, since the limit of the leading term as $\eta \to 1$ exists:

$$\lim_{\eta\to 1}(\eta-1)\ln^2|\eta-1| = \lim_{\delta\to 0}\delta\ln^2\delta = 0 \quad . \qquad (3.48)$$

Hence, the Cauchy principal value for the integral over [a,b] exists, and integrals of the form

$$\int_0^\infty f(\eta)\ln|\eta-1|d\eta$$

exist.

We can use similar arguments for an integrand of the form $f(\eta)\ln^2|\eta-1|$. After integration by parts, the function for the integrated part becomes $f(\eta)\left[(\eta-1)\ln^2|\eta-1| - 2(\eta-1)\ln|\eta-1| + 2(\eta-1)\right]$. This function vanishes as $\eta\to1$, and is bounded for finite b. The leading term in the new integrand as $\eta\to1$ becomes $t_2(\eta)\left[(\eta-1)\ln^3|\eta-1|\right]$, where $t_2(\eta)$ is bounded and continuous over [a,b]. The limit of this term as $\eta\to1$ exists:

$$\lim_{\eta\to1} t_2(\eta)\left[(\eta-1)\ln^3|\eta-1|\right] = t_2(1)\lim_{\delta\to0} \delta\ln^3\delta = 0 \quad . \qquad (3.49)$$

Hence, the new integrand is continuous at $\eta = 1$, the Cauchy principal value over [a,b] exists, and integrals of the form

$$\int_0^\infty f(\eta)\ln^2|\eta-1|d\eta$$

exist.

Finally, we consider an integrand of the form $f(\eta)(\eta-1)^{-1}$. We divide the range of integration into three parts, as before. The integrals over $\eta = [0,a]$ and $\eta = [b,\infty]$ obviously exist.

For the integral over $\eta = [a,b]$, we integrate by parts:

$$P \int_a^b f(\eta)(\eta-1)^{-1}d\eta = P \left|_a^b f(\eta)\ln|\eta-1| - P \int_a^b f'(\eta)\ln|\eta-1|d\eta \right. . \quad (3.50)$$

The integrated term can be rewritten

$$\lim_{\delta\to 0} \left\{ \left|_a^b f(\eta)\ln|\eta-1| - \left|_{1-\delta}^{1+\delta} f(1)\ln|\eta-1| \right.\right\} . \quad (3.51)$$

The first expression in Eq. (3.51) is bounded for finite b. The second expression vanishes, since

$$\lim_{\delta\to 0} (f(1)\ln\delta - f(1)\ln\delta) = 0 . \quad (3.52)$$

The integral on the right in Eq. (3.50) can be rewritten

$$P \int_a^b [t_1(\eta)\ln|\eta-1| + t_2(\eta)\ln^2|\eta-1|]d\eta , \quad (3.53)$$

where $t_1(\eta)$ and $t_2(\eta)$ are bounded and continuous over $[a,b]$. We have already established that the Cauchy principal value of an integral over $[a,b]$ with an integrand of the form $t_1(\eta)\ln|\eta-1|$ or $t_2(\eta)\ln^2|\eta-1|$ exists. Hence, the integral in Eq. (3.47) exists, and integrals of the form

$$\int_0^\infty f(\eta)(\eta-1)^{-1}d\eta$$

exist.

Hence, the Cauchy principal values of all of the singular parts of Eqs. (3.2), (3.3), (3.21), and (3.22) exist, and the integrals in these four expressions exist.

C. The Basic Integration Routine

The numerical techniques were influenced by three basic considerations. First, a relative error tolerance for numerical integration refers to an entire expression, not just the integral part. As discussed below and in Chapter 5, we require a relative error tolerance of 10^{-4} for each (r;V)-dependent expression, and a relative error tolerance of 10^{-6} for each V-dependent expression. For a V-dependent calculation, taking the relative error of the entire expression reduces the work of numerical integration since the analytic part tends to be large. For some (r;V)-dependent calculations, taking the relative error of the entire expression is the only reasonable approach over certain ranges of r where the analytic and integral contributions partially cancel. In practice, the analytic parts are taken under the integral sign for a finite interval of integration. We can write

$$A + \int_0^b f(q)dq = \int_0^b [f(q) + \frac{A}{b}]dq \quad , \tag{3.54}$$

where A is the analytic part.

Second, the integration routine was chosen for general reliability, not for specialized features. All numerical integration was done with one basic program, employing adaptive high-order Gaussian quadrature. We choose to transform the integrals to remove any difficulties that the routine cannot handle.

This process gives more valuable results than choosing specialized routines to treat the integration difficulties directly. The basic routine handled a variety of test integrals dependably, returning solutions that were safely within the required error tolerances. In addition the logic and coding in this routine was traced and found adequate. This was not the case with several more specialized programs, some of which performed erratically and some of which contained logic problems. We choose to sacrifice ease of programming for trustworthiness of results.

Third, the overall integration schemes, including the methods of removing integration difficulties, were designed to be handled efficiently by CRAY-1 computers. On vector machines such as these, it is much faster to perform a large number of arithmetic operations than to make a small number of decisions. If we transform a set of integrals so that all can be handled in essentially the same way by the integration routine, we avoid decision making during program execution. This is particularly important for (r;V)-dependent expressions, where the routine must evaluate thousands of integrals for each volume used.

We describe below the details of the computer routine and our treatment of the major integration difficulties.

The basic numerical integration program used is the subroutine QAG, a globally adaptive integrator using pairs of Gauss-Kronrod quadrature formulas for the integration rules. Rules of varying degrees of precision can be chosen. The program also contains provisions for detection of bad convergence and round-off error. QAG is based on the routine AIND[24] and is part of QUADPACK,[25] an integration subroutine package for the numerical computation of definite one-dimensional integrals. The package contains both double and single precision variants of QAG; we use the faster single precision version. For CRAY-1 computers, single precision gives ~ 14 significant figures.

1. Adaptivity

In a globally adaptive scheme, the interval of integration is subdivided into a set of subintervals:

$$[x_0, x_1], [x_1, x_2] , ... [x_{n-1}, x_n] .$$

The subintervals will be large where the integrand is easy to handle, and small where the integrand is difficult. The same integration rule is used to estimate $\int_{x_i}^{x_{i+1}} f(x)dx$ over each interval. The results of the numerical integration, as well as the results of the error estimates for the subintervals, are then summed.

An example of the interval bisection scheme used in QAG will demonstrate this. We wish to integrate f(x) over the interval [a,b]. We specify both a relative error tolerance and an absolute error tolerance. As soon as either tolerance is satisfied, the routine returns an answer for the integral and the error. In practice, if we desire a relative error tolerance we set the absolute error tolerance to ~ 0, and vice versa.

We first attempt to integrate over the entire interval. If either tolerance is satisfied, the routine ends. If not, we divide the interval into two equal parts and estimate the integral and the absolute error over each part. We add the two integral contributions, add the two errors, and decide if either tolerance is satisfied. If not, we divide the interval with the largest error estimate into two parts. This process repeats; the next interval to be subdivided is always the one with the largest error estimate. If neither tolerance can be satisfied, the routine returns the current estimates for the integral and the error, plus information about the kind of difficulty encountered. Such abnormal exits are discussed below.

The primary advantage of an adaptive routine is economy in the number of integrand evaluations required. The primary disadvantage is inefficiency on a vector machine; the process of interval subdivision requires decision making, and decision making is costly. For the integrals necessary to determine the elastic constants of sodium, the most important advantage of adaptivity is

the ability to "throw" most of the error, and most of the subintervals, into the awkward region around $q = 2k_f$. The adaptive routine will also subdivide an interval to allow for a larger contribution to the integral from smaller q, and will automatically provide small intervals for rapid oscillations at large r. These advantages outweigh the inefficiencies. The routine can be made more efficient by choosing a set of subintervals and using this set as a starting point for the integration. The particular set will depend on the nature of the integrand and on the value of r. This would reduce the number of decisions to subdivide. However, the routine was fast enough to be economical without requiring this modification.

2. Integration Rules

To estimate the error over each subinterval, we calculate two different estimates of the integral over the subinterval. The error is then taken as the magnitude of the difference between these estimates.

We use n-point Gaussian quadrature for the first estimate of the integral over each subinterval:

$$\int_a^b f(x)dk \sim \sum_{k=1}^{n} w_k f(x_k) \quad , \tag{3.55}$$

where w_k is the weight for point k of an n-point rule, and all x_k are in the interior of [a,b]. This rule is exact for all polynomials of class P_{2n-1}.[26]

We wish to perform a second evaluation of the integral over the subinterval, hopefully a more accurate evaluation than the first. This second evaluation then becomes the best estimate for the subinterval. A difficulty with Gaussian integration is that the abscissas, $\{x_k\}$, for any rule of order n are distinct from the abscissas for a rule of any other order, with the exception of the midpoint in odd-order rules.[26] If we perform a second Gaussian integration with a higher-order rule, we need a completely new set of integrand evaluations.

Instead, we use a method developed by Kronrod.[27] For the second evaluation of the integral, n+1 new abscissas are added to the original set of abscissas. The new abscissas are real, located in the interior of [a,b], and are separated by the original n abscissas. The new rule is exact for P_{3n+1} and hence is of higher accuracy than the original n-point rule. Note that a 2n+1-point Gauss rule would be exact for P_{4n+1}, and hence of higher accuracy than a 2n+1-point Gauss-Kronrod rule. This sacrifice of accuracy is outweighed by the saving of n integrand evaluations for each subinterval. For thousands of calculations of complicated integrands, the Kronrod extension can represent a significant saving in computer time.

The choice of n for the pair of integration rules (n,2n+1) depends on two major factors. A higher-order rule requires fewer interval subdivisions and is better suited to an integrand with fast oscillations than a lower-order rule. A lower-order rule

helps to minimize round-off error. We choose $n = 15$; the Gauss-Kronrod pair (15,31) represents a reasonable compromise between higher precision and lower round-off error.

As noted above, the error for a subinterval is calculated by taking the absolute value of the difference between the application of the n-point rule and the 2n+1-point rule. We assume that the latter rule is more accurate; this is not unreasonable if the integrand is continuous over the subinterval, and if the higher-order rule is not significantly contaminated by round-off error. This is, of course, not rigorous. The method is actually a sampling process, since the error tolerance is calculated from a finite sample of points.[28]

To evaluate the integrals at the beginning of this chapter, we need to use the error estimates returned by the integration routine. However, we can obtain information about the reliability of these estimates by using the routine to evaluate test integrals whose solutions are known in closed form. The test integrands and intervals can be chosen to mimic the general form of the actual integrals in Eqs. (3.1)-(3.3) and (3.18)-(3.22) over various ranges of q. The actual errors in the computer calculations of the test integrals were always at least an order of magnitude smaller than the error estimates returned by QAG. Calculation of the actual integrals necessary to evaluate the elastic constants, using relative error tolerances varying from 10^{-4} to 10^{-8}, also indicated that the error estimates returned by QAG were over an order of

magnitude too high. This indicates that the integration routine is reliable, albeit considerably too accurate for the required tolerances. For our estimate of the absolute error in an integral evaluated by routine QAG, we will take 10% of the error calculated by the routine. This represents an upper bound for the numerical integration error.

3. Abnormal Exits

As noted above, the program will stop evaluating an integral upon encountering certain integration difficulties, and will return estimates for the integral and the error, along with information about the kinds of difficulties encountered. These estimates are less reliable than those where the program stops when the tolerances are satisfied. The routine provides three kinds of abnormal exits, in addition to the normal exit where either the absolute error or the relative error is satisfied.

The first abnormal exit, for bad integrand behavior at a point of the integration range, is not a problem as long as the integrand is sufficiently smooth. This exit only occurs when interval subdivision has proceeded until the spacing of the abscissas x_k for the 2n+1 point rule is too small to resolve. Hence, we require an integrand to be continuous over the interval of integration. There should be no sharp peaks and, preferably, no strong derivative singularities on the interval of integration. In addition, any singularity off the interval of integration should be sufficiently distant or weak. The transformation of the integrals

in Eqs. (3.2), (3.3), (3.21), and (3.22) to fit these conditions is discussed below. In practice, we only require an integrand to be bounded and piecewise continuous over the interval of integration, but the positions of any jump discontinuities must be known. QAG can then be directed to subdivide the interval at these points, and the jumps present no problem. If the interval of integration is not divided at jump discontinuities, QAG tends to be very inefficient, with an increased risk of an abnormal exit for bad integrand behavior or for an excessive number of integrand evaluations.

The second abnormal exit, for an excessive number of integrand evaluations, is not a problem as long as the integrand is sufficiently smooth, and as long as the interval of integration is not too large. The maximum number of subintervals is set to be large enough so that weak derivative singularities can be located, and small enough to provide an abnormal exit before too much computer time has elapsed on any one integral.

The third abnormal exit, for round-off error, is not a serious problem as long as care is taken when specifying error tolerances and the orders of the integration rules, and as long as coding designed to minimize round-off is used to specify the functional form of the integrands. An abnormal exit will occur if both the error estimate and the integral estimate over a subinterval do not change significantly upon many repeated

subdivisions. This behavior is typical of integrals with cancellation of positive and negative areas.

An abnormal exit for round-off error will also occur if the error estimate repeatedly increases after a large number of subdivisions has been made. It should be noted that a certain amount of round-off error can accumulate even with a normal exit. This underscores the necessity of checking the reliability of an integration routine with test functions, as well as comparing the results of the routine for different tolerances.

D. Integration Difficulties

In order to use the integration routine QAG, we require a finite interval to subdivide. However, the integrals in expressions (3.1-3.3) and (3.18-3.22) all possess an infinite upper limit of integration. We handle this problem by dividing the range of integration for each integral into a finite interval, $q = [0,b]$, and a semi-infinite one, $q = [b,\infty]$. We will discuss first the numerical techniques for handling the integrals over the finite range. For now, we take $b > 2k_f$; this confines all of the singularities and derivative singularities to the finite part of the interval of integration. We will discuss the choice of b in more detail when we treat the problems associated with integration over the semi-infinite interval, $q = [b,\infty]$.

1. Singularities

For adaptive n-point Gauss-Kronrod quadrature over a finite range of integration, the greatest accuracy can be achieved with the smallest number of integrand evaluations if several conditions are met. The integrand should be continuous (or bounded and piecewise continuous) over the interval of integration. The first 2n derivatives should be bounded over the interval of integration, and there should be no integrand singularities in the complex plane near the interval of integration.[26] If any of these conditions is not satisfied, obtaining the desired accuracy will be more difficult.[29] If the integrand is not bounded, obtaining the desired accuracy may be impossible. We note that none of the integrands in Eqs. (3.1-3.3) and (3.18-3.22) satisfy the conditions above for the interval of integration [0,b]. There are singularities near the interval of integration, as well as a derivative singularity at $q = 2k_f$ for each integrand. In addition, several of the integrands are unbounded at $q = 2k_f$. We treat each of these problems below.

None of the off-interval singularities represents a significant problem. Each integrand contains two poles on the imaginary axis, at $q = \pm 2i$, from the terms in Q of the form

$$(1 + \rho^2 q^2)^{-2} = (1 + q^2/4)^{-2} \quad . \tag{3.56}$$

In addition, the integrands in Eqs. (3.2), (3.3), (3.21), and

(3.22) contain branch points at $\eta = -1$, from the $\ell n|\eta+1|$ and $\ell n^2|\eta+1|$ terms. None of these singularities is close enough to $q = 0$ to have a significant effect on the integrand at small q.

The on-interval derivative singularity also does not represent a significant problem. Each integrand contains a weak logarithmic derivative singularity at $\eta = 1$, from the $(\eta-1)\ell n|\eta-1|$ term in the dielectric function, $\varepsilon(q)$. We can use the (15,31)-point integration rules for an integrand of this type over an interval containing the singularity; only a modest number of subdivisions is necessary for good accuracy.

The on-interval singularities, however, do represent a significant problem. All of these singularities result from taking volume derivatives of the dielectric function, and the integrands containing these singularities are unbounded at $\eta = 1$ ($q=2k_f$). Equations (3.3) and (3.22) contain the strong singularity, $(\eta-1)^{-1}$, and the weak singularity, $\ell n^2|\eta-1|$. Equations (3.2), (3.3), (3.21), and (3.22) contain the weak singularity, $\ell n|\eta-1|$.

Ordinary Gaussian quadrature tends to produce large errors for singular integrands, even if the singularities are weak.[29] If any of the abscissas used in the quadrature falls on the singularity, of course, the computed integral will diverge. The errors will tend to be smaller for an adaptive routine, but even if the abscissas manage to "miss" the immediate region around the singularity, which is possible for a single integration over a logarithmic singularity, the routine will be inefficient.

In order to use adaptive Gaussian quadrature, we require continuous integrands (or bounded, piecewise-continuous integrands, as discussed above). Further, we require bounded, or at most, weakly singular first derivatives. Briefly, the procedure is as follows. We first transform each $(\eta-1)^{-1}$ integrand singularity by integration by parts. The resulting integrand will contain only $\ell n|\eta-1|$ and $\ell n^2|\eta-1|$ singularities (see Eqs. (3.50-3.53)). We then "subtract out" the singularity[30] over a finite interval for each divergent term in our integrands. The result is a set of continuous integrands with weak singularities in the first derivatives, plus some analytic terms.

For the $(\eta-1)^{-1}$ term in Eq. (3.3), we integrate by parts over the entire range of integration, with $\eta = q/2k_f$ as the integration variable:

$$\int_0^{\infty} \frac{4k_f V_a}{3} \frac{Q}{D^2} \frac{\varepsilon_2 \eta}{(\eta+1)(\eta-1)}\, d\eta = P \left|_o^{\infty} \frac{4k_f V_a}{3} \frac{Q\varepsilon_2 \eta}{D^2\,(1+\eta)} \ell n|\eta-1|\right.$$

$$- P \int_0^{\infty} \frac{4}{3} k_f V_a \frac{d}{d\eta}\left[\frac{Q\varepsilon_2 \eta}{D^2\,(\eta+1)}\right] \ell n|\eta-1|\, d\eta \quad . \qquad (3.57)$$

The integrated part in Eq. (3.57) can be rewritten

$$\lim_{\delta\to 0} \left\{ \left|_o^{\infty} \frac{4}{3} k_f V_a \frac{Q}{D^2} \frac{\varepsilon_2 \eta}{(\eta+1)} \ell n\,|\eta-1| - \right|_{1-\delta}^{1+\delta} C(1) \ell n|\eta-1| \right\} \quad , \quad (3.58)$$

where the slowly varying terms are taken at $\eta = 1$, and $C(1)$ is a

constant. The first expression in Eq. (3.58) vanishes. The second expression also vanishes, by Eq. (3.52). The integral on the right in Eq. (3.57) can be rewritten

$$P\int_0^\infty 2k_f(f_7(q)\ln|\eta-1| + f_8(q)\ln^2|\eta-1|)d\eta \quad , \tag{3.59}$$

where

$$f_7(q) = \frac{-2}{3}\frac{V_a\varepsilon_2}{D^2}\frac{1}{\eta+1}(1-\rho^2q^2)\left(\frac{\beta}{\pi^2}\frac{q^2}{(1+\rho^2q^2)^3} - \frac{\beta^2}{8\pi^3}\frac{q^4}{(1+\rho^2q^2)^5}\right)$$

$$+\frac{2}{3}\frac{V_a\varepsilon_2}{D^2}\frac{Q}{\eta+1}\left(\frac{\eta}{\eta+1} - 4Y\right)$$

$$+\frac{2}{3}\frac{V_a\varepsilon_2}{D^3}\frac{Q}{\eta+1}\left[2+4Y+4\varepsilon_1Y^2 - 6V_a\varepsilon_2(1-Y)\ln|\eta+1|\right] \quad , \tag{3.60}$$

and

$$f_8(q) = \frac{4V_a^2\varepsilon_2^2}{D^3(\eta+1)}Q(1-Y) \quad . \tag{3.61}$$

The functions $f_7(q)$ and $f_8(q)$ are bounded and continuous over $0 \leq \eta \leq \infty$, and their leading terms at large η vanish faster than η^{-3} as $\eta\to\infty$. By Eqs. (3.44)-(3.49), the integral in Eq. (3.59) exists.

We can now rewrite the integrand in Eq. (3.3), replacing the strongly singular $(\eta-1)^{-1}$ term with weaker logarithmic singularities. This gives

$$\frac{\Omega^{**}}{N} = g_3(V) + \int_0^\infty \{f_3(q) + (f_4(q) + f_7(q))\ln|\eta-1|$$

$$+ \frac{f_5(q)}{(\eta+1)}(\eta-1)\ln^2|\eta-1|\}dq \quad . \tag{3.62}$$

Note that the new $\ln^2|\eta-1|$ term is continuous at $\eta = 1$, by Eq. (3.48). The $(\eta-1)^{-1}$ term in Eq. (3.22) can be treated in the same way. This gives

$$\phi^{**} + \frac{2}{3}\phi'^{*} = 2\int_0^\infty \{[f_3(q) + (f_4(q) + f_7(q))\ln|\eta-1|$$

$$+ \frac{f_5(q)}{(\eta+1)}(\eta-1)\ln^2|\eta-1|]\frac{\sin qr}{qr}$$

$$+ \frac{2}{3}[f_1(q) + \frac{\eta}{\eta+1}f_2(q)\ln|\eta-1|](\cos qr - \frac{\sin qr}{qr})\}dq \quad . \tag{3.63}$$

We still need to transform the singular terms in Eqs. (3.2), (3.21), (3.62), and (3.63). These singularities are all of the form $f(\eta)\ln|\eta-1|$ and can all be handled in the same fashion. We "subtract out" each of these singularities on a part of its finite interval of integration that includes the singularity. The general method for "subtracting out" a singularity is to replace a singular integrand $f(x)$ with the integrand $f(x) - g(x)$. The new integrand should be continuous with as many bounded derivatives as possible. The integral of $g(x)$, which should be known in closed form, is then added.

We take $f(x) = f(\eta)\ln|\eta-1|$, $g(x) = f(1)\ln|\eta-1|$, and "subtract out" the singularity on the interval $\eta = [0,a]$, where $a \gtrsim 1$. This gives

$$\int_0^b f(\eta)\ln|\eta-1|d\eta = \int_0^a [f(\eta) - f(1)]\ln|\eta-1|d\eta + P\int_0^a f(1)\ln|\eta-1|d\eta + \int_a^b f(\eta)\ln|\eta-1|d\eta \quad . \tag{3.64}$$

The first integrand on the right of Eq. (3.64) is bounded at its limits of integration, and continuous over [0,a], since, from the discussion following Eq. (3.47),

$$\lim_{\eta\to 1} [f(\eta)-f(1)]\ln|\eta-1| = f(1) \lim_{\eta\to 1} [(\eta-1)\ln|\eta-1|]\ln|\eta-1| = 0 \quad . \tag{3.65}$$

The second integral on the right has the elementary solution $f(1)[(a-1)\ln(a-1) - a]$. The third integrand on the right is bounded and continuous over $\eta = [a,b]$, since there is no singularity on its interval of integration.

The third integrand does have an off-interval singularity at $\eta = 1$. From the previous discussion of the effects of similar off-interval singularities, we choose $a = 2$; the singularity at $\eta = 1$ should then have virtually no effect on the integration. For the purposes of integration over q, we note that $2k_f \sim 1$ for the range of volumes used, and $\eta = 2$ corresponds to $q \sim 2$. Hence, we choose the interval $q = [0,2]$ to subtract out the singularity. We can now rewrite each of the singular integrands in Eqs. (3.2),

(3.62), (3.21), and (3.63) as a piecewise continuous integrand with a jump discontinuity at q = 2, plus an analytic term. We have

$$\frac{\Omega^*}{N} = g_2(V) + f_2(2k_f)P(2)$$

$$+ \int_0^\infty \{f_1(q) + (f_2(q) - f_2(2k_f)\omega(q))\ln|\eta-1|\}dq \quad , \tag{3.66}$$

$$\frac{\Omega^{**}}{N} = g_3(V) + (f_4(2k_f) + f_7(2k_f))P(2)$$

$$+ \int_0^\infty \{f_3(q) + \frac{f_5(q)}{\eta+1}(\eta-1)\ln^2|\eta-1|$$

$$+ [(f_4(q) + f_7(q)) - (f_4(2k_f) + f_7(2k_f))\omega(q)]\ln|\eta-1|\}dq \quad , \tag{3.67}$$

$$\phi^* = f_2(2k_f)\frac{\sin 2k_f r}{k_f r}P(2) + 2\int_0^\infty \{f_1(q)\frac{\sin qr}{qr}$$

$$+ (f_2(q)\frac{\sin qr}{qr} - f_2(2k_f)\omega(q)\frac{\sin 2k_f r}{2k_f r})\ln|\eta-1|\}dq \quad , \tag{3.68}$$

$$\phi^{**} + \frac{2}{3}\phi'^* = (f_4(2k_f) + f_7(2k_f))\frac{\sin 2k_f r}{k_f r}P(2)$$

$$+ \frac{2}{3}f_2(2k_f)(\cos 2k_f r - \frac{\sin 2k_f r}{2k_f r})P(2)$$

$$+ 2\int_0^\infty \{[f_3(q) + \frac{f_5(q)}{\eta+1}(\eta-1)\ln^2|\eta-1|]\frac{\sin qr}{qr}$$

$$+ \frac{2}{3}f_1(q)(\cos qr - \frac{\sin qr}{qr})$$

$$+ \left[\left(f_4(q) + f_7(q)\right) \frac{\sin qr}{qr} - \left(f_4(2k_f) + f_7(2k_f)\right)\omega(q) \frac{\sin 2k_f r}{2k_f r} \right]$$

$$\times \ln |\eta-1| + \frac{2}{3} \left[\frac{\eta f_2(q)}{\eta+1} \left(\cos qr - \frac{\sin qr}{qr}\right) \right.$$

$$\left. - \frac{f_2(2k_f)\omega(q)}{2} \left(\cos 2k_f r - \frac{\sin 2k_f r}{2k_f r}\right) \right] \ln|\eta-1| \Big\} dq \quad , \tag{3.69}$$

where

$$P(2) = (2 - 2k_f) \ln \left| \frac{1-k_f}{k_f} \right| - 2 \quad , \tag{3.70}$$

and

$$\omega(q) = 1 \text{ for } q \leq 2 \quad , \tag{3.71}$$

$$\omega(q) = 0 \text{ for } q > 2 \quad . \tag{3.72}$$

It should be noted that there are removable (or apparent) singularities at $q = 2k_f$ $(\eta=1)$ for any integrand of the form $\left[f(\eta) - f(1)\right]\ln|\eta-1|$ as well as for any integrand containing the factor ε_1. In these cases, the limit of the integrand as $q \to 2k_f$ exists, but the $\ln|\eta-1|$ factors diverge. The limit of the integrand is taken only if an abscissa of the integration rule falls on $q = 2k_f \pm 10^{-14}$.

There are also removable singularities at $q = 0$ for all integrands, since ε_1, ε_2, etc., diverge at this point. This presents no problems for two reasons. First, Gaussian integration does not use interval endpoints as abscissas. Second, the

integrands are quite smooth for $q = [0,0.5]$, even for large r. This interval is never subdivided so finely that machine accuracy for q near zero is a problem, and it is therefore not necessary to specify a limit as $q \to 0$ in the integrand evaluation routines.

2. Infinite Upper Limit of Integration

The integrals in Eqs. (3.1), (3.18)-(3.20), and (3.66)-(3.69) are all amenable to adaptive integration if the semi-infinite range of integration $[0,\infty]$ is replaced with a finite range $[0,b]$. This leaves the problem of integration over the remaining semi-infinite interval $[b,\infty]$. The method of integration over the semi-infinite range depends on the nature of the integrand; the nonoscillatory V-dependent integrals and the oscillatory (r;V)-dependent integrals must be handled differently. In the former case, the semi-infinite interval can be mapped onto a finite interval, using a change of variable. In the latter case, a series of integrations over a finite part of the semi-infinite interval can be used to extrapolate the value of the integral over the entire interval.

a. V-dependent Integrals. We treat the simpler case of the V-dependent integrals first. We make the change of variable[26]

$$t = b/q \tag{3.73}$$

for the interval $[b,\infty]$. This gives

$$\int_b^\infty f(q)dq = \int_0^1 \frac{b}{t^2} f\left(\frac{b}{t}\right) dt \quad . \tag{3.74}$$

The transformation provides a finite interval for the integration routine. The transformed integrand is bounded and continuous over the interval of integration for $b > 2k_f$. We show first that the integrand is bounded at zero (it is certainly bounded at 1 for $b > 2k_f$). The leading term in the integrand at large q goes as $q^{-4}\ln q$ for Eq. (3.67), and as q^{-4} for Eqs. (3.1) and (3.66). Hence, the leading term in each transformed integrand goes to zero faster than t, as $t \to 0$. The transformed integrands are also continuous, since f(q) is continuous for $q > 2k_f$. Hence, the transformed integrals exist and are suitable for evaluation by QAG.

For efficient numerical integration we choose b large enough so that the magnitude of the integrand f(q) is monotonically decreasing for $q > b$. For all of the V-dependent integrals, $b > 7$ satisfies this requirement. Ideally, b should be chosen to minimize the combined number of interval subdivisions for q = [0,b] and t = [0,1]. We find that b = 8 gives reasonable results for each of the three V-dependent expressions.

b. (r;V)-dependent Integrals. Evaluation of the (r;V)-dependent integrals over the interval $[b,\infty]$ presents a more difficult problem. These integrands contain sin qr and cos qr terms, with r between 5 and 27. The change of variable described above is in general not suitable for such oscillatory integrands.

Instead, we transform each integral over $[b,\infty]$ to an infinite series, and speed up convergence with the Euler transformation.[26]

To obtain an infinite series, we note that an integrand which oscillates around zero contributes alternating positive and negative areas to the integral. We can treat these areas as terms in an infinite alternating series and sum the series. An integrand containing both sine and cosine terms can be divided into two integrands; there will then be two such series. For large q, the leading terms in the (r;V)-dependent integrands go as $q^{-3}\sin qr$ (3.20), $q^{-4}\cos qr$ (3.19 and 3.69) and $q^{-5}\sin qr$ (3.18 and 3.68). Hence, the resulting infinite series will converge.

We set the minimum value of b such that the magnitude of the nonoscillatory factor of each integrand is monotonically decreasing for $q > b$; the error in the series sum can then be taken as the magnitude of the first neglected term. As an estimate of the sum of the infinite series, this process gives very poor results for the (r;V)-dependent integrands, since the infinite series converge very slowly. For b ranging from 15 to 25, and for alternating series of 5-10 terms, the error is of the order of the sum itself. This is not a serious problem for small r ($r \sim 5$-10) for all of the (r;V)-dependent integrals except Eq. (3.20), the uncertainty in the sum of the infinite series is usually much smaller than the numerical integration error. For larger r, however, the oscillations in the finite interval make the contribution of the tail of the integrand relatively more

important. For the slowly converging integrand in Eq. (3.20), the contribution of the tail of the integrand is of the same order as the value of the integral over [0,b] for b > 10. The tail of the integrand is also important in cases where the integral over [0,b] and the analytic part of the expression tend to cancel.

To speed up convergence of the alternating series, we apply an Euler transformation. The formal transformation can be written[26]

$$u_0 - u_1 + u_2 - \ldots\ldots = \frac{1}{2} u_0 - \frac{1}{4} \Delta u_0 + \frac{1}{8} \Delta^2 u_0 - \ldots\ldots, \quad (3.75)$$

where

$$\Delta u_0 = u_1 - u_0 \ ,$$

$$\Delta^2 u_0 = \Delta(\Delta u_0) = u_2 - 2u_1 + u_0 \ , \quad (3.76)$$

etc. If the original series on the left of Eq. (3.75) is convergent, it can be proved that the transformed series on the right is convergent, and that both series converge to the same value. This transformation is particularly convenient for the (r;V)-dependent expressions; the transformed series converges much faster than the original series for all of these integrals.

In general, the slower the original series converges, the faster the transformed series converges and the more accurate the extrapolation becomes.[26] In order to improve the accuracy of the

extrapolation we integrate over five loops of the sine or cosine function ($\Delta q = 5\ \pi/r$) for each term of the series. This large interval gives smaller differences between series terms than a small interval containing only one loop per term. In addition, an interval containing five loops requires no subdivision by QAG for a (15,31) point rule and a relative error tolerance of $< 10^{-7}$.

We can also improve the accuracy of the extrapolation by increasing b. In this case, the accuracy of a sum of n terms of the original series also improves, but the accuracy of an extrapolation using a linear combination of these n terms improves much more quickly.

We take the extrapolation error to be the magnitude of the last term in the transformed series. This quantity tends to be somewhat larger than the actual error, and can serve as a cautious estimate of the uncertainty in the extrapolation.

For efficient extrapolation, we choose b large enough so that the magnitude of the nonoscillatory factor of the integrand is monotonically decreasing for $q > b$. For all of the (r;V)-dependent integrands, $b > 7$ satisfies this requirement. We also find that for $r > 4$ and $b > 15$, extrapolation using 2-20 terms of the transformed series gives better accuracy than merely summing 2-20 terms of the original series. We therefore choose $b = 16$ and extrapolate using the second through the tenth terms of the alternating series. The first term, which is simply added to the

extrapolation sum, is the integral from b to the nearest node of the integrand on $[b,\infty]$.

3. Round-off Error

Evaluation of the (r;V)-dependent expressions presents another noticeable problem. These expressions involve only the effective potential, $\phi(r;V)$, and its derivatives with respect to r and V. From Fig. 3, it can be seen that $\phi(r;V)$ is oscillatory with respect to r, with several nodes between r = 5 and 27. Each of the four other expressions is likewise oscillatory.

Near any of these nodes there will be considerable cancellation of positive and negative areas for the integrals. This is a definite source of round-off error, as discussed above under abnormal exits. We can minimize round-off error, of course, by requiring as large an error tolerance as possible. We can also accept a few isolated occurrences of round-off error near the nodes, since the absolute error will be very small.

The general procedure is merely to identify, during integration program execution, any cases where the relative error tolerance is not satisfied due to round-off error. These cases can be examined later. For a relative error tolerance of 10^{-4}, we find that round-off error is not a significant problem.

E. Numerical Integration Procedure

We can now summarize the complete integration procedure. The three V-dependent expressions that we need to evaluate are given by Eqs. (3.1), (3.66), and (3.67). The five (r;V)-dependent expressions are given by Eqs. (3.18)-(3.20) and (3.68)-(3.69). The factors $g_i(V)$, $h_i(r)$, and P(2) are given by Eqs. (3.4)-(3.6), (3.23)-(3.25) and (3.70), respectively. The factors $f_i(q)$ are given by Eqs. (3.7)-(3.12) and (3.60)-(3.61); the individual parts of the $f_i(q)$ are given by the equations following Eq. (3.12).

We divide each interval of integration into a finite and a semi-infinite part, and take all of the analytic parts under the integral sign for the finite interval, as illustrated in Eq. (3.54). This gives, for example, for Eq. (3.1),

$$\int_0^b \left[\frac{Q\varepsilon_1}{D} + \frac{g_1(V)}{b}\right] dq + \int_b^\infty \frac{Q\varepsilon_1}{D}\, dq \quad . \tag{3.77}$$

The extension to the other expressions is obvious.

1. Procedure for V-dependent Integrals

For each V-dependent expression, we take b = 8 and apply a change of variable to the integral over q = [b,∞], as given in Eqs. (3.73)-(3.74). The transformed integral now has a finite range of integration, t = [0,1]. We require a relative error tolerance of 10^{-6} for both the integral over q = [0,8] and the integral over t = [0,1]. Since the value of the integral over

[0,8] dominates each expression, the relative error for each expression will be less than 10^{-6}. Evaluation of all three expressions for a given V takes only a fraction of a second of computer time on the CRAY-1, and entails no integration difficulties for the range of volumes given in Eq. (3.30).

2. Procedure for (r,V)-dependent Integrals

For each (r;V)-dependent expression we take b = 16. For the [16,∞] interval (but not for the finite interval) we divide any integrand containing both sine and cosine terms into two integrands.

For each integrand, we generate the first ten terms of an infinite series. For an integrand containing a sin qr term, we integrate over the intervals

$$q = [16,b'],\ [b',b' + 5\pi/r],\ldots,\ [b' + 40\pi/r,\ b' + 45\pi/r] \quad , \tag{3.78}$$

where b′ is the first node of sin qr on the interval q = [16,∞]. We extrapolate the value of the infinite series by taking the Euler transformation given in Eq. (3.75), where u_0 corresponds to the second term of the series in Eq. (3.78).

For example, for Eq. (3.18) we then have

$$\phi = \int_0^{16} \left[\frac{2Q\varepsilon_1}{D}\frac{\sin qr}{qr} + \frac{h_1(r)}{16}\right] dq + \int_{16}^{b'} \frac{2Q\varepsilon_1}{D}\frac{\sin qr}{qr}\, dq + \text{extrapolation sum} \quad , \tag{3.79}$$

where the extrapolation sum is the sum of the first nine terms of the transformed series. This procedure is easily extended to an expression containing both sine and cosine terms in its integrand.

We require a relative error tolerance of 10^{-4} for each (r;V)-dependent expression; two iterations of the integral over [0,16] suffice for QAG to return a calculated error estimate that satisfies this tolerance, except for a few isolated cases of round-off error. We apportion the error tolerance among the various integral contributions as follows. For the first iteration of the integral over [0,16], we require a relative error tolerance of 8.5×10^{-5}. For an integral containing only a sin qr term, we require a relative error tolerance of 4.0×10^{-7} for the integration over [b,b'] and for each integration over [b'+mπ/r, b'+(m+5)π/r], where the values of m are given in Eq. (3.78). We then take the extrapolation error to be the magnitude of the last extrapolation term. For an integral containing both sin qr and cos qr terms, we require a relative error tolerance of 2.0×10^{-7} for each integral on the range of integration [b,∞].

If the relative integration error calculated by routine QAG for the entire expression is greater than 10^{-4}, and round-off error is not present, we repeat the integration over [0,16]. For this second iteration, we require an absolute error tolerance E_{abs}:

$$E_{abs} = 10^{-4} \left| \int_0^{\infty} f(q)dq \right| - \text{err}\,[16,\infty] \quad , \qquad (3.80)$$

where the integral in the first term is the previous result for the (r;V)-dependent expression, and err [16,∞] is the total calculated error over the semi-infinite range. Evaluation of all five (r;V)-dependent expressions for a given V and r takes between 0.3 and 0.6 seconds on the CRAY-1, with minimal integration difficulties.

CHAPTER 4

MOLECULAR DYNAMICS PROCEDURES

We now consider the details of our molecular dynamics simulations. We wish to calculate the pressure and the adiabatic elastic constants for bcc sodium at each of the temperatures given in Table I. We first establish an appropriate system of units for these calculations. We then discuss the setup of the MD runs and the interpretation of the MD output.

A. Units

As discussed in Chapter 2, we use atomic units for length and energy. From Eq. (2.4), we have, for length in Bohr radii and energy in Rydbergs,

$$a_0 = 1 \quad , \tag{4.1}$$

$$e^2/2a_0 = 1 \quad . \tag{4.2}$$

We take the mass of a sodium ion, M_0, as unity:

$$M_0 = 1 \quad . \tag{4.3}$$

The natural time unit is

$$t_0 = a_0 \left(\frac{2\, M_0 a_0}{e^2}\right)^{1/2} \quad , \tag{4.4}$$

which corresponds to $\sim 7\times10^{-15}$ seconds. The temperature is measured in Kelvins (K), and the pressure in Ry/a_0^3.

B. Molecular Dynamics Setup

The computer simulations were performed using the continuous potential MD routine MOLDY developed at Los Alamos National Laboratory. Principal collaborators for this version of the code included G. K. Straub, S. K. Schiferl, B. L. Holian, J. R. Beeler, and J. D. Johnson. We have already described this code's algorithms for integration of the equations of motion and implementation of periodic boundary conditions. We discuss below the initial setup of an MD routine for the calculation of pressure and elastic constants.

For all MD runs, we use a cubic computational box. For a typical number of atoms N = 686, this gives a box length of $\ell = 7a$ for bcc structures, where a is the lattice parameter. We use the experimental volumes (in terms of V_a, the volume per atom) for bcc sodium at atmospheric pressure for all of our calculations. We use the thermal expansion data of Adlhart et al.[31] to obtain volumes for the temperature range 300 K-371 K; we use the thermal expansion data of Siegel and Quimby[32] to obtain volumes for the temperature range 80 K-300 K. Both sets of experimental data were scaled to agree with the lattice parameter measured by Feder and Charbnau[33] at 298.15 K. We calculate the volume for bcc sodium at 0 K by extrapolation from the above measurements. The volumes and numbers of atoms used in our computer simulations are listed in Table I.

The static lattice calculations with N = 43904 were performed for the purpose of investigating the effects of varying the range of the effective potential.

To calculate the ensemble averages in Eq. (1.20) and Eqs. (1.24)-(1.26), we set up the MD routine to compute the following mechanical quantities for each time step Δt: E_{KI}, $\sum \phi^*$, $\sum \phi' x x$, $\sum \phi' x y$, $\sum \phi'$, $\sum (\phi^{**} + \frac{2}{3}\phi'^*)$, $\sum (\phi''-\phi')x^4$, and $\sum (\phi''-\phi')x^2y^2$, where E_{KI} is the total kinetic energy of the ions in the computational box. The sums are taken over all distinct pairs of indices K,L: K is taken over all ions in the computational box; L is taken such that the distance

$$r_{KL} = |\underset{\sim}{r}_K - \underset{\sim}{r}_L| \tag{4.5}$$

is within the range of the effective potential, and $L \neq K$. The routine will also calculate the total mechanical energy E_T:

$$E_T = E_{KI} + \sum \phi(r,V) = H - \Omega(V) \quad . \tag{4.6}$$

The MD routine must be supplied with a table of all five (r;V)-dependent expressions (see Chapter 3) for each volume used. The routine is then directed to interpolate from the table to find the necessary values of the expressions. We choose a linear interpolation scheme, which requires a minimum number of operations per look-up. We discuss below the choice of the interval, the minimum r, and the maximum r for the table.

The interval, Δr, is chosen to be small enough so that the effects of interpolation errors on any pressure or elastic constant calculation can be ignored (see Chapter 5). We take $\Delta r = 0.01$; the relative interpolation error for any (r;V)-dependent expression is then less than 2×10^{-5}.

We choose a minimum r, r_{min}, to indicate an energetically unlikely configuration for the MD system. If the MD routine encounters $r < r_{min}$, a warning message will be sent and the particular run can be examined for errors. We take

$$\phi\,(r_{min};V) \sim 10\,\langle E_{KI}/N\rangle \quad . \tag{4.7}$$

As discussed below, the initial conditions for an MD run are chosen so that the equilibrium time average of the ion kinetic energy differs by less than 10% from the initial ion kinetic energy. Hence, we can select r_{min} according to the desired temperature T, and

$$\phi\,(r_{min};V) \sim 17\ kT \quad . \tag{4.8}$$

The values of r_{min} used in these simulations are given in Table I. For the bcc static lattice calculations at $V_a = 254.921\ a_0^3$, we choose $r_{min} = 6.91\ a_0$, since the nearest neighbor distance for the perfect crystal is approximately $6.918\ a_0$.

The maximum r, r_{max}, determines the range of the (r,V)-dependent expressions. If the MD routine encounters $r > r_{max}$, the values of all of these expressions are taken to be zero. The value of r_{max} is chosen to satisfy several criteria. First, by the nearest image convention (see Chapter 1), $r_{max} < \ell/2$, where ℓ is the length of the computational cell. Second, the possible values of r_{max} are limited to zeros of the force function $-\phi'/r$, so that the force between two particles as they move out of range passes smoothly to zero. Third, r_{max} should be large enough to minimize the errors in the simulation due to the effects of this finite cutoff. We choose r_{max} to be the fourth node of $-\phi'/r$ following the initial well (see Fig. 4). The errors due to use of a finite cutoff are discussed in Chapter 5. The values of r_{max} are given in Table I.

The MD time step Δt should be small enough so that the total energy H (or the total mechanical energy $E_T = H - \Omega(V)$) is conserved, and so that the fluctuations of $\sum\phi_{xx}$, $\sum\phi_{xy}$, etc., are adequately sampled. To calculate a reasonable time step for energy conservation, we take $\sim 1/50$ of the characteristic oscillation period T_0 of a sodium ion in the MD system. Swanson[22] estimated $T_0 \sim 74\ t_0$; this gives $\Delta t \sim 1.5\ t_0$.

To calculate a reasonable time step for adequate sampling of the fluctuations, we take $\sim 1/50$ of the characteristic time Δt_F for the fluctuations in $\sum\phi_{xx}$. We define Δt_F to be the average time between local maxima (or local minima) for a mechanical quantity in

an equilibrium MD system[10] (see Fig. 5). For $\sum\phi_{xx}$ at T ~ 298 K and $V_a = 266.17\ a_0^3$, we find Δt_F to be ~ 20 t_0; this gives $\Delta t = 0.4\ t_0$.

We find the time step $\Delta t = 0.4\ t_0$ to be satisfactory for our MD runs. For this time step, there is no long term trend in the total energy, and the total mechanical energy E_T fluctuates by only a few parts in 10^5. Hence, the total energy is conserved to within the accuracy of our simulations. We will discuss the problems of fluctuation sampling in Chapter 5.

We begin an MD trajectory by specifying N, V_a, Δt, and a set of initial positions and velocities for the ions. We choose initial conditions to approximate the desired equilibrium state; relaxation to a steady state should then occur quickly. The resulting system should have cubic symmetry and approximately the correct temperature for the given volume.

These initial conditions take the form of a Maxwell distribution of the velocities of the ions, and a Gaussian distribution of the displacements of the ions from a perfect bcc lattice. For each component of velocity a set of values is assigned from a random Gaussian distribution with a rms width of $(kT)^{1/2}$. For each component of displacement the Gaussian distribution has a rms width of $(\overline{u_{xT}^2})^{1/2}$, where

$$(\overline{u_{xT}^2})^{1/2} = B_T/8\pi \quad , \tag{4.9}$$

and B_T is the thermal Debye parameter.[34]

In practice, we generate an initial velocity distribution so that the desired temperature is ~ 95% of the value of the parameter T in the width of the distribution. We then integrate the equations of motions for 250 time steps but rescale the velocities of the ions at each time step so that the total kinetic energy remains constant. After 250 time steps the scaling ceases and the system is allowed to relax. After a few hundred more time steps the kinetic energy usually reaches a steady state and the temperature of the system can be estimated. The trajectory can be restarted with slightly different initial conditions if the estimated temperature is not sufficiently close to the desired value.

C. Interpretation of Molecular Dynamics Data

We now consider the evaluation of MD time averages for the mechanical quantities in Eqs. (1.20) and (1.24)-(1.26). We follow the procedures given in Schiferl and Wallace[10] for determining equilibration times and for establishing confidence limits for MD ensemble averages; an extension of these methods is used for evaluation of fluctuation averages. A brief outline of these procedures and their application to calculations of the pressure and the elastic constants is given below. Tests for symmetry of an MD system will also be described.

1. Confidence Limits for Ensemble Averages

As discussed in Chapter 1, the output of an MD run for a mechanical quantity A consists of values of A calculated at each time step:

$$A_i = A(i\Delta t),\ i = 1,2 \ldots\ . \tag{4.10}$$

These "raw data" are highly correlated, and not quite normally distributed for our MD systems. To obtain data which are normally distributed and approximately random, while preserving the weight function for time averages of A(t), we construct coarse-grained, or time-smoothed data. The series of points A_i, over a time interval $\tau = mn\Delta t$, is divided into sequential nonoverlapping segments k, $k = 1,2, \ldots\ldots n$. Each segment has m points, and the mean and variance of the A_i for segment k are denoted a_k and S_k^2, respectively. The n values of a_k constitute a sample, drawn from a population with mean $\langle A \rangle$. The sample mean and variance are $\bar{A}$ and s_A^2, respectively:

$$\bar{A} = \frac{1}{n} \sum_{k=1}^{n} a_k\ , \tag{4.11}$$

$$s_A^2 = \frac{1}{n-1} \sum_{k=1}^{n} (a_k - \bar{A})^2\ . \tag{4.12}$$

If the sample passes statistical tests for normality, for lack of

long term trend, and for randomness, we can assign confidence limits for the ensemble average <A>:

$$\langle A \rangle = \bar{A} \pm \frac{\alpha_n s_A}{\sqrt{n}} \quad , \tag{4.13}$$

where α_n is the 0.975 fractile of "Student's" t distribution with n-1 degrees of freedom. For $n \geq 24$, $\alpha_n \sim 2$.

We need to rewrite the equations for the pressure and the elastic constants in a form more suitable for the sampling described above. From Chapter 1, we have

$$P = O_P(\Omega) + K_P + L_P \quad , \tag{4.14}$$

$$C_{11}^S = O_{11}(\Omega) + K_{11} + L_{11} + F_{11} + X_1 + X_2 \quad , \tag{4.15}$$

$$C_{12}^S = O_{12}(\Omega) + L_{12} + F_{12} + X_1 + X_2 \quad , \tag{4.16}$$

$$C_{44} = O_{44}(\Omega) + K_{44} + L_{44} \quad . \tag{4.17}$$

The strictly volume-dependent terms, $O_\alpha(\Omega)$, are given by

$$O_P(\Omega) = - \Omega^*/V \quad , \tag{4.18}$$

$$O_{11}(\Omega) = (\Omega^{**} - \Omega^*)/V \quad , \tag{4.19}$$

$$O_{12}(\Omega) = (\Omega^{**} + \Omega^*)/V \quad , \tag{4.20}$$

$$O_{44}(\Omega) = - \Omega^*/V \quad . \tag{4.21}$$

The kinetic energy terms, K_α, are given by

$$K_p = NkT/V \quad , \tag{4.22}$$

$$K_{11} = 2NkT/V \quad , \tag{4.23}$$

$$K_{44} = NkT/V \quad . \tag{4.24}$$

The linear terms, L_α, are given by

$$L_p = - \langle \sum \phi_{rr} \rangle / V \quad , \tag{4.25}$$

$$L_{11} = \langle \sum \left[\phi^{**} + \frac{2}{3} \phi'^{*} - \phi^{*} + (\phi'' - \phi') f_x^4 \right] \rangle / V \quad , \tag{4.26}$$

$$L_{12} = \langle \sum \left[\phi^{**} + \frac{2}{3} \phi'^{*} + \phi^{*} + (\phi'' - \phi') f_x^2 f_y^2 \right] \rangle / V \quad , \tag{4.27}$$

$$L_{44} = \langle \sum \left[-\phi^{*} + (\phi'' - \phi') f_x^2 f_y^2 \right] \rangle / V \quad , \tag{4.28}$$

where

$$\phi_{rr} = \phi^{*} + \phi'/3 \quad . \tag{4.29}$$

The fluctuation terms, F_α, are given by

$$F_{11} = - \beta \langle \left[\sum \phi_{xx} - \langle \sum \phi_{xx} \rangle \right]^2 \rangle / V \quad , \tag{4.30}$$

$$F_{12} = - \beta \langle \left[\sum \phi_{xx} - \langle \sum \phi_{xx} \rangle \right] \left[\sum \phi_{yy} - \langle \sum \phi_{yy} \rangle \right] \rangle / V \quad , \tag{4.31}$$

$$F_{44} = - \beta \langle \left[\sum \phi_{xy} - \langle \sum \phi_{xy} \rangle \right]^2 \rangle / V \quad , \tag{4.32}$$

where

$$\beta = (kT)^{-1} \quad . \tag{4.33}$$

By symmetry, we can rewrite F_{12} as

$$F_{12} = - \beta \left\langle \frac{3}{2} \left[\sum \phi_{rr} - \left\langle \sum \phi_{rr} \right\rangle \right]^2 - \frac{1}{2} \left[\sum \phi_{xx} - \left\langle \sum \phi_{xx} \right\rangle \right]^2 \right\rangle / V \quad . \tag{4.34}$$

We obtain smaller uncertainties for the ensemble averages of the fluctuations in C_{12} if we use Eq. (4.34) instead of Eq. (4.31). We can also rewrite F_{44} as

$$F_{44} = - \beta \left\langle \left[\sum \phi_{xy} \right]^2 \right\rangle / V \quad , \tag{4.35}$$

since the ensemble average $\left\langle \sum \phi_{xy} \right\rangle = 0$ for a symmetric system. We will discuss tests for symmetry below.

The correction terms, X_α, are given by

$$X_1 = - \frac{NkT}{V} \frac{(\gamma c - 1)^2}{c} \quad , \tag{4.36}$$

$$X_2 = \frac{NkT}{V} \gamma^2 c \quad , \tag{4.37}$$

where X_1 is the ensemble correction, X_2 is the isothermal-adiabatic correction, γ is the Grüneisen parameter, and c is given by Eq. (1.38).

We begin our evaluation of an MD run by determining the equilibration time for the kinetic energy, plus confidence limits for the temperature. Using the procedure given above, we coarse-grain the kinetic energy, E_{KI}. If a coarse-grained sample of n values, over a time interval τ, passes the statistical tests referred to above, we can assign confidence limits according to

$$T = \frac{2}{3Nk}\left[\overline{E_{KI}} \pm \frac{\alpha_n s_K}{\sqrt{n}}\right] , \tag{4.38}$$

where $\overline{E_{KI}}$ is the sample mean, and s_K^2 is the sample variance. The raw data points in this interval τ can be written $A(t_e + i\Delta t)$, $i = 0,1,2 \ldots$, where the kinetic energy equilibration time, t_e, measures the time elapsed since the beginning of the trajectory. We will use Eq. (4.38) to define the temperature of the MD system, and we will use only that portion of the run with $t > t_e$ for equilibrium calculations.

To determine confidence limits for the linear terms, L_α, we coarse-grain the bracketed expressions in Eqs. (4.25)-(4.28). If a coarse-grained sample passes the statistical tests, we proceed as in Eq. (4.13).

To calculate confidence limits for the fluctuation terms in C_{11} and C_{12}, we will need to coarse-grain two mechanical quantities over the same time interval. We demonstrate this procedure for the fluctuation average in F_{11}.

We first coarse-grain the quantity $\sum \phi_{xx}$. If a sample of n values over the interval τ passes the statistical tests, we can assign confidence limits according to

$$\langle \sum \phi_{xx} \rangle = \overline{\sum \phi_{xx}} \pm \frac{\alpha_n s_x}{\sqrt{n}} \quad , \tag{4.39}$$

where $\overline{\sum \phi_{xx}}$ is the sample mean, and s_f^2 is the sample variance. We then coarse-grain the quantity $(\sum \phi_{xx} - \overline{\sum \phi_{xx}})^2 = f_{11}$ over the interval τ. If a sample of m values passes the statistical tests, we can assign confidence limits according to

$$\langle (\sum \phi_{xx} - \langle \phi_{xx} \rangle)^2 \rangle = \overline{f_{11}} \pm \left[\frac{\alpha_m s_f}{\sqrt{m}} + \frac{(\alpha_n s_x)^2 (n-1)}{n \chi^2} \right] \quad , \tag{4.40}$$

where $\overline{f_{11}}$ is the sample mean, s_f^2 is the sample variance, and χ^2 is the 0.025 fractile of the chi-squared distribution for n-1 degrees of freedom.[35] The first term inside the square brackets in Eq. (4.40) is the uncertainty in the average fluctuation of $\sum \phi_{xx}$ around $\overline{\sum \phi_{xx}}$. The second term is the uncertainty in the average fluctuation of $\overline{\sum \phi_{xx}}$ around $\langle \sum \phi_{xx} \rangle$, i.e., the uncertainty in the variance of $\overline{\sum \phi_{xx}}$.

We need to coarse-grain only one expression to obtain the fluctuation average in C_{44}. From Eq. (4.35), we coarse-grain the quantity $[\sum \phi_{xy}]^2$ and assign confidence limits as in Eq. (4.13).

2. Symmetry

To derive Eqs. (4.14)-(4.17) and (4.34)-(4.35), we assumed that the equilibrium MD systems possessed cubic symmetry. We will need to test this assumption for each of our MD runs.

Cubic symmetry requires that

$$\langle \sum f(r) \hat{r}_i \hat{r}_j \rangle = \frac{1}{3} \delta_{ij} \langle \sum f(r) \rangle \quad , \tag{4.41}$$

where f(r) is any r-dependent function. To check the symmetry of a particular MD system, we first test for the equality of $\langle \sum \phi' \hat{r}^2 \rangle$ and $\langle \sum \phi'/3 \rangle$, using a two-sample test for the equality of two population means when the two population variances are different.[35] We then test the hypothesis that $\langle \sum \phi_{xy} \rangle = 0$, using an ordinary t - test.[35] Before applying either of these tests, we take coarse-grained samples and establish that our samples satisfy statistical tests for normality, lack of long-term trend, and absence of both positive and negative correlation. All of the MD systems listed in Table I easily satisfied these tests for a 5% level of significance.

CHAPTER 5

RESULTS AND DISCUSSION

A. Comparison of Theory and Experiment

Our results for the adiabatic elastic constants of bcc sodium are given in Table II. The calculated values for $T > 0$ are compared with the experimental atmospheric-pressure data of Diederich and Trivisonno,[36] Martinson,[37] and Fritsch et al.[38] in Fig. 6. The relative uncertainties in the experimental data, for 95% confidence limits, are approximately 2-3%. The agreement of our MD data with experiment is quite good, particularly for the magnitudes of C_{11} and C_{12}. The agreement with experiment is excellent for the temperature dependences of all three elastic constants.

The agreement of theory and experiment for the temperature dependences illustrates a definite advantage of molecular dynamics (and Monte Carlo) techniques, compared to lattice dynamics calculations, for conditions where classical statistics are valid and anharmonic effects are important. MD and Monte Carlo methods both involve direct calculation of anharmonic effects, eliminating the problems inherent in perturbation treatments of anharmonicity. Evidence that anharmonic effects are significant for bcc sodium at $T > 100$ K, and that anharmonic perturbation theory breaks down for

these temperatures, is given by Straub et al.[7] and by Swanson et al.[4]

We have ignored the effects of the calculated pressure on the elastic constants, in order to compare experimental and theoretical elastic constants at the same densities and temperatures. From Table II, the theoretical pressures are all less than 1.2 kbar. These pressures are quite small, and their differences from zero can be neglected.

1. Quantum Effects

We have omitted quantum effects in our calculations. This approach is generally correct for temperatures such that $T \geq \theta_{H\infty}$, where $\theta_{H\infty}$ is the high-temperature harmonic Debye temperature. For sodium, $\theta_{H\infty} \sim 167$ K.[14] For $T < \theta_{H\infty}$, there will be deviations between classical and quantum calculations, and hence between classical calculations and experimental data. For the elastic constants of sodium, however, these deviations are very small for $T \gtrsim 100$ K.

The deviations can be discussed in terms of approximate temperature dependences.[39] In the classical regime, we expect the elastic constants to vary linearly with temperature. For calculations employing classical statistics, such as our MD simulations, this linear dependence will extend to T = 0 K. In the quantum regime, we expect the values of the elastic constants to approach 0 K with zero slope. We will ignore the small zero-point

vibrational contribution to the elastic constants. Wallace[9] estimates this contribution to be less than 0.6 kbar.

From Fig. 6, small quantum effects in the experimental data are present at the lowest temperatures. These effects take the form of slight deviations from the straight line dependence of $C_{\alpha\beta}$ on T. The MD calculations, of course, do not reproduce this quantum low-temperature curvature. Even at 100 K, however, this curvature is very small, and the experimental results are still approximately classical. For T > 100 K, this indicates that quantum effects on the elastic constants can be ignored.

2. Electronic Excitations

We have neglected the effects of electronic excitations on the pressure and the elastic constants. For temperatures such that $kT \ll e_F$, where e_F is the Fermi energy, we can estimate these effects by treating the excitations as a contribution to the free energy, F_e, where[14]

$$F_e = -\frac{1}{2}\Gamma T^2 \quad . \tag{5.1}$$

For free electrons,

$$\Gamma = \frac{N\pi^2 k^2 mZ}{\hbar^2 k_f^2} \quad , \tag{5.2}$$

where k is Boltzmann's constant, m is the electron mass, and Z is the valence. For sodium, in our units, we can write

$$\frac{\Gamma}{N} = 2.068\times10^{-11}\ V_a^{2/3}\ \frac{\text{Ry K}^2}{\text{atom}} \quad . \tag{5.3}$$

The electronic excitation contributions to the pressure and to the elastic constants are given by

$$P^e = \frac{\Gamma T^2}{3NV_a} \quad , \tag{5.4}$$

$$C_{11}^e = \frac{4\Gamma T^2}{9NV_a} \quad , \tag{5.5}$$

$$C_{12}^e = -\frac{2\Gamma T^2}{9NV_a} \quad , \tag{5.6}$$

$$C_{44}^e = \frac{\Gamma T^2}{3NV_a} \quad . \tag{5.7}$$

These contributions are negligible for the solid under the conditions of our simulations. The maximum excitation contribution to an elastic constant is ~ 0.024 kbar, at T = 340. The maximum contribution to the pressure is ~ 0.017 kbar.

3. The Calculation of C_{44}

The main deficiency of our model appears to be in the calculation of the magnitude of the shear constant, C_{44}. The

temperature dependence agrees well with experiment, but the calculated values of C_{44} are consistently too small.

It is probably not possible to obtain both good agreement with measured bulk properties and good agreement with the measured shear constant from second-order pseudopotential perturbation theory. As discussed in Chapter 3, the three adjustable parameters were fitted to experimental results for the binding energy, the lattice spacing, and the bulk modulus of bcc sodium at zero temperature and pressure.[8] The calculated value of the shear constant, C_{44}, at zero temperature and pressure was approximately 6 kbar smaller than the experimental value.[9] Conversely, Suzuki et al.[40] fitted a pseudopotential to experimental results for the shear constant of bcc sodium, but failed to obtain agreement with the measured value of the bulk modulus.

The most likely source of the discrepancy between experiment and theory for the value of C_{44} is the use of only second-order perturbation theory. We have assumed that we can neglect terms higher than second order in the pseudopotential. However, Harrison[41] indicates that those higher-order terms which introduce three-body interactions can be significant in the determination of crystal structures. The contributions to C_{44} of the strain derivatives of these three-body terms could account for the large, nearly constant difference between experimental and theoretical values for C_{44}, in the form of a geometrical resistance to shear that is not contained in the second-order theory.

B. Theoretical Contributions

Table II gives the various contributions to the theoretical pressure and elastic constants. Several distinctive features of these contributions should be noted. First, some of the fluctuation terms are quite large. At T = 340 K, the magnitude of the fluctuation term in C_{11} is ~ 20% of the elastic constant. For C_{44}, the corresponding figure is ~ 37%. As discussed below, fluctuation terms are notoriously difficult to calculate accurately.

We also note that the strictly volume-dependent terms, $O(\Omega)$, are very large for P, C_{11}, and C_{44}, ranging from - 22 kbar to - 40 kbar. The contribution of $O(\Omega)$ to C_{12}, 5 kbar, is much smaller, but not negligible. Finally, we note that the ensemble correction, X_1, is small but significant at higher temperatures.

Table III shows the effect of the volume dependence of the effective potential on the pressure and the elastic constants. The volume-dependent terms in this table are defined as the contributions to the linear and fluctuation terms that would be zero if the volume derivative of $\phi(r;V)$ were identically equal to zero. The r-dependent terms are the contributions of the position derivatives of $\phi(r;V)$. For example, the volume-dependent part of the linear term in C_{11} is $\langle\sum(\phi^{**} + 2/3\ \phi'^{*} - \phi^{*})\rangle/V$. The corresponding r-dependent part is $\langle\sum(\phi'' - \phi')x^4\rangle/V$.

The most striking feature of this table is the large size of the volume-dependent linear terms: ~ 12 kbar for P and C_{44}, and ~ 25 kbar for C_{11}. These three terms decrease slightly with increasing volume and temperature. The contributions of the volume-dependent fluctuation terms to the elastic constants are not significant.

C. Other Theoretical Work

We discuss briefly two other theoretical calculations of the elastic constants of bcc sodium. Glyde and Taylor[42] performed lattice dynamics calculations for temperatures from 5 K to 361 K. Cohen et al.[43] performed Monte Carlo calculations at temperatures of 293 K and 361 K.

The calculations of Glyde and Taylor are based on an empirical electron-ion potential which was fitted to spectroscopic term values of the isolated ion. The fitted potential was used to construct an effective ion-ion potential. The authors calculated phonon frequencies in the self-consistent harmonic approximation, with a cubic anharmonic term included as a perturbation. The elastic constants were calculated from the long-wavelength limit of the phonon dispersion curves. The results of Glyde and Taylor differ from experiment considerably more than the present MD results; our agreement with experiment is better for both the magnitudes and temperature dependences of the elastic constants.

The calculations of Cohen et al. are based on a pseudopotential model which includes exchange and correlation effects. The pseudopotential was used to construct an effective ion-ion potential. The stresses and the elastic constants were obtained by taking the expressions derived by Hoover et al.[44] for the adiabatic elastic constants of argon. These expressions are the strain derivatives of the Helmholtz free energy for a volume-independent pair potential.

These Monte Carlo calculations are seriously flawed by several problems. First, the volume dependence of the effective potential was ignored. The form of the effective potential, however, is not volume independent. The volume dependence enters through the dielectric function, $\varepsilon(q)$, in the integrand of the expression for $\phi(r;V)$, and through a volume-dependent term in an interpolation approximation for the effect of exchange and correlation on the screening. These are the same kinds of volume dependences that we encounter in our effective potential. From Table III, it can be seen that the contributions of the volume derivatives of our effective potential to the pressure and the elastic constants are significant. The contributions of these volume derivatives to P, C_{11}, and C_{44}, in particular, are very large.

Second, the authors make a conceptual error in the comparison of their calculations of the elastic constants with

experiment. They evaluate the stress-strain derivatives, or Birch coefficients, $B_{ijk\ell}$, where[14]

$$B_{ijk\ell} = \frac{\partial \tau_{ij}}{\partial \eta_{k\ell}} \quad , \tag{5.8}$$

and, in Voigt notation:

$$B_{11} = C_{11} - P \quad , \tag{5.9}$$

$$B_{12} = C_{12} + P \quad , \tag{5.10}$$

$$B_{44} = C_{44} - P \quad . \tag{5.11}$$

The pressure P used by the authors is the pressure calculated from the equations of Hoover et al.[44] for a volume-independent potential. This pressure, which we will call $\tilde{P}$, is ~ 7 kbar. The authors then compare the theoretical Birch coefficients at ~ 7 kbar with the experimental elastic constants at ~ 0 kbar. These are considerably different physical quantities. From Martinson's[37] analysis, the experimental Birch coefficients at 7 kbar are larger than the experimental Birch coefficients at 0 kbar by ~ 27-38%.

Third, following these Birch coefficient calculations, the authors introduce a strictly volume-dependent potential, $\Omega(V)$, for the purpose of investigating electron gas contributions to the elastic constants. However, the contributions to the elastic constants of $\Omega^* = V\partial\Omega(V)/\partial V$ were ignored.

The form of $\Omega(V)$ is given by Basinski et al.:[45]

$$\Omega(V) = N \left(\frac{3}{5} e_F + X(\rho_0) + \frac{A}{V}\right) , \qquad (5.12)$$

where e_F is the Fermi energy, $X(\rho_0)$ is the exchange and correlation energy per electron of a uniform electron gas, and A is an adjustable parameter. $X(\rho_0)$ is given by Eq. (2.75) above. The value of A is determined by requiring the total pressure P, including the Ω^* contribution, to be zero.

The authors calculated the contributions of $\Omega^{**} = V^2\partial^2\Omega(V)/\partial V^2$ to the C_{11} and C_{12} elastic constants for the form of $\Omega(V)$ above. They obtained $\Omega^{**}/V = 2.36$ kbar for T = 293 K, and 1.46 kbar for T = 361 K. These contributions were considered negligible. The contributions of Ω^* to the elastic constants are considerably larger. We have, for a volume-independent pair potential, $\phi(r)$,

$$PV = -\Omega^* + NkT - \langle \sum \phi'/3 \rangle = -\Omega^* + \tilde{P}V \quad . \qquad (5.13)$$

Introducing the condition P = 0 gives

$$\Omega^*/V = \tilde{P} \quad . \qquad (5.14)$$

Hence, the authors' neglect of the contribution of Ω^* to the elastic constants gives an error of $-\tilde{P}$ for C_{11} and C_{44}, and $+\tilde{P}$ for C_{12}. Taking the Birch coefficients gives the same mathematical result as including the contribution of Ω^* in the elastic constants, but not the same physical interpretation.

Finally, we note that an appropriate form for $\Omega(V)$ for pseudopotential sodium can be derived without requiring an empirical expression with an adjustable parameter. We show how to derive such an expression for $\Omega(V)$ in Chapter 2 of this dissertation, using only the information necessary to determine the effective potential. The functional form of $\Omega(V)$ is given by the bracketed terms in Eq. (2.92), and by Eq. (2.99). This form differs significantly from the parameterized expression in Eq. (5.12). While the first two terms in Eq. (2.92) and Eq. (5.12) are identical, none of the remaining terms in our expression for $\Omega(V)$ goes as V^{-1}.

D. Sources of Computational Error

By far the largest source of computational error in our calculations is the statistical error in the MD averages. We will discuss this statistical error below. We will also discuss several smaller sources of computational error: integration and interpolation error, cutoff error, and system size effects.

1. Statistical Error

The error bars in Fig. 6 correspond to the statistical uncertainties in the MD averages. The various contributions to these uncertainties are given in Table IV. To obtain the uncertainty in the total correction term $X_1 + X_2$, we take the relative uncertainties in γ, the Grüneisen parameter, and C_v, the specific heat, to be $\sim 2\%$, where the values of C_v and γ are obtained from Ref. 7.

The dominant statistical uncertainty in any elastic constant calculation is clearly the uncertainty in the fluctuation term. The uncertainty in a fluctuation average is given by Eq. (4.40); this uncertainty goes approximately as $1/\sqrt{\tau}$, where τ is the length of the averaging interval. For the averages of fluctuations of $\sum\phi_{xx}$, $\sum\phi_{rr}$, and $\sum\phi_{xy}$, we require an averaging interval of the order of $10^4\ \Delta t$ for a relative accuracy of 15-20%. The computer time required for such long runs is considerable for N = 686, a run of 12000 time steps requires about two hours on the CRAY-1; for N = 1458, a run of 12000 time steps would require over six hours. Hence, the accuracy of these calculations cannot be significantly improved without the use of an inordinate amount of computer time.

2. Integration and Interpolation Error

By integration error, we refer to the effect of errors in the numerical integrations on the calculations of the pressure and the elastic constants. The integration error in a strictly

volume-dependent term, $O(\Omega)$, can be determined directly from the numerical integration errors for Ω^* and Ω^{**}. As discussed in Chapter 3, the numerical integration routine QAG calculates an integral plus an estimate of the absolute error in the integration. This absolute error is a considerable overestimate of the actual absolute error: we take 10% of the absolute error calculated by QAG for a particular integral as an upper bound for the numerical integration error of the integral. This error in $O(\Omega)$ contributes less than 8×10^{-6} kbar to the pressure and the elastic constants, and can be neglected.

The integration errors in the linear terms can be estimated as follows. We begin by calculating an upper bound for the integration error in each of the seven position-dependent mechanical quantities that form the output of the MD routine. Each of these quantities has the form

$$A = \sum_{K,L}' f(r_{KL};V)\, \hat{r}_i^m \hat{r}_j^n \quad . \tag{5.15}$$

A list of these quantities and the ranges of the indices K,L are given in Chapter 4. We calculate an upper bound for the integration error in A, $E_U(A)$, where

$$E_U(A) = \sum_{K,L}' |E[f(r_{KL};V)]\hat{r}_i^m \hat{r}_j^n| \quad , \tag{5.16}$$

and $E[f(r_{KL};V)]$ is an upper bound for the numerical integration error in $f(r_{KL};V)$. The MD routine calculates the sum in Eq. (5.16)

in the same fashion that it calculates the sum in Eq. (5.15). The necessary values of $E[f(r_{KL};V)]$ are obtained by linear interpolation from a table of the numerical integration errors. We can then combine $E_U(\sum\phi^*)$, $E_U[\sum(\phi''-\phi')\hat{x}^4]$, etc., and take time averages to estimate the integration errors in the linear terms.

We obtain a relative integration error of less than 1×10^{-5} for each linear term. From Chapter 4, the relative interpolation error for any of the $(r;V)$-dependent expressions is less than 2×10^{-5}. We estimate an upper bound for the relative integration and interpolation error of a linear term to be less than 3×10^{-5}. This relative error corresponds to a maximum absolute error of less than 4×10^{-3} kbar; this error can be neglected.

The integration and interpolation errors in the fluctuation terms can be estimated as follows. We begin by writing the time average of the fluctuations of a mechanical quantity A as

$$\overline{(A(t) - \bar{A} + \Delta(t) + \delta)^2} \quad , \tag{5.17}$$

where $\Delta(t)$ is the integration and interpolation error in $A(t)$, and δ is the corresponding error in the time average $\bar{A}$. The integration and interpolation error, $E_F(A)$, for the fluctuation average of A is then

$$E_F(A) = \overline{2(A(t)-\bar{A})\Delta(t)} + \overline{\Delta(t)^2} + \delta^2 \quad . \tag{5.18}$$

We calculate an upper bound for this error, $E_{UF}(A)$, by taking absolute values for the factors in the first time average of Eq. (5.18). The second and third terms on the right can then be neglected, and we obtain

$$E_{UF}(A) = \overline{2|(A(t)-\bar{A})||\Delta(t)|} \quad . \tag{5.19}$$

To estimate $\Delta(t)$, we note that $\sum\phi_{xx}$, $\sum\phi_{rr}$, and $\sum\phi'_{\hat{x}\hat{x}}$ do not vary from their respective mean values by more than 1%. In addition, the relative integration and interpolation error for each of these mean values is less than 3×10^{-5}. Hence, for fluctuations in $\sum\phi_{xx}$ and $\sum\phi_{rr}$, we take

$$\Delta(t) = 3\times10^{-5}\ \overline{\sum\phi_{xx}} \quad , \tag{5.20}$$

and

$$\Delta(t) = 3\times10^{-5}\ \overline{\sum\phi_{rr}} \quad , \tag{5.21}$$

respectively. For fluctuations in $\sum\phi_{xy}$, we take

$$\Delta(t) = 3\times10^{-5}\ \overline{\sum\phi'_{\hat{x}\hat{x}}} \quad . \tag{5.22}$$

We can approximate $\overline{|A(t)-\bar{A}|}$ in Eq. (5.19) by the rms value S, where

$$S^2 = \overline{(A(t)-\bar{A})^2} \quad . \tag{5.23}$$

We then obtain, for the upper bound $E_{UF}(A)$ of the integration and interpolation error in a fluctuation average of A,

$$E_{UF}(A) = 6\times10^{-5}\ |\Delta(t)|S \quad . \tag{5.24}$$

The maximum error in a fluctuation term, F_α, due to integration and interpolation error contributes less than 0.2 kbar to the corresponding elastic constant. This error is negligible compared to the statistical error.

3. Cutoff Error

By cutoff error, we refer to the errors in the pressure and the elastic constants that result from setting the values of the (r;V)-dependent expressions to zero for $r > r_{max}$. We can analyze in some detail the effects of varying r_{max} for a static lattice. Figures 7-10 show the results of such static lattice calculations for the linear terms in the pressure and the elastic constants. The linear term in the pressure, L_p, converges asymptotically to a constant as r_{max} is increased. For $r_{max} \gtrsim 23\ a_0$, the relative cutoff error in L_p is less than 1%. In contrast, L_{11}, L_{12}, and L_{44}

exhibit large oscillations and pronounced beats; convergence is very slow. We estimate, for $r_{max} \geq 20\ a_0$, a cutoff uncertainty of less than 1 kbar for L_{11} and L_{44}, and less than 0.5 kbar for L_{12}.

We cannot apply this analysis to finite temperature calculations, since the necessity of taking time averages does not reasonably allow repeated calculations with different cutoffs. However, the sharp peaks and the clear beat frequencies exhibited by L_α as a function of r_{max} are properties of a perfect lattice. For time averages for a lattice of vibrating ions, these structures should be less pronounced, and the cutoff error should be smaller.

4. System Size Effects

By a system size effect, we refer to the difference between an intensive thermodynamic quantity calculated in the thermodynamic limit ($N \to \infty$) and the same quantity calculated for a small system. At present, there is no rigorous way to calculate this difference. However, the computational error associated with the number of particles in a system is assumed to be of order N^{-1} for systems with periodic boundary conditions.

We can investigate the effect of system size on our data by comparing two MD calculations of the pressure and the elastic constants. We performed one calculation with N = 686 atoms, and another with N = 1458 atoms. The two systems were set up with the same volume per atom and the same cutoff. In addition, the temperatures of the two equilibrium systems were approximately the same: T ~ 296 K for N = 1458, and T ~ 297 K for N = 686. The

results are given in Table II and Fig. 6. Within the limit of the statistical uncertainties, we found no significant system size effects.

TABLE I

MD RUN PARAMETERS

T_d is the desired temperature (see discussion following Eq. (4.9)).
a is the lattice parameter.

V_a (a_0^3)	T_d (K)	N	a (a_0)	r_{min} (a_0)	r_{max} (a_0)
254.921	Static Lattice	686	7.989	6.91	24.72
254.921	Static Lattice	43904	7.989	6.91	6.91-110.12
256.400	100	686	8.004	5.64	24.73
260.916	200	686	8.051	5.19	24.78
266.170	298.15	686	8.105	4.90	24.83
266.170	298.15	1458	8.105	4.90	24.83
268.637	340	686	8.130	4.80	24.86

TABLE II

CONTRIBUTIONS TO THE RESULTS FOR THE PRESSURE AND THE ELASTIC CONSTANTS

All entries are in kbar.

	Quantity	Total	$O(Q)$	K_α	L_α	F_α	Corrections X_1	Corrections X_2
			Strictly V-dependent	Kinetic Energy	Linear	Fluctuations	Ensemble	Isothermal-Adiabatic
Static Lattice	P	0.20	-22.8377	0	23.04	0	0	0
N = 686	C_{11}	79.7	-40.1284	0	119.84	0	0	0
	C_{12}	70.2	5.5470	0	64.62	0	0	0
	C_{44}	54.8	-22.8377	0	77.60	0	0	0
T = (99.5±0.2) K	P	1.06	-22.7369	0.362	23.44	0	0	0
N = 686	C_{11}	81.1	-39.9633	0.724	123.29	-3.7	-0.81	1.56
	C_{12}	69.4	5.5105	0	62.59	-0.6	-0.81	1.56
	C_{44}	50.2	-22.7369	0.362	74.84	-2.2	0	0
T = (198.7±0.4) K	P	1.12	-22.4390	0.710	22.85	0	0	0
N = 686	C_{11}	78.1	-39.4749	1.420	122.37	-7.7	-1.63	3.09
	C_{12}	66.9	5.4031	0	58.69	1.4	-1.63	3.09
	C_{44}	41.7	-22.4390	0.710	69.87	-6.5	0	0
T = (295.7±0.5) K	P	1.09	-22.1027	1.036	22.15	0	0	0
N = 1458	C_{11}	72.8	-38.9213	2.073	120.99	-13.6	-2.77	4.97
	C_{12}	64.9	5.2840	0	54.50	2.9	-2.77	4.97
	C_{44}	34.6	-22.1027	1.036	64.63	-9.0	0	0
T = (297.2±0.5) K	P	1.10	-22.1027	1.042	22.16	0	0	0
N = 686	C_{11}	73.7	-38.9213	2.083	121.11	-12.8	-2.79	5.00
	C_{12}	64.9	5.2840	0	54.56	2.8	-2.79	5.00
	C_{44}	35.4	-22.1027	1.042	64.67	-8.2	0	0
T = (339.7±0.6) K	P	1.11	-21.9466	1.181	21.88	0	0	0
N = 686	C_{11}	72.5	-38.6635	2.362	120.70	-14.5	-3.60	6.19
	C_{12}	62.9	5.2296	0	52.58	2.5	-3.60	6.19
	C_{44}	30.2	-21.9466	1.181	62.23	-11.3	0	0

TABLE III

CONTRIBUTIONS OF THE EFFECTIVE POTENTIAL $\phi(r;V)$
TO THE PRESSURE AND THE ELASTIC CONSTANTS

All entries are in kbar.

	Quantity	L_α (Linear)		F_α (Fluctuations)	
		V-dependent	r-dependent	V-dependent	r-dependent
Static Lattice	P	12.58	10.46	0	0
N = 686	C_{11}	24.76	95.10	0	0
	C_{12}	- 0.40	65.03	0	0
	C_{44}	12.58	65.03	0	0
T = (99.5±0.2) K	P	12.42	11.02	0	0
N = 686	C_{11}	25.01	98.28	0.2	-3.9
	C_{12}	0.17	62.42	0.3	0.3
	C_{44}	12.42	62.42	0	-2.2
T = (198.7±0.4) K	P	12.19	10.66	0	0
N = 686	C_{11}	25.39	96.97	0.4	-8.1
	C_{12}	1.02	57.68	0.6	0.8
	C_{44}	12.19	57.68	0	-6.5
T = (297.2±0.5) K	P	11.93	10.24	0	0
N = 686	C_{11}	25.67	95.45	0.8	-13.6
	C_{12}	1.81	52.75	0.7	2.1
	C_{44}	11.93	52.75	0	-8.2
T = (339.7±0.6) K	P	11.80	10.08	0	0
N = 686	C_{11}	25.75	94.95	1.0	-15.5
	C_{12}	2.15	50.43	0.9	1.6
	C_{44}	11.80	50.43	0	-11.3

TABLE IV

STATISTICAL UNCERTAINTIES IN THE MD RESULTS

	Quantity	Total Statistical Uncertainty (kbar)	ΔK_α Kinetic Energy Uncertainty (kbar)	ΔL_α Linear Uncertainty (kbar)	ΔF_α Fluctuation Uncertainty (kbar)	ΔX Correction Uncertainty (kbar)	τ Averaging Interval (10^3 Δt)
T = (99.5±0.2) K	P	0.002	0.001	0.001	0	0	8.1
N = 686	C_{11}	0.9	0.001	0.07	0.8	0.02	8.1
	C_{12}	0.6	0	0.07	0.6	0.02	8.1
	C_{44}	0.5	0.001	0.07	0.4	0	6.6
T = (198.7±0.4) K	P	0.005	0.001	0.003	0	0	11.2
N = 686	C_{11}	1.7	0.003	0.15	1.5	0.04	11.2
	C_{12}	1.1	0	0.07	1.0	0.04	11.2
	C_{44}	1.1	0.001	0.08	1.0	0	11.2
T = (295.7±0.5) K	P	0.007	0.002	0.005	0	0	7.7
N = 1458	C_{11}	3.3	0.004	0.17	3.1	0.06	7.7
	C_{12}	2.4	0	0.07	2.2	0.06	7.7
	C_{44}	1.7	0.002	0.08	1.6	0	6.0
T = (297.2±0.5) K	P	0.005	0.002	0.003	0	0	13.0
N = 686	C_{11}	2.3	0.003	0.19	2.1	0.06	13.0
	C_{12}	1.7	0	0.09	1.5	0.06	13.0
	C_{44}	1.2	0.002	0.10	1.1	0	13.0
T = (339.7±0.6) K	P	0.007	0.002	0.005	0	0	12.0
N = 686	C_{11}	2.6	0.004	0.23	2.3	0.07	12.0
	C_{12}	1.9	0	0.11	1.8	0.07	12.0
	C_{44}	2.5	0.002	0.12	2.3	0	10.0

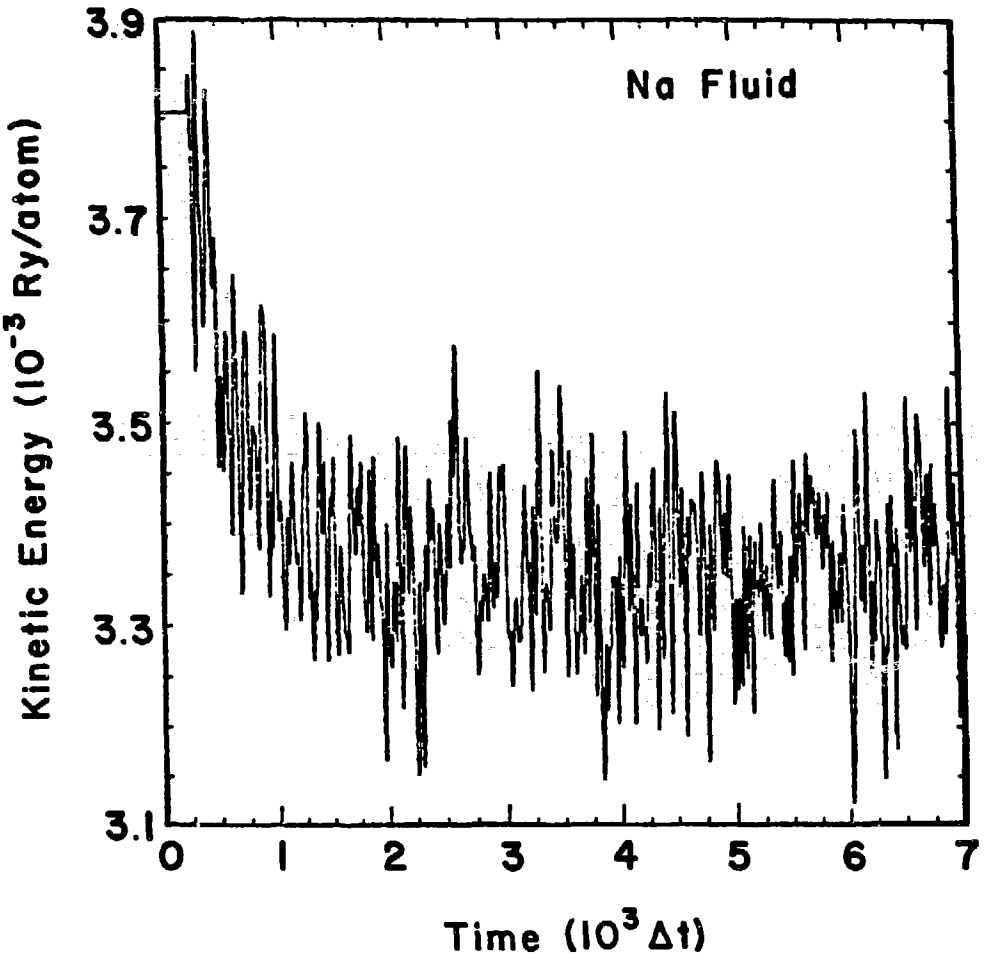

Fig. I. Equilibration of MD Data: Changing Mean of the Kinetic Energy

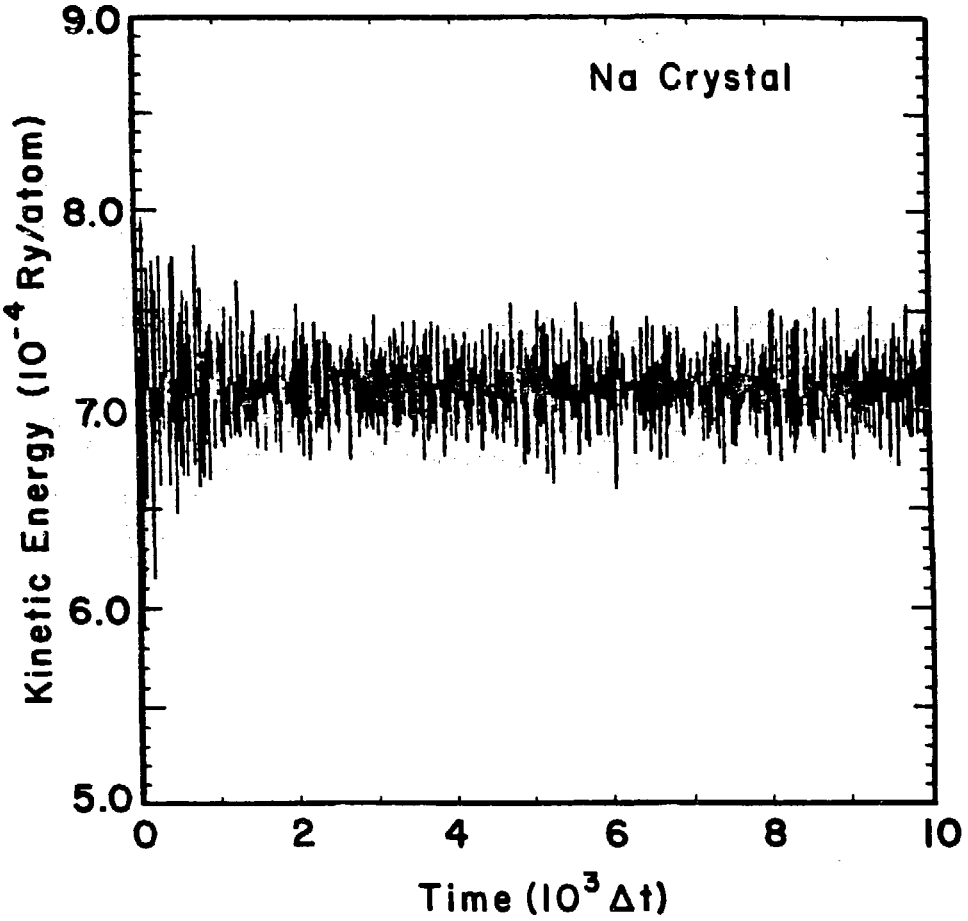

Fig. 2. Equilibration of MD Data: Changing Bandwidth of the Kinetic Energy

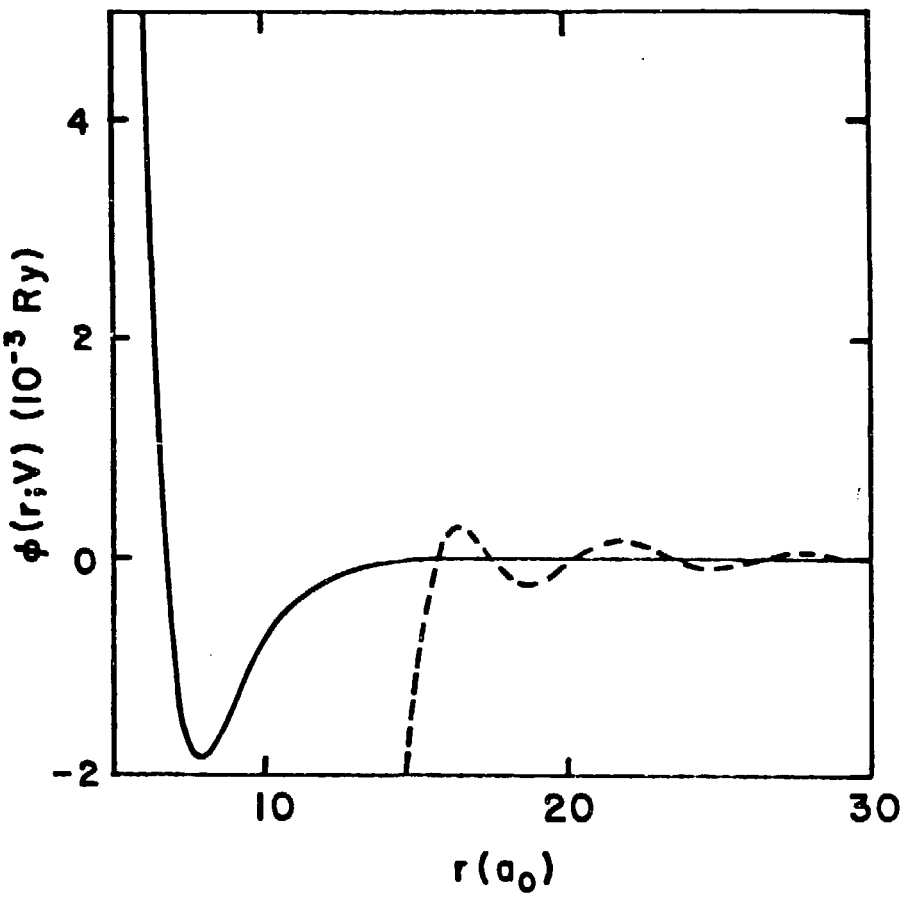

Fig. 3. The Effective Ion-Ion Potential $\phi(r;V)$

The volume per atom is $V_a = 256.4\, a_0^3$.
The dashed curve is $\phi(r;V) \times 100$.

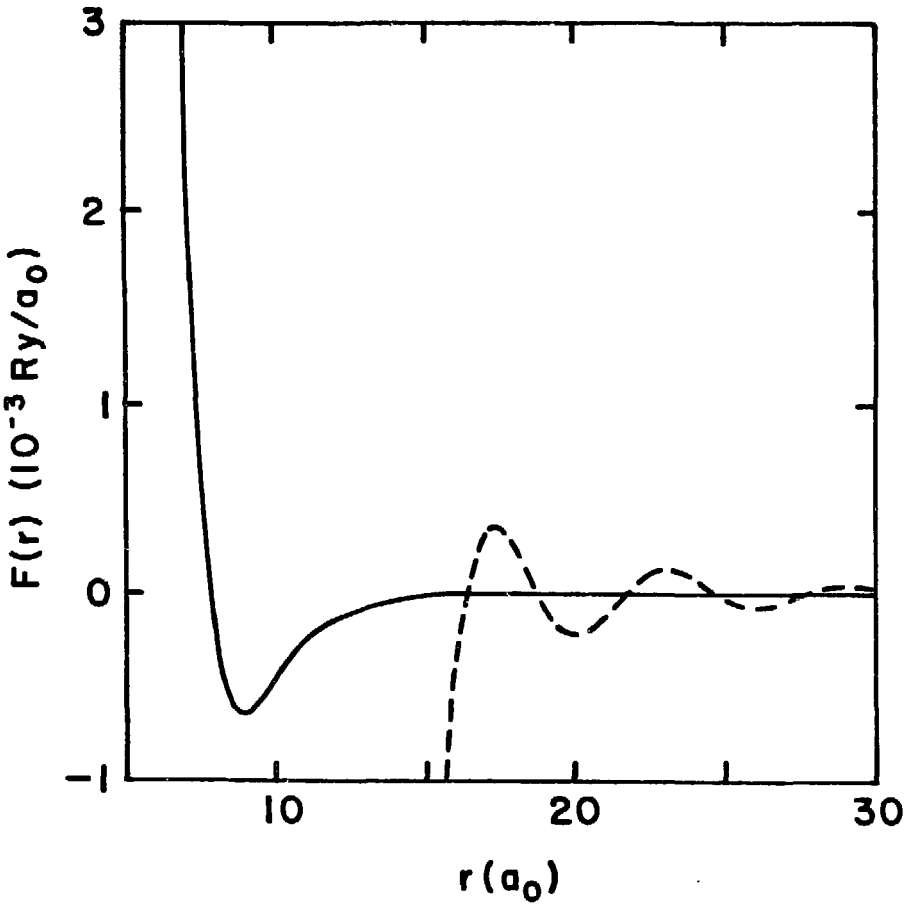

Fig. 4. The Effective Pairwise Force F(r)

The volume per atom is $V_a = 256.4\, a_0^3$.
The dashed curve is F(r)×100.

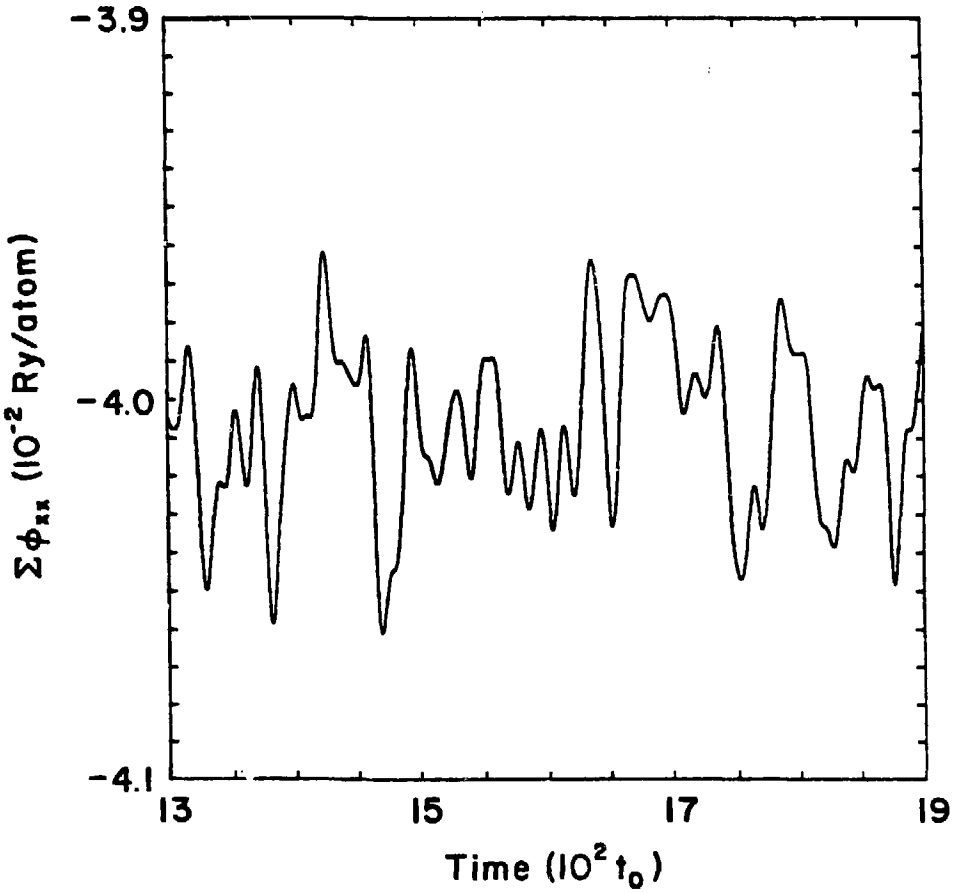

Fig. 5. Determination of the Fluctuation Time Δt_F

The average time between relative maxima is $\Delta t_F \sim 20 t_0$.

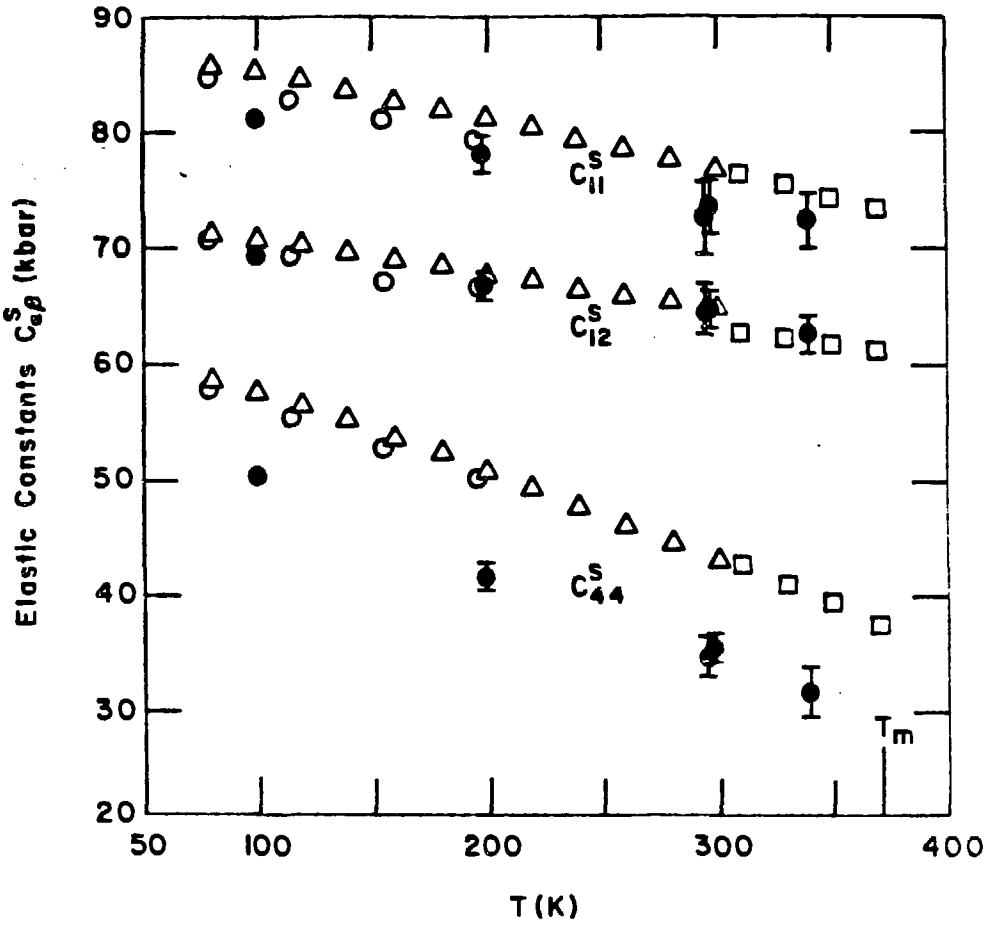

Fig 6. Adiabatic Elastic Constants $C^S_{\alpha\beta}$ vs Temperature

●, MD results
O, Diederich and Trivisonno (Ref. 36)
△, Martinson (Ref. 37)
□, Fritsch et al. (Ref. 38)

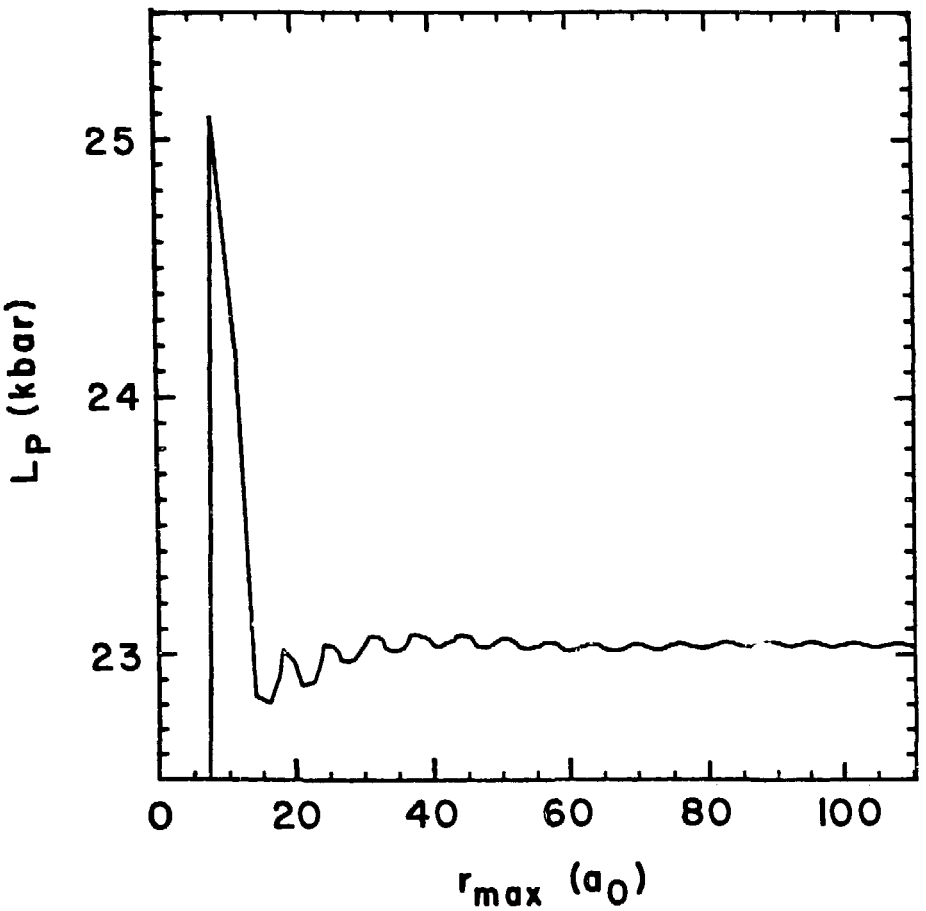

Fig. 7. Effects of Finite Potential Range: L_P vs r_{max} for the Static Lattice

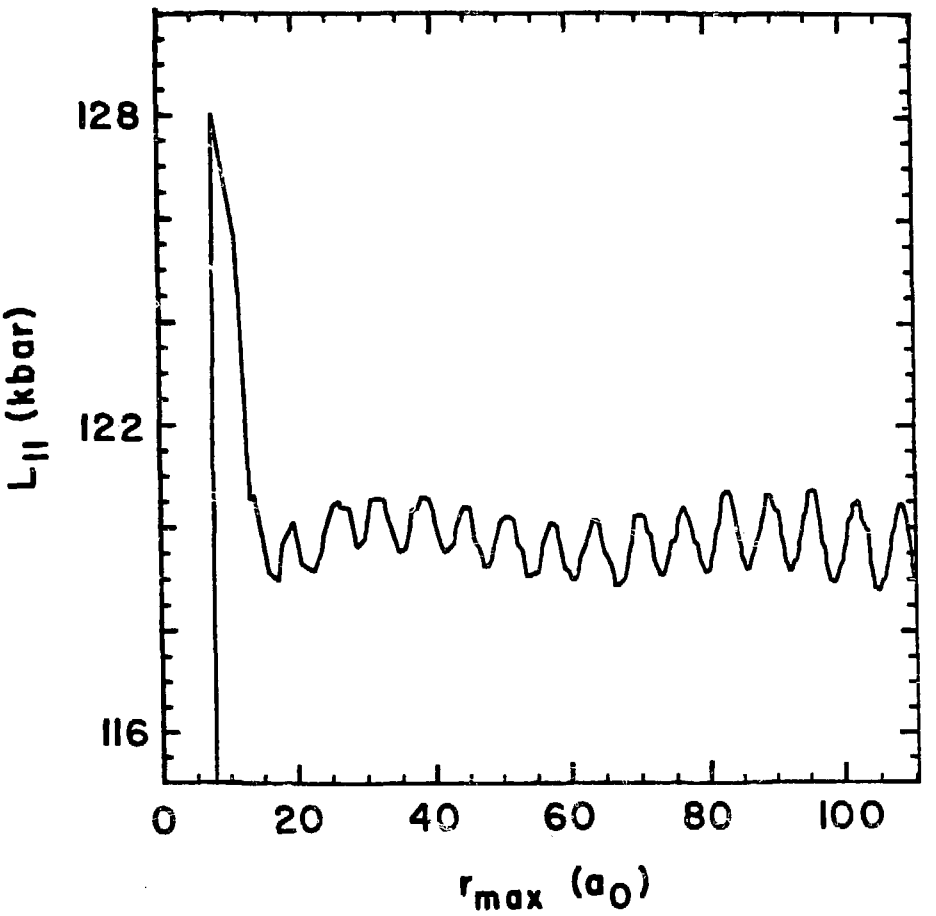

Fig. 8. Effects of Finite Potential Range: L_{11} vs r_{max} for the Static Lattice

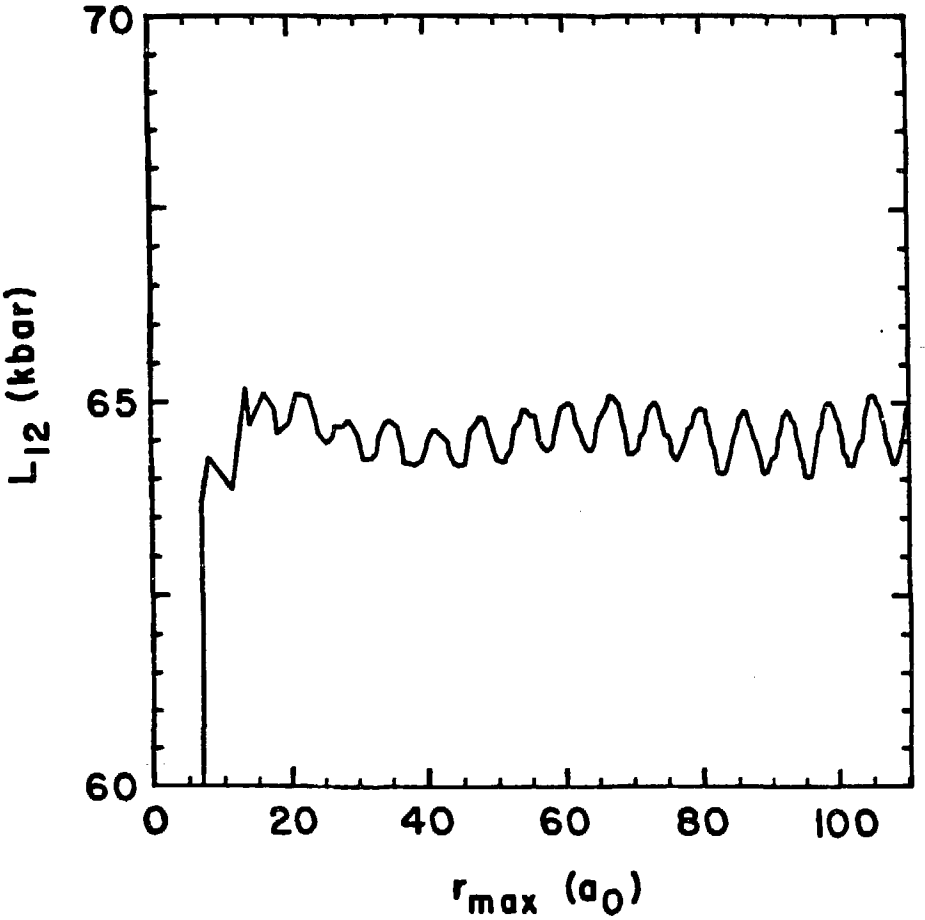

Fig. 9. Effects of Finite Potential Range: L_{12} vs r_{max} for the Static Lattice

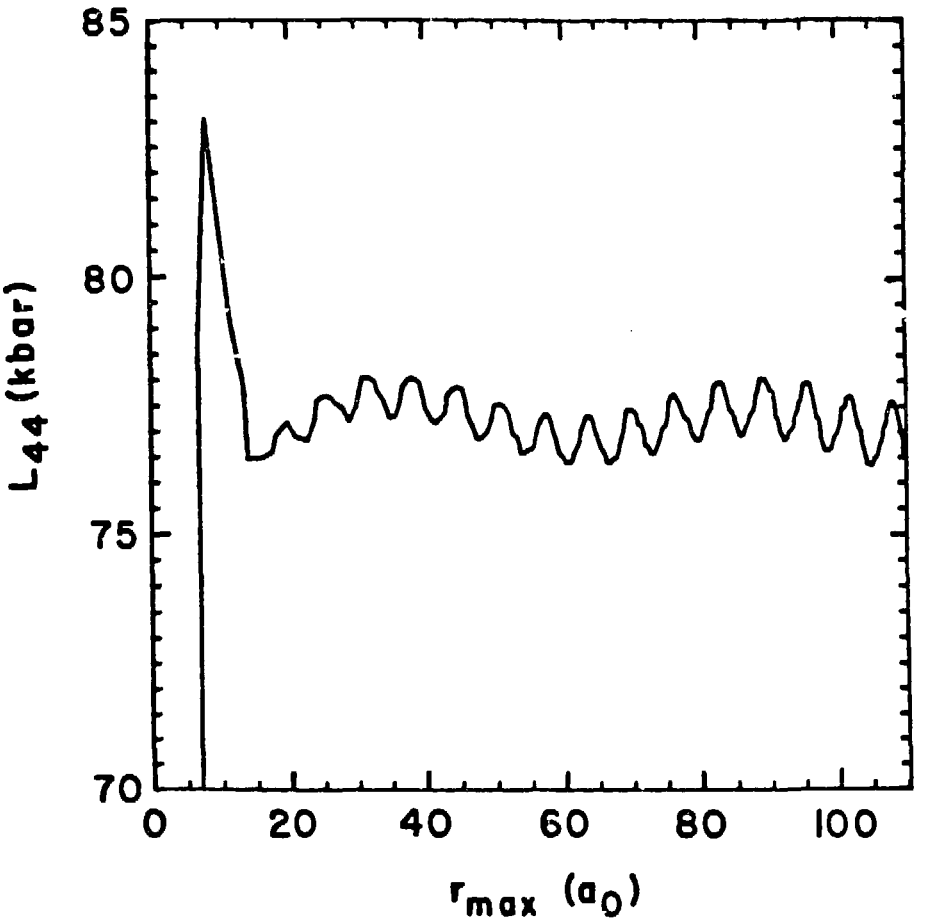

Fig. 10. Effects of Finite Potential Range: L_{44} vs r_{max} for the Static Lattice

ACKNOWLEDGMENTS

I gratefully acknowledge the support of Los Alamos National Laboratory, the Northwest College and University Association for Science (NORCUS), and the University of Arizona, whose cooperation made the time and facilities available for this study. This work was supported in part by a Los Alamos Graduate Research Assistanceship, and in part by a NORCUS (University of Washington) Laboratory Graduate Participant appointment, under Contract DE-AM06-76-RL02225 with the U.S. Department of Energy.

I especially appreciate the guidance, encouragement, and friendship of Dr. Duane C. Wallace, my mentor and Los Alamos advisor, and his insistence that one should do physics right. I also appreciate many helpful discussions with Dr. James D. Johnson and Dr. Milton S. Shaw, on equation-of-state matters, with Dr. Thomas R. Bement, on statistics and numerical techniques, and with Dr. Galen K. Straub and Dr. Brad L. Holian, on computer simulations. I would also like to thank Dr. John W. Shaner, for pushing me in the direction of statistical mechanics.

I appreciate the encouragement of my University of Arizona advisor, Prof. Roald K. Wangsness, and his efforts on behalf of an in absentia student. I also received encouragement of many indispensable kinds from Prof. Jose D. Garcia, Prof. Leon Blitzer, Prof. Chang-Yun Fan, Prof. K.-C. Hsieh, Prof. Donald R. Huffman,

Prof. Richard A. Young, Prof. Bruce R. Barrett, and Prof. Royal W. Stark.

I would like to thank Dr. John F. Barnes, for arranging Los Alamos divisional support, and Dr. Donald C. Wolkerstorfer, for extending the facilities of Group X-4 for this work. I would also like to thank Dr. Bryan B. Valett, Program Director for NORCUS, for arranging many months of support. I particularly appreciate the efforts of several individuals in Group X-DO at Los Alamos National Laboratory, without whose administrative expertise this cooperative project would have been impossible: Mr. Terry R. Gibbs and Ms. Carolyn R. Brown, for smoothly managing several changes in funding sources, Mr. John D. Klein, for computer liaison, and Mrs. Lydia G. Martinez, for arranging access to computer terminals and computer time.

I owe very special thanks to Ms. Yvonne Johnson for skilled and unfailingly good-natured typing of this manuscript. Finally, I would like to thank my husband, Dr. David Schiferl, for many useful discussions and for assistance with the figures.

REFERENCES

1. C. Herring, Phys. Rev. 57, 1169 (1940).

2. J. C. Phillips and L. Kleinman, Phys. Rev. 116, 287 (1959).

3. W. A. Harrison, Pseudopotentials in the Theory of Metals (Benjamin, New York, 1966).

4. R. E. Swanson, G. K. Straub, B. L. Holian, and D. C. Wallace, Phys. Rev. B 25, 7807 (1982).

5. G. K. Straub, S. K. Schiferl, and D. C. Wallace, Phys. Rev. B 28, 312 (1983).

6. B. L. Holian, G. K. Straub, R. E. Swanson, and D. C. Wallace, Phys. Rev. B 27, 2873 (1983).

7. G. K. Straub, R. E. Swanson, B. L. Holian, and D. C. Wallace, in Ab Initio Calculation of Phonon Spectra, edited by J. T. Devreese (Plenum, New York, 1983), p. 137.

8. D. C. Wallace, Phys. Rev. 176, 832 (1968).

9. D. C. Wallace, Phys. Rev. 182, 778 (1969).

10. S. K. Schiferl and D. C. Wallace, J. Chem. Phys. (to be published).

11. D. C. Wallace, S. K. Schiferl, and G. K. Straub, Phys. Rev. A 30, 616 (1984).

12. D. C. Wallace and G. K. Straub, Phys. Rev. A 27, 2201 (1983).

13. W. W. Wood, in Fundamental Problems in Statistical Mechanics, edited by E. D. G. Cohen (North-Holland, Amsterdam, 1975), Vol. 3, p. 331.

14. D. C. Wallace, Thermodynamics of Crystals (Wiley, New York, 1972).

15. F. Reif, Fundamentals of Statistical and Thermal Physics (McGraw-Hill, New York, 1965).

16. V. Heine, in Solid State Physics: Advances in Research and Applications, Vol. 24, edited by H. Ehrenreich, F. Seitz, and D. Turnbull (Academic Press, New York, 1970), p. 1.

17. M. L. Cohen and V. Heine, in Solid State Physics: Advances in Research and Applications, Vol. 24, edited by H. Ehrenreich, F. Seitz, and D. Turnbull (Academic Press, New York, 1970), p. 38.

18. J. Hubbard, Proc. Roy. Soc. (London) A243, 336 (1957).

19. C. Kittel, Quantum Theory of Solids (Wiley, New York, 1963).

20. D. Pines and P. Nozières, The Theory of Quantum Liquids (Benjamin, New York, 1966), Vol. 1.

21. M. J. Lighthill, Fourier Analysis and Generalized Functions (Cambridge University Press, London, 1958).

22. R. E. Swanson, Report No. LA-8877-T (Los Alamos National Laboratory, Los Alamos, 1981).

23. F. G. Fumi and M. P. Tosi, J. Phys. Chem. Solids 25, 31 (1964).

24. R. Piessens, Angew. Informatik 9, 399 (1973).

25. E. de Doncker, SIGNUM Newsletter 13, 12 (June, 1978).

26. P. J. Davis and P. Rabinowitz, Methods of Numerical Intergration (Academic Press, New York, 1975).

27. A. S. Kronrod, Nodes and Weights of Quadrature Formulas (Consultants Bureau, New York, 1965).

28. J. R. Rice, in Mathematical Software, edited by J. R. Rice (Academic Press, New York, 1971).

29. J. Pachner, Handbook of Numerical Analysis Applications (McGraw-Hill, New York, 1984).

30. V. I. Krylov, Approximate Calculation of Integrals, translated by A. H. Stroud (MacMillan, New York, 1962).

31. W. Adlhart, G. Fritsch, A. Heidemann, and E. Lüscher, Phys. Lett. 47A, 91 (1974).

32. S. Siegel and S. L. Quimby, Phys. Rev. 54, 76 (1938).

33. R. Feder and H. P. Charbnau, Phys. Rev. 149, 464 (1966).

34. International Tables for X-ray Crystallography (Kynoch Press, Birmingham, 1962), Vol. III.

35. G. W. Snedecor and W. G. Cochran, Statistical Methods (Iowa University Press, Ames, 1967).

36. M. E. Diederich and J. Trivisonno, J. Phys. Chem. Solids 27, 637 (1966).

37. R. H. Martinson, Phys. Rev. 178, 902 (1969).

38. G. Fritsch, F. Geipel, and A. Prasetyo, J. Phys. Chem. Solids 34, 1961 (1973).

39. D. Leibfried and W. Ludwig, in Solid State Physics: Advances in Research and Applications, Vol. 12, edited by F. Seitz and D. Turnbull (Academic Press, New York, 1961), p. 275.

40. T. Suzuki, A. V. Granato, and J. F. Thomas, Jr., Phys. Rev. 175, 766 (1968).

41. W. A. Harrison, Phys. Rev. B 7, 2408 (1973).

42. H. R. Glyde and R. Taylor, Phys. Rev. B 5, 1206 (1972).

43. S. S. Cohen, M. L. Klein, M. S. Duesbery, and R. Taylor, J. Phys. F: Metal Phys. 6, 337 (1976).

44. W. G. Hoover, A. C. Holt, and D. R. Squire, Physica 44, 437 (1969).

45. Z. S. Basinski, M. S. Duesbery, A. P. Pogany, R. Taylor, and Y. P. Varshni, Can. J. Phys. 48, 1480 (1970).

☆ U.S. GOVERNMENT PRINTING OFFICE:1985—576-034 / 20026